Durham E-Theses

A study of high energy muons and neutrinos underground

Creed, D.R.

How to cite:

Creed, D.R. (1967) *A study of high energy muons and neutrinos underground*, Durham theses, Durham University. Available at Durham E-Theses Online: http://etheses.dur.ac.uk/4086/

Use policy

The full-text may be used and/or reproduced, and given to third parties in any format or medium, without prior permission or charge, for personal research or study, educational, or not-for-profit purposes provided that:

- a full bibliographic reference is made to the original source
- a link is made to the metadata record in Durham E-Theses
- the full-text is not changed in any way

The full-text must not be sold in any format or medium without the formal permission of the copyright holders.

Please consult the full Durham E-Theses policy for further details.

Academic Support Office, Durham University, University Office, Old Elvet, Durham DH1 3HP
e-mail: e-theses.admin@dur.ac.uk Tel: +44 0191 334 6107
http://etheses.dur.ac.uk

A Study of High Energy Muons and Neutrinos Underground

A Thesis submitted to the
University of Durham for the
Degree of Doctor of Philosophy

by

D.R. Creed, B.Sc.

September 1967

Contents

Abstract

The results are presented of an investigation into the flux of cosmic ray muons underground at a depth of 7500 m.w.e. in the Kolar Gold Fields, South India.

Muons from the decay of pions produced in the first high energy interactions of energetic cosmic rays in the upper atmosphere were observed to arrive from directions close to the vertical. The angular distribution, depth-intensity relation and electromagnetic interaction products of the muons are discussed and conclusions are drawn about the behaviour of these characteristics at very great depths.

An examination is made of the way in which muons loose energy in various media and from this study the range-energy relations for muons in standard rock and sea water are constructed. A comparison of recent underwater and underground measurements at depths down to 1500 m.w.e. is made and it is shown that the sea level energy spectra derived from measurements under the two types of media are nearly identical and close to the spectrum given by Osborne et al. (1964).

At angles close to the horizontal, muons were detected in the underground laboratory from the interactions of neutrinos with nucleons in the surrounding rock wall. Definite evidence was obtained, by means of a visual neon flash tube technique, that the

neutrino interactions are mainly non-elastic in character, and that the rate of muons observed agrees well with theory, though on the presently available statistics it is not possible to decide whether or not the role played by the theoretically predicted intermediate boson is significant.

The results from comparable experiments are presented, and the future development and aims of the Kolar Gold Fields experiment discussed.

Preface

The experimental and analytical studies reported in this thesis were performed by the author in conjunction with other members of an international collaboration team composed of groups from the Tata Institute of Fundamental Research, Bombay; Osaka City University, Japan and Durham University. The author was a research student attached to the Durham group, under the supervision of Professor A.W. Wolfendale, in the period August 1964 to September 1967 during which time he spent 18 months in the Kolar Gold Fields, South India, the site of the experimental work.

Relieving a Durham colleague in the Summer of 1964, the author helped to bring an earlier experiment to a satisfactory conclusion. This work, reported by Achar et al. (1965a, b) and Creed et al. (1965) confirmed the cosmic ray muon depth-intensity measurements made by Miyake et al. (1964a) and provided new information on the electromagnetic accompaniment of muons by the use of neon flash tube detectors. Brief details of the experiment are given here, particular reference being given to the analysis of the electromagnetic accompaniment.

Whilst in Durham the author made a study of energy loss mechanisms, giving close attention to the apparent discrepancy between muon intensity measurements under rock and water. It is

reported here, and also by Creed and Wolfendale (1967), that the apparent differences in measurements under the two media are due to normalisation procedures, and that when taken with a suitable range-energy relation, derived from the muon energy loss curves, the sea level muon energy spectra estimated from the two sets of intensity measurements for the different media are in close agreement.

Since the start of the K.G.F. neutrino experiment in January 1965 the author has been responsible for the installation of the major part of the neon flash tube detectors, and their associated optics and electronics, in the seven telescopes built. Whilst in the Kolar Gold Fields he was responsible for the daily running of the flash tube detectors and for the analysis of the photographic records.

Results from the K.G.F. neutrino experiment have been published by Achar et al. (1965c,d,e,f) and Menon et al. (1966a,b; 1967a,b). The present experiment brings these reports up to date and compares the experiment with similar studies reported at the 10th International Cosmic Ray Conference in Calgary.

Chapter 1

INTRODUCTION.

The study of cosmic radiation has added considerably to our knowledge of the structure of the atomic nucleus and has been instrumental in the discovery of many new fundamental particles. Beginning with the observations made in the 1900s that the charge on an electroscope gradually leaked away at a rate that could not be entirely explained by background radioactivity, and that the degree of ionisation within an ionisation chamber increased with height above about 2000 metres, it became clear that an ionising radiation was entering the Earth from outside the atmosphere. In the last fifty years many advances in the understanding of this radiation have been made, but the problems still to be solved are considerable.

The primary cosmic radiation incident on the Earth's atmosphere is known to consist mainly of protons and helium nuclei with a small admixture of heavier nuclei of mass up to, and possibly exceeding that of uranium, as well as a low flux of primary electrons. In addition there is thought to be a flux of neutrinos and X- and γ-rays, though quantitative measurements on these components are difficult to make. Above an energy of a few GeV the origin of the radiation is uncertain, but the very high

energies that have been observed indicate that a substantial part is of galactic and even extra-galactic origin. The high energy processes inherent in supernovae and galactic nuclei give rise to the belief that they may constitute at least partial sources, whilst the recent discovery of other energetic celestial objects, such as quasars, has opened speculation on new modes of production. On the other hand, some of the low energy component comes from the Sun and, if charged and of sufficiently low energy, enters the Earth's atmosphere after a period of oscillation within the van Allen radiation belts. The origin of cosmic rays is reviewed by Ginzburg and Syrovatsky (1964).

On entry into the upper atmosphere the nuclear active particles undergo collision with air nuclei with an interaction length of about 80 $g.cm^{-2}$. High energy cosmic rays produce 'jets' in which many pions and a lesser number of kaons, nucleon-antinucleon pairs and hyperons are produced. The nucleons undergo further interactions at a lower energy deeper inside the atmosphere, whilst the pions decay or interact depending on their heights of production, relativistic lifetimes and energies. The neutral pions decay with a very short lifetime into γ-rays which initiate high energy photon-electron showers in the atmosphere that may survive to sea level. The kaons and hyperons decay into pions, as well as γ-rays, electrons and neutrinos, through a variety of modes. The decay products of the pions: muons and neutrinos, also continue to sea level since they are weakly interacting particles. The cosmic ray

flux at sea level thus consists mainly of muons and neutrinos, and smaller numbers of electrons and γ-rays, with a very small contamination of nucleons and pions. The highly energetic primaries generate photon-electron showers which survive to sea level, with the secondaries mentioned, in the form of extensive air showers (EAS).

Many experiments investigating the nature of the cosmic radiation at sea level and at mountain altitudes have been carried out in the last few decades. A picture of the propagation of the interaction products of cosmic ray primaries has been built up in terms of the multiplicity of the production of secondaries, the energies transferred in interactions and the decay probabilities and interaction cross-sections of the particles generated, and a reasonably clear idea has been obtained of the processes involved, at least up to medium energies.

Two of the more recent problems to be investigated were those of the muon and neutrino components at very great depths underground. The muons from highly energetic primaries, created as the result of the decay of pions and kaons produced in the very first interactions ('atmospheric' muons), penetrate to great depths in the Earth whereas all the remaining components, other than the neutrinos, are absorbed in the first few metres of ground. The flux of muons underground had been investigated from the earliest days of cosmic ray studies, and increasing interest was shown in measuring the flux at the greatest possible depths to

throw light on the energy loss mechanisms effective at high energies, and to investigate the very energetic end of the sea level muon energy spectrum. Additionally, it was expected that the flux of neutrinos both from the primary cosmic radiation and from muon, pion and kaon decays should produce a small but measurable flux of secondary muons and electrons within the Earth, and that at great depths it would be possible to measure at least the secondary muon flux against the natural radioactivity and atmospheric muon backgrounds.

It is with these aspects that this work is concerned.

Chapter 2

THE STATUS OF MUON AND NEUTRINO STUDIES.

2.1 Muons.

The existence of mesons was first predicted by Yukawa in 1935, who in modifying Fermi's theory of β-decay, showed that the exchange particle representing nuclear forces must have a mass very much greater than that of the electron which Fermi had assumed acted as the mediator. Adopting a wave function similar to Schroedinger's equation to represent the meson, Yukawa used the information obtained from scattering experiments, that the nuclear force decreases approximately exponentially in distances of the order of 2.8×10^{-13} cm, to predict a mass of approximately $150m_e$ for the meson. He assumed the meson underwent decay, and information from β-decay indicated that its lifetime would be about 10^{-8} seconds.

It had long been known that the cosmic radiation consisted of a soft component, soon identified as electrons, and a hard component that did not fit the characteristics of any known particle. The direct determination of the mass of the penetrating particles by Anderson and Neddermeyer, and independently by Street and Stevenson in the period 1936-38, gave a result of the order of $200m_e$. These particles were at first thought to be Yukawa mesons

since they were observed to decay into an electron and, it was assumed, neutrinos. However their lifetime proved to be 100 times longer than that predicted, and the strong interactions with matter, essential to the Yukawa hypothesis, were not observed. The discovery of another particle in 1947, the π-meson (pion), which had characteristics that fitted the Yukawa particle resolved the dilemma and established the μ-meson (muon) as a decay product of the pion.

The characteristics of the muon listed in table 2.1 were established in the next couple of decades. Other than direct investigation through the use of accelerators, the chief method used to study muons was their underground and underwater detection with cloud chambers, ionisation counters, Geiger counters and scintillators, since at depths greater than a few tens of feet of rock the only remaining components of the cosmic radiation at surface are muons, neutrinos and their secondaries.

Table 2.1 Basic Properties of the Muon.

Mass	$(206.768 \pm 0.003)m_e$
Charge	$(1.00000 \pm 0.000005)e$
Lifetime	$(2.212 \pm 0.001)10^{-6}$ sec.
Spin	$\frac{1}{2}$

2.1.1 Underground Experiments.

Work by early underground experimenters yielded some useful results. Determination of the absolute rate of muons at various depths enabled the sea level muon spectrum to be calculated if an energy loss relation was assumed. The derived sea level spectrum could be checked against that measured directly by magnetic spectrographs up to energies of the order of 10^3 GeV and used to extend the knowledge of the spectrum beyond these energies. The muon spectrum threw light on the mode of propagation of air showers in the atmosphere, and on the primary cosmic radiation incident on the top of the atmosphere.

However there were several difficulties associated with finding an accurate depth-intensity relation for muons. The muons were always accompanied by a soft component consisting of low energy electrons which could give rise to spurious counts. The introduction of layers of absorber within the detectors helped to reduce this effect, but without the use of visual detectors there was always the possibility of recording a higher rate than actually existed.

To obtain a vertical intensity from a measured rate the angular distribution of the muons had to be known, unless the detector was collimated and observed only muons arriving from near vertical directions. This became particularly important at great depths where detector apertures had to be large to observe a reasonable rate. Geiger hodoscopes were used, but ideally visual detectors were needed. Additionally, accurate measurements had to

be made of the nature and extent of the overburden above the detectors. In many cases the exact chemical composition and amount of all the rocks within the overburden was not established, and only approximate allowances were made for the surface topography.

In order to compare intensities measured under different materials the concept of 'metres water equivalent' (m.w.e.) was adopted, which initially was the depth of experimentation in metres times the mean density of the overburden. It was realised later that the energy loss of muons was a complicated function of the atomic weight, A, and atomic number, Z, of an absorber and that direct comparison of intensities at depths expressed in m.w.e. was not possible. As a result a 'standard rock' was assumed with $Z = 11$, $A = 22$ and density $= 2.65\ g.cm^{-3}$, so that a genuine comparison could be made.

Despite these difficulties useful results were gathered and the sea level muon spectrum defined out to energies of the order of 2000 GeV, corresponding to depths of about 3500 m.w.e. It was realised that errors in the estimation of muon energy losses through nuclear interactions and electron pair production, as well as errors from the effect of fluctuations in the total energy loss would introduce an increasing inaccuracy into the derived muon spectrum at high energies. This necessitated an investigation into the electromagnetic interactions of muons at various depths to uncover any anomalies and to check the total rate of accompaniment of muons by a soft component against that expected from the proposed

underground spectrum.

Recently, experiments were proposed to investigate the muons produced from neutrino-nucleon interactions in rock, and to distinguish these muons from the remnant atmospheric muons, even at very great depths, required an accurate knowledge of the angular distribution and intensity of atmospheric muons down to depths in the region of 9000 m.w.e.

Since the review article by Barrett et al. (1952), a number of experiments have been reported. Results from experiments performed at depths greater than 3000 m.w.e. are discussed in chapter 4 where the best estimate of the depth-intensity relation under standard rock is derived for depths between 3000 and 9000 m.w.e. The work of Higashi et al. (1966) on muon intensities under sea water is also examined in chapter 4, and it is concluded that there is no significant difference between underwater and under rock measurements down to a depth of 1500 m.w.e. Comparative studies under different types of absorber, particularly sea water and Kolar rock should, in theory, enable the energy loss components to be evaluated at high energies. This aspect of underground work is discussed in the same chapter.

Of the more recent experiments those of Miyake et al. (1964a) and Achar et al. (1965a) are probably the most significant. Working in the Kolar Gold Fields, both teams established the depth-intensity relation of cosmic ray muons to greater depths than had previously been achieved. The earlier work did not include the

use of visual detectors and as a result suffered from some of the uncertainties already mentioned. The later work by Achar et al. confirmed the findings of Miyake et al. by the use of neon flash tubes to examine the angular dependence and electromagnetic interactions of the muons, as well as paving the way for the Kolar Gold Fields neutrino experiment which used similar detectors.

The KGF neutrino experiment, which is the main subject of discussion in this work, although primarily designed to detect the muons produced by neutrino interactions has a considerable aperture for atmospheric muons arriving from between 15^{o} and 50^{o} projected zenith angle. At the great depth at which the experiment is sited, 7500 m.w.e., the atmopheric muons recorded come from the decay of pions produced in the upper atmosphere by the very first interactions of high energy primaries, and since the apparatus can detect any gross anomaly in rate, direction or energy (the latter through the degree of electromagnetic interactions and scatter of the muons in the lead absorbers), of the atmopheric muons, it can give valuable information about the primary spectrum and the character of high energy interactions, as well as giving the most accurate assessment of the vertical muon intensity yet obtained at comparable depths.

2.2 Neutrinos: A Historical Review

First postulated by Pauli in 1932 so that the concepts of momentum and spin conservation might hold in β-decay, the idea of

the neutrino was soon incorporated into Fermi's theory of weak interactions which successfully explained the shape of the electron energy spectrum emitted by an element undergoing β-decay. It was supposed that neutrinos existed as particles and anti-particles and examination of the end point of the beta energy spectrum suggested that neutrinos should have a very small, if not zero mass. Discovery of the muon in the late 1930s and an examination of its interaction characteristics lead to the conclusion that along with the electron and neutrino it underwent weak interactions as predicted by the universal Fermi interaction. The theory of weak interactions remained essentially the same until the existence of parity non-conservation was confirmed by the observations of Wu et al. on the asymmetric production of beta rays from Co^{60} in 1957.

Earlier, in 1953, Reines and Cowan working with the Savannah River reactor made the first observation of the absorption of neutrinos by nuclei, giving the neutrino full status as a fundamental particle. They found an interaction cross-section of approximately 10^{-44} cm^2 at a neutrino energy of 1 MeV, in accordance with the predictions of the universal Fermi interaction.

The present form of the weak interaction theory was developed by Feynman and Gell-Mann in 1958. Describing the weak interactions in terms of vector and axial vector coupling, the V - A theory proposed four types of neutrinos, particle and anti-particle each associated with the electron (ν_e, $\bar{\nu}_e$) or the muon (ν_μ, $\bar{\nu}_\mu$). Successfully describing β-decay, muon decay and

absorption, and the branching ratio of the pion into an electron and a neutrino or a muon and a neutrino, the theory met with difficulties at high momentum transfers. For example, the effective interaction Lagrangian which accounts for muon decay:

$$\mu^+ \longrightarrow e^+ + \nu_e + \bar{\nu}_\mu$$

represents the interaction of four fermions at a single space-time point and predicts a cross-section for, say,

$$\bar{\nu}_\mu + e^+ \longrightarrow \bar{\nu}_e + \mu^+$$

that increases with the square of the c.m.s. momentum. A conflict with the unitarity limit of the cross-section ($\lambda^2/8\pi$) is reached at an energy of about 300 GeV. From this it follows that there must be an alternative mechanism that comes into operation well before an energy of 300 GeV. To remove the obstacle that the interaction takes place at a single space-time point the intermediate vector boson was introduced with a role similar to that of the photon in electromagnetic interactions. The introduction of this non-locality at high energies and the fact that the mediating particle must appear virtually, ensured a large amplitude for the reaction:

$$\mu \rightarrow e + \gamma$$

but this was not observed experimentally. T.D. Lee argued that this was explained by a selection rule and that the only one consistent with all the known facts about muon decay was the two neutrino hypothesis:

$\pi^+ \longrightarrow \mu^+ + \nu_\mu$, $\pi^+ \rightarrow e^+ + \nu_e$ and $\nu_\mu \neq \nu_e$.

The difficulties inherent in observing weak interactions at high energies against the background of strong and electromagnetic interactions were overcome by using neutrinos as bombarding particles following suggestions made independently by M.Schwartz and B. Pontecorvo. Studies of the existing accelerators showed that they were capable of yielding sufficient intensities of neutrinos to observe their weak interactions at energies of the order of 1 GeV.

The first experiment demonstrating the separate existence of electron and muon neutrinos was carried out in 1962 by Danby et al. at the Brookhaven National Laboratory. The results gave strong support to the two neutrino theory. Subsequent experiments at CERN using an energy spectrum of neutrinos calculated to be peaked at a value below 1 GeV and extending effectively up to the region of 10 GeV confirmed this result and investigated the nature of the elastic and inelastic interaction cross-sections for neutrino-nucleon collisions. No clear evidence for the intermediate boson (W) was found, the lower limit to its mass m_W being set at about 2 GeV depending on the branching ratio of the W through leptonic or non-leptonic modes. (Bernardini et al. 1965). The neutrino flip hypothesis was found to be false with 90% certainty, confirming the non-interchange of the electron and muon associated neutrinos. Some of the experimentally determined properties of neutrinos are listed in table 2.2.

Table 2.2 Basic Properties of Neutrinos

	Electron neutrino	Muon neutrino
Mass	< 0.2 KeV	< 1 MeV
Charge	$< 10^{-19} e$	$< 5 \times 10^{-6} e$
Spin	$\frac{1}{2}$ if $m = 0$	$\frac{1}{2}$ if $m = 0$
Helicity	> 0.95	> 0.80

The behaviour of weak interactions at high energies could only be investigated up to a few GeV at CERN and Brookhaven with the existing experimental arrangements. Within the next few years the particle intensities will be raised by a factor of up to 100, but this will be the probable limit of these machines. Better statistics will be available for intensities up to 10 GeV, but it will not be until the next generation of machines is built that mean neutrino energies of about 20 GeV with maximum energies of 100 GeV will be available. Within 8 months the Sherpukhov accelerator will raise the maximum available proton energy to 70 GeV from its present limit of 30 GeV, and the design study by the Lawrence Radiation Laboratory for a 200 GeV machine should give the neutrino energies mentioned within six years.

However, an investigation of weak interactions can be made by using the neutrinos from pion, kaon and muon decay in the atmosphere. Because of the very low cross-sections even at high energies, assuming no resonance interactions, the Earth is

effectively transparent to neutrinos and at any point underground the flux of neutrinos is roughly isotropic. The interaction of neutrinos of atmospheric origin within the Earth's crust will produce a very low flux of muons and electrons, but as pointed out by Markov and Zheleznykh (1961), the muons produced will travel considerable distances and there will be an effective target thickness of rock surrounding the detector that is equal to the range of the muons in rock. Compensation for the falling neutrino intensity at high energies is gained from the increased range of the muons in rock, and it was thought that it should be possible to measure the rate of muons from neutrino interactions, though it was unlikely that the interactions themselves would occur within the detecting apparatus.

Following the work of Miyake et al. (1964) who reported no events from two vertical muon telescopes each of 1.5 m^2 area at a depth of 9200 ft. below ground in 60 days of operation, it became clear that it was possible to operate successfully detectors at a depth where the neutrino-induced muon intensity was of the same order of magnitude as the residual muon intensity from the atmosphere. Two experiments were started in late 1964 and early 1965. One, the Johannesburg experiment, was sited in the East Rand Proprietary Mines, South Africa and was run by a group from the Case Institute, Ohio and Witwatersrand University. (Reines et al. 1965). The other, the KGF experiment, was sited in the Kolar Gold Fields, Southern India and was run jointly by groups from the Tata

Institute of Fundamental Research, Bombay (TIFR), Osaka City University, Japan and Durham University. (Achar et al. 1965e). The author is a member of this last group.

2.3 Present Underground Experiments

The Johannesburg experiment is sited at a depth of 8500 m.w.e. standard rock and uses tanks of mineral oil based liquid scintillator stacked in two parallel vertical walls as the primary detectors. Each tank is 56 cm high, 12.7 cm thick and 5.5 m long and is viewed by four five inch photomultipliers. The walls, separated by 1.8 m, are three tanks high and, for the initial stages of the experiment, were six tanks long. The thickness of the tanks ensures that a minimum ionising muon traversing a single tank must deposit at least 20 MeV in the scintillator, which is well above the energies of the natural radioactive processes. The arrangement gives a maximum aperture in the horizontal direction where the neutrino flux is peaked by a factor of about two over the vertical flux, and minimum aperture in the vertical direction where any residual atmospheric muons might be expected to be seen. Pulse height analysis of the photomultiplier outputs indicates the energy deposition of the muon, and if it traverses a tank in each wall the azimuth angle can be estimated. To date several categories of event have been observed, a full discussion of the latest available results from the experiment is given in chapter 6. Undoubtedly muons from neutrino interactions have been

recorded, but the interpretation of some of the more complex coincidences involving two or more adjacent tanks in the same wall is difficult.

Some of the difficulties of interpretation are overcome in the KGF experiment by the use of visual detectors as well as scintillator elements. Using two vertical walls of plastic scintillator 5 cm thick, 3 m high and 2 m long with a separation of 85 cm, as primary detectors, walls of lead and neon flash tubes are positioned between the scintillators to give visual evidence of the tracks of particles traversing the apparatus and information on any interactions occurring within the lead walls. A description of the initial and subsequent phases of the experiment is given in chapters 3 and 7, but the shallower depth, 7500 m.w.e. standard rock, at which the experiment is sited gives rise to the detection of a large number of atmospheric muons.

Recently, an experiment has been initiated by members of the University of Utah to investigate the interactions of neutrinos with a detector bulk of 2000 tons incorporating a novel type of cylindrical spark counter. (Bergeson et al. 1965). Although situated at a depth of about 1500 m.w.e. the sense of travel of a particle is determined in the most favorable case by four independent Cerenkov measurements and three time of flight measurements allowing upward travelling neutrino secondaries to be distinguished. Track location is made within the spark counters by a sonic technique giving an accuracy of 3 mm along the length

of the counter. The counter arrangement, described with the latest results from the experiment in chapter 6, gives an angular resolution of about 10^{-6} steradians.

Experiments of the type described should give valuable information about absolute rates of neutrino-induced muons underground which will allow some estimate to be made of the dominant mode and character of neutrino-nucleon interactions if the flux of neutrinos generated in the atmosphere from muon, pion and kaon decays is known to a reasonable accuracy. The problem of the atmospheric neutrino flux has been studied by Cowsik et al. (1966) and Osborne et al. (1965) and it appears that their estimates do not differ greatly.

The arrival times and directions of muons reflect the original directions of the muon initiating neutrinos, and the apparent neutrino origins can be examined on the celestial sphere for any anisotropy, since there may be a low flux of muon neutrinos from some celestial objects. This form of 'neutrino astronomy' is more likely to be productive when the experiment is designed to detect electrons resulting from low energy electron neutrino interactions, since a large number of electron neutrinos are generated in the Sun and other stars. An experiment of this type, initiated by Davis (1964), to detect the inverse β-decay caused by low energy electron neutrinos in a large volume of detector, has already put an upper limit on the Sun's central temperature of 18×10^6 ^{o}K by an estimate of the upper limit of the electron neutrino flux from

the Sun. (Kocharov 1965). However, it must be made clear that the present work deals primarily with the muon induced component from neutrino interactions of the type:

$$\bar{\nu}_\mu + p \rightarrow n + \mu^+ \quad \text{and} \quad \nu_\mu + n \rightarrow p + \mu^-$$

Information on the energy of muons traversing detectors can be gained from a study of the scattering in an absorber and from the rate of accompaniment by a soft component produced in the rock or absorber walls. These aspects are examined in chapters 3 and 8. A more direct method is to put large volumes of magnetised iron within the detectors and measure the deflection of the muons. This approach has been used recently by the KGF group with the introduction of two 14 k.gauss magnets underground and has been adopted by the Utah group who are incorporating magnets in their detector. It is hoped that the maximum detectable momentum of the KGF spectrographs will be 20-30 GeV/c which will allow, with sufficient exposure time, an estimate to be made of the neutrino-induced muon energy spectrum, a vital piece of information needed for the interpretation of the total rate of events. A discussion of the KGF spectrographs is given in chapter 7.

It is apparent that the type of experiment described above has an effective role to play in the advancement of our knowledge of weak interactions whilst the new generation of accelerators is under construction. Whether they will continue in their usefulness once accelerators can produce neutrino energies of up to 100 GeV depends on the discoveries made in the field of weak interactions

and in the new subject of neutrino astronomy.

Chapter 3

ELECTROMAGNETIC INTERACTIONS UNDERGROUND

3.1 Introduction

An experiment using visual detectors for the first time at great depths underground was carried out in 1964 by a combined group from TIFR and Durham University. (Achar et al. 1965a,b). This experiment, sited in the Kolar Gold Fields, Southern India, was followed by the KGF neutrino experiment, as mentioned in chapter 2. Both experiments have yielded data on the accompaniment of muons by secondaries, and the production of secondaries within detectors, through the use of neon flash tubes. It is the analysis of this data which is discussed in this chapter.

3.2 The Joint TIFR-Durham Experiment

A full account of this experiment has been given by Pattison (1965) and only a brief outline of the experimental arrangement will be given here. Figure 3.1 is a diagram of the apparatus used. Two such units were operated consecutively at a depth of 816 m.w.e. and simultaneously at depths of 1812 m.w.e. and 4100 m.w.e. (All depths are for KGF rock with $Z^2/A = 6.29$). The coincidence requirements demanded a fourfold coincidence between a pulse from the Geiger counters (each of sensitive

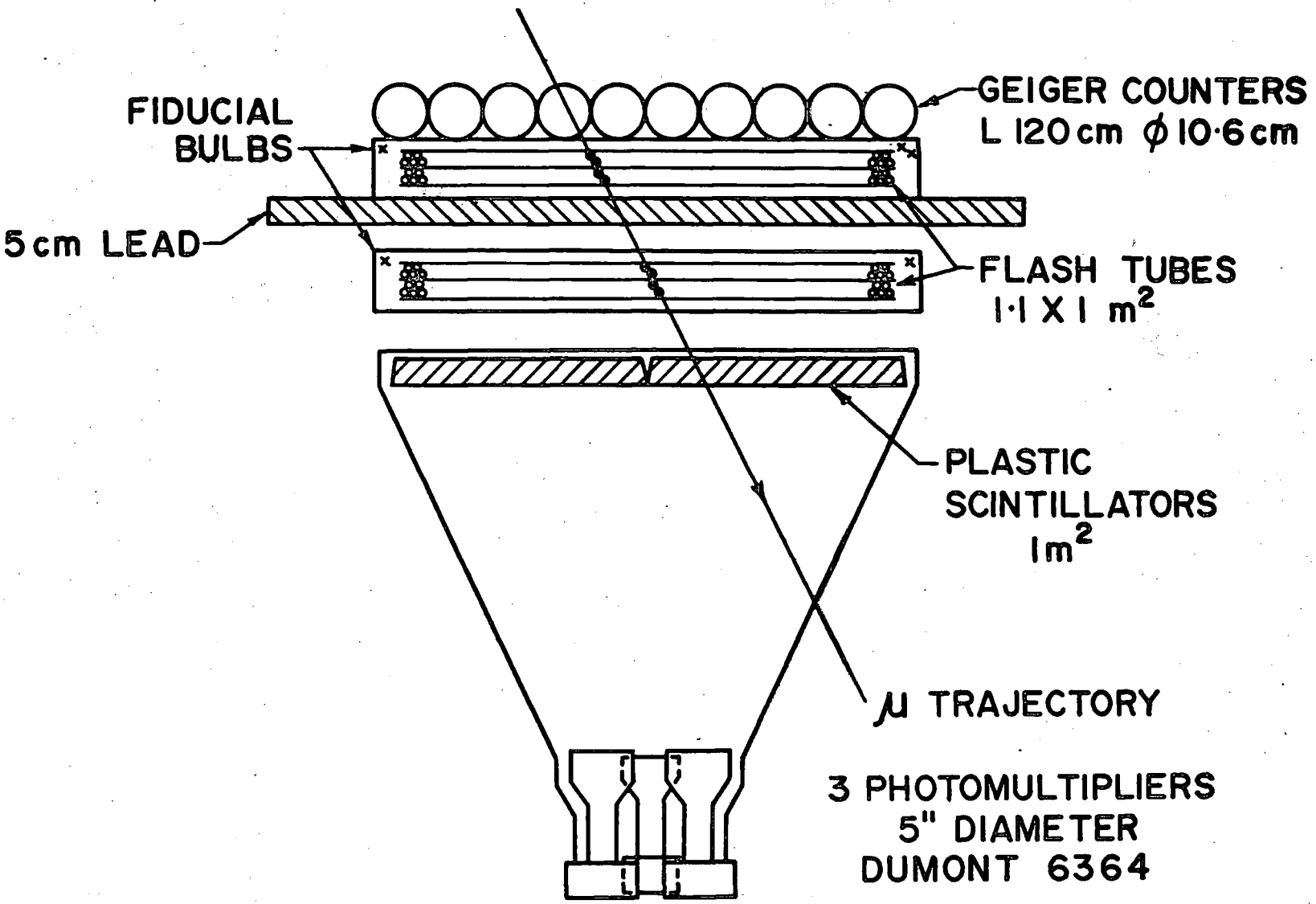
FIDUCIAL BULBS
GEIGER COUNTERS
L 120 cm ϕ 10·6 cm
5 cm LEAD
FLASH TUBES
1·1 X 1 m²
PLASTIC SCINTILLATORS
1 m²
μ TRAJECTORY
3 PHOTOMULTIPLIERS
5" DIAMETER
DUMONT 6364
0 10 20 30 cm

Figure 3.1

length 111 cm and diameter 10.6 cm) and pulses from the three photomultipliers viewing the 1 m square scintillator, within a 4 μs resolving time. The two sets of four layers of neon flash tubes (each 111 cm long and of 1.8 cm external diameter) were pulsed after each coincidence and the events photographed through a mirror system. A lead layer, 5 cm thick, was placed between the two sets of flash tubes.

It was found that the flash tube records could be divided into two groups: those that could be interpreted as the result of electromagnetic interactions and those showing clear evidence of more than one penetrating particle.

3.2.1 Multiple Penetrating Particles

An analysis of the multiple penetrating particle events (MPP) was made by Creed et al. (1965) who attempted to account for the observed number of double particles on the assumption that they originated in EAS as double muons, and that pion-muon pairs were generated by nuclear interactions of the muons in rock. The EAS contribution was derived using an adaptation of the simple model of Brooke et al. (1964) for the propagation through the atmosphere of the various components resulting from primary protons. The model enabled the probability of two muons falling within the detecting area of 1.1 m^2 per unit to be calculated. A check of the method was made by computing the expected vertical intensities at the three depths of operation and comparing the

values with the observed intensities. A good agreement was found.

The contribution to MPP from nuclear interactions of muons was calculated by using the cross-sections for shower production at the relevant depths taken from the review by Fowler and Wolfendale (1958) and it was assumed that most of the energy lost by the muon went into the production of a single pion.

The probability of two muons from an air shower falling within the detecting area added to the probability of a muon and a pion from a nuclear interaction being registered simultaneously gave a rate of double particle events that was in reasonable agreement with the observed rates at the three depths. Further confirmation was obtained by examining the projected lateral distributions of the double particle events and comparing them with the calculated distributions on the EAS model. The conclusion was that MPP at the depths of observation could be adequately explained by the simultaneous observation of more than one muon produced by the same primary nucleon in the atmosphere, and by the local nuclear interactions of the muons, except for a possible excess of events with very small track separations.

3.2.2 Electromagnetic Interactions

The flash tube records that were interpreted as being the result of electromagnetic interactions of the muons were divided as follows:

a) secondaries visible above the lead absorber:

(i) single electrons incident from the rock above the apparatus

(ii) electron showers incident from the rock

(iii) single low energy electrons (δ-rays) generated within the top tray

b) secondaries visible below the lead absorber:

(i) single electrons generated within the lead

(ii) electron showers produced in the lead

(iii) single low energy electrons (δ-rays) generated within the bottom tray.

The frequencies of occurrence of each type of event were determined for the three depths at which the apparatus was operated, and from the total numbers of events observed the probabilities plotted in figures 3.2 and 3.3 were calculated. It should be noted that these figures are not the same as those given by Creed et al. (1965) and by Pattison (1965), since they are the result of a more accurate examination of the majority of the events made by the author. In the new figures, allowance is made for the 'out of geometry' events (i.e. ones where the primary muon did not pass through both planes of the detector, the fourfold coincidence coming from energy deposition by the accompanying secondary particles), and a more careful criterion is taken for the 'in tray' accompaniment. The figures for showers do not include penetrating showers where there was a simultaneous observation of different developments of the same electron shower

Figure 3.2

Percentage of Electromagnetic Accompaniment from the Rock.

⊙ δ-rays in the top tray

● Electron Showers

× Single knock-on electrons

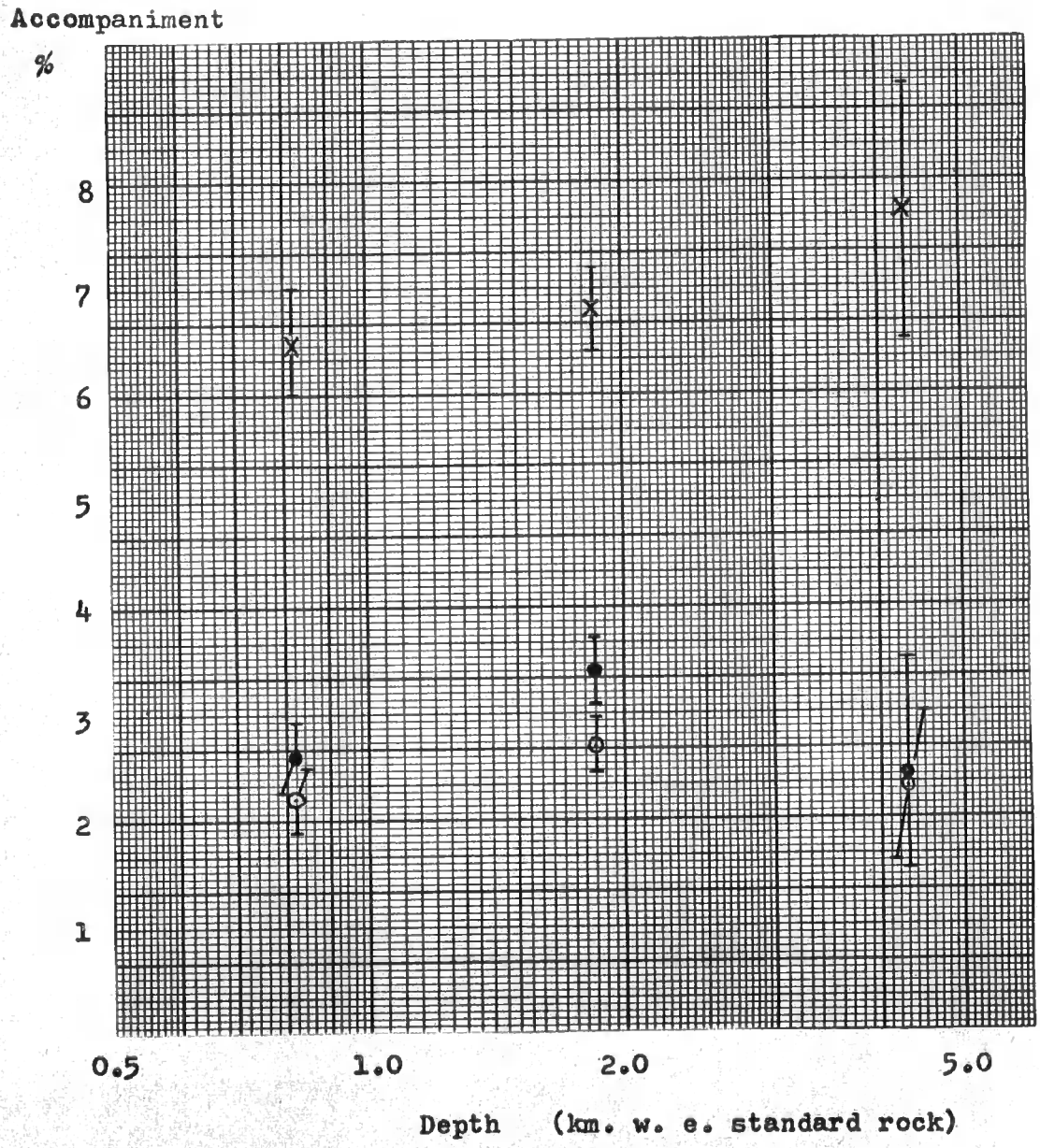

Figure 3.3

Percentage of Electromagnetic Accompaniment from the Lead.

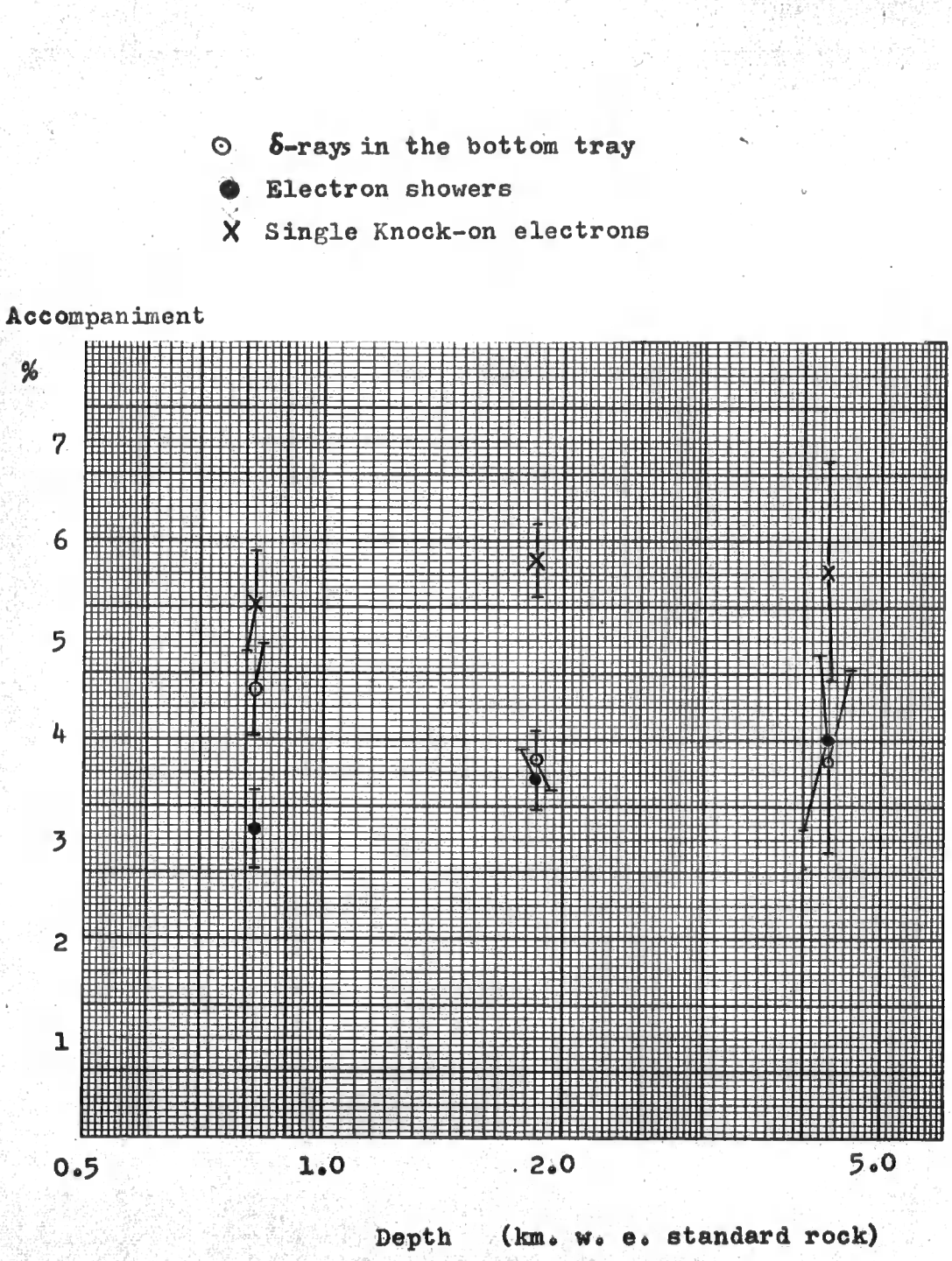

in upper and lower trays.

A knowledge of the arrival directions of the muons enabled the probabilities of the various types of accompaniment with projected zenith angle to be calculated. The results for 1812 m.w.e. are displayed in figures 3.4 and 3.5 where the error estimations are made by assuming a Poissonian distribution and are based on the figures of Regner (1951). No values are shown beyond 45° because there the statistics are extremely poor.

Figures 3.2 and 3.3 show quantitatively the increase in accompaniment with depth corresponding to the increase of the mean energy of atmospheric muons with depth. The large value for the δ-ray production in the bottom tray is probably due to low energy electrons from the lead being counted as δ-rays produced within the lower tray. A similar situation would not occur with the upper tray since the rock ceiling was approximately 1 m above the Geiger counters at the two shallower depths and 2 m above them at the greatest depth. This difference in ceiling height probably accounts for the reduction in shower probability from the rock at 4100 m.w.e. No increase with depth was found for δ-rays, this is because the probability of collision loss is insensitive to muon energy as explained in section 4.2.1.

The angular dependence of the various types of accompaniment, shown in figures 3.4 and 3.5 for the middle depth, is explained qualitatively by the increase with projected zenith angle of the mean muon energy and the muon path length through the

Figure 3.4

Variation of the Probability of Accompaniment of Muons from the Rock with Projected Zenith Angle.

1812 m.w.e.

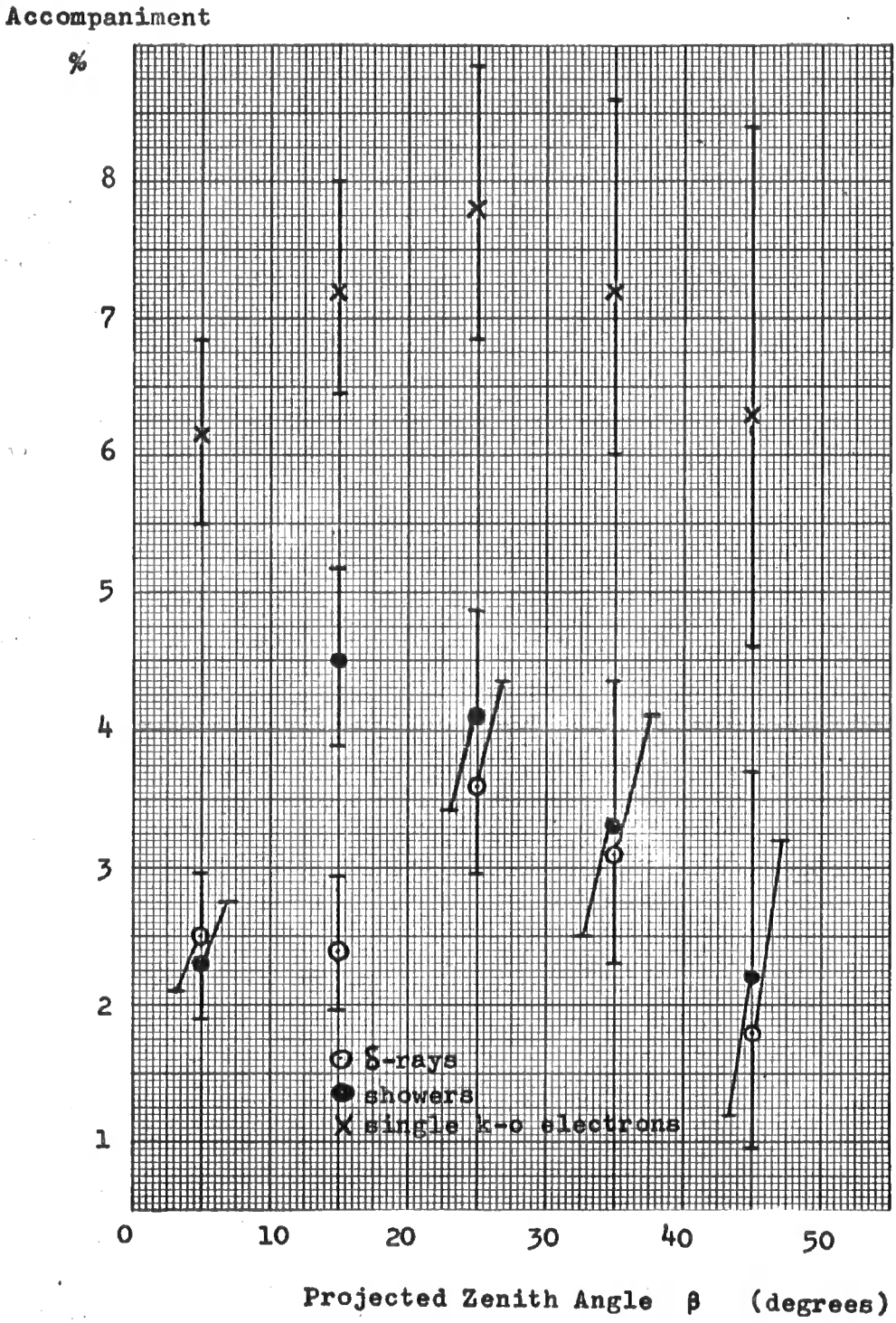

Figure 3.5

Variation of the Probability of Accompaniment of Muons from the Lead with Projected Zenith Angle.

1812 m.w.e.

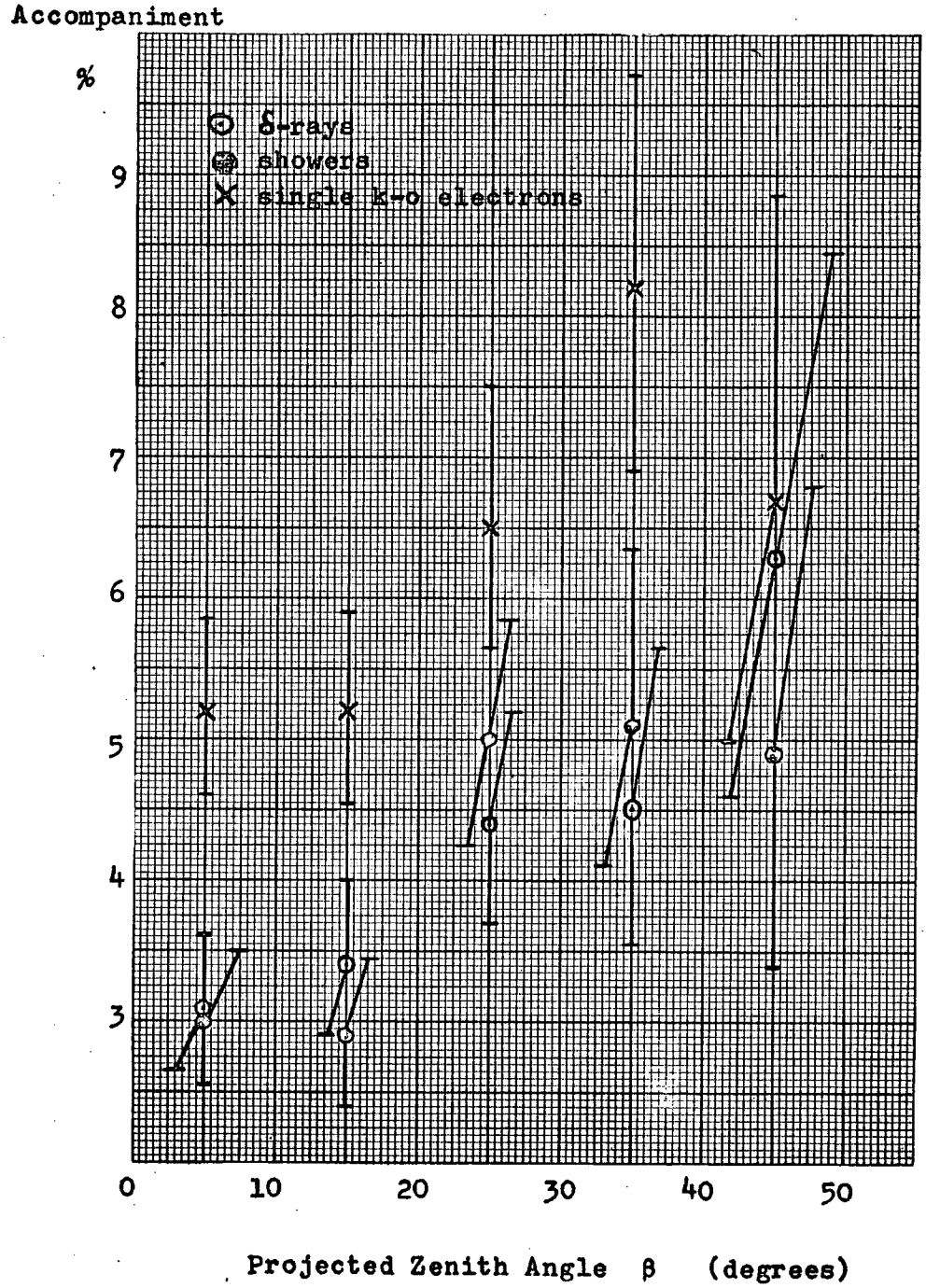

lead and neon flash tubes. The probability of electron showers being observed coming from the rock does not increase with angle because there is no increased path length in the absorber. Rather, it shows a decrease corresponding to the decrease of telescope aperture with increasing angle.

In broad outline the electromagnetic interactions observed at the three depths are understood. The total rate does not increase much with depth, but neither does the expected mean muon energy, as explained in section 3.5.

3.3.1 The KGF Neutrino Experiment: the Experimental Arrangement

The first two detector arrays were assembled in the Spring of 1965 and were designated the titles 'Neutrino Telescopes 1 and 2'. In their final completed state they were identical. (Figure 3.6). Two vertical walls of plastic scintillator each 2 m long, 3 m high and separated by 85 cm formed the primary detecting area of each telescope. Each wall was constructed from six scintillator elements each one metre square and 5 cm thick, the elements being made of four identical square blocks. Two adjacent DuMont 6364 five inch diameter photomultipliers were housed at the apex of a cone covering each scintillator element. Neon flash tubes were used as the visual detectors acting as the secondary detecting area. Each tube had an external diameter of 1.8 cm and was 2 m long. The tubes were arranged horizontally in trays 1 m high, 2 m long and 8 cm wide, giving four columns of flash tubes in each tray. Three trays

K.G.F. NEUTRINO TELESCOPE

Telescope 1 or 2

Front Elevation

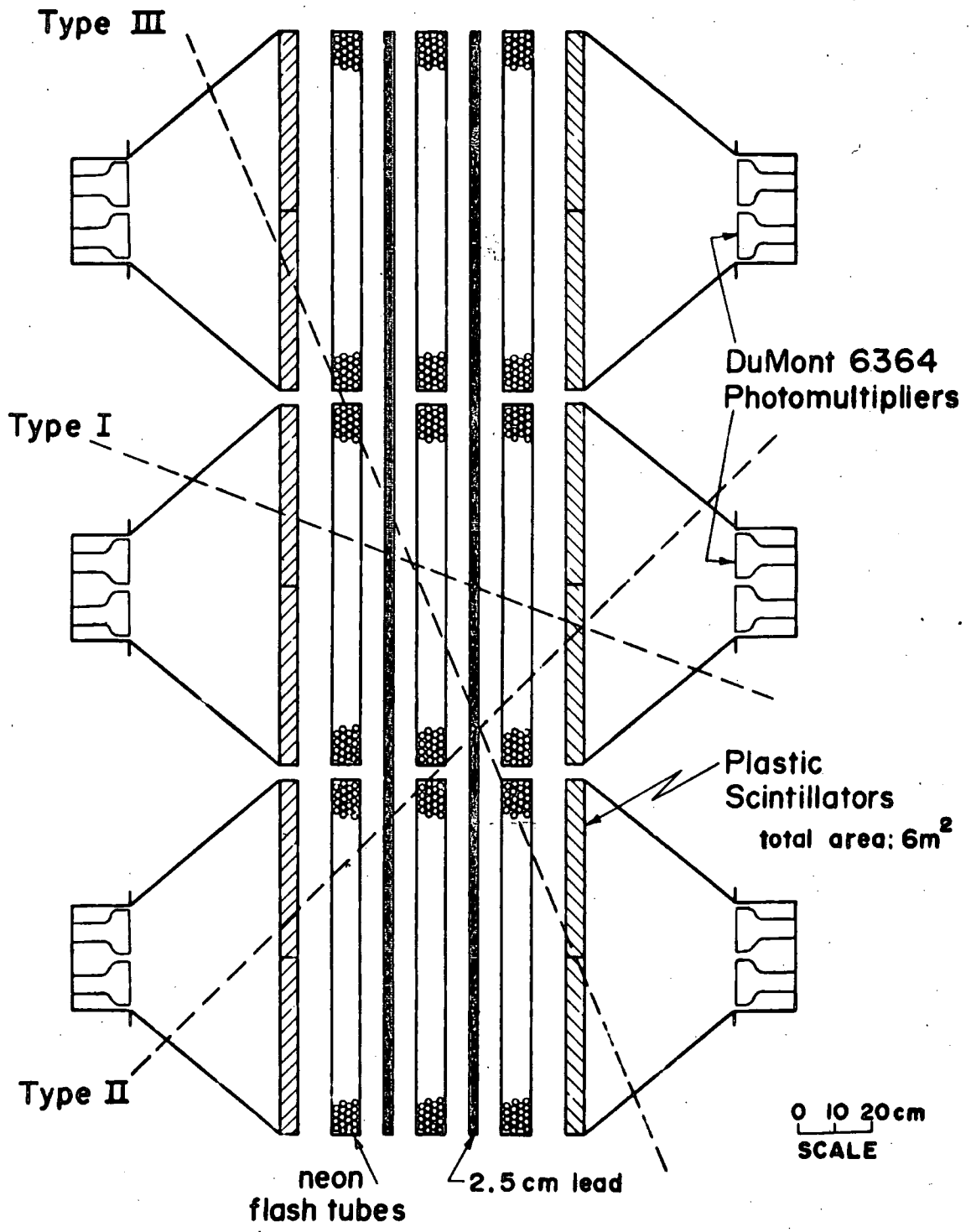

Figure 3.6

sufficed to cover one wall, so that nine trays were used in each telescope to erect three flash tube arrays between the scintillator walls. A 2.5 cm thick lead absorbing wall was placed between each adjacent flash tube array, making a total absorber thickness of 5 cm.

The passage of a particle through both scintillator walls of a telescope was registered by a fourfold coincidence between a pair of photomultipliers on one wall and any pair on the other. A block diagram of the circuitry used is shown in figure 3.7. The two pulses from adjacent photomultipliers were added and delayed and fed to the Y plates of an oscilloscope, the pulses from the six pairs of photomultipliers on one wall going to the same oscilloscope. When a fourfold coincidence occurred the oscilloscopes' sweeps were triggered and the added pulses appeared, the amount of the delay indicating the corresponding scintillator element. The four oscilloscopes, one for each wall, were viewed by a single open shutter camera. After a delay of 30 μs, which allowed the oscilloscopes to complete their sweeps, a high voltage pulse was applied to the centre electrodes of the flash tube trays of both telescopes. Two open-shutter cameras viewed the neon flash tubes of each telescope and recorded the flashes resulting from the passage of an ionising particle through the arrays. The master pulse gate was closed for 12 seconds after each fourfold coincidence making both telescopes insensitive while a cycling system operated. This cycling system initiated the advance of the

Figure 3.7

Block Diagram of Scintillator Circuitry for Telescopes 1 and 2

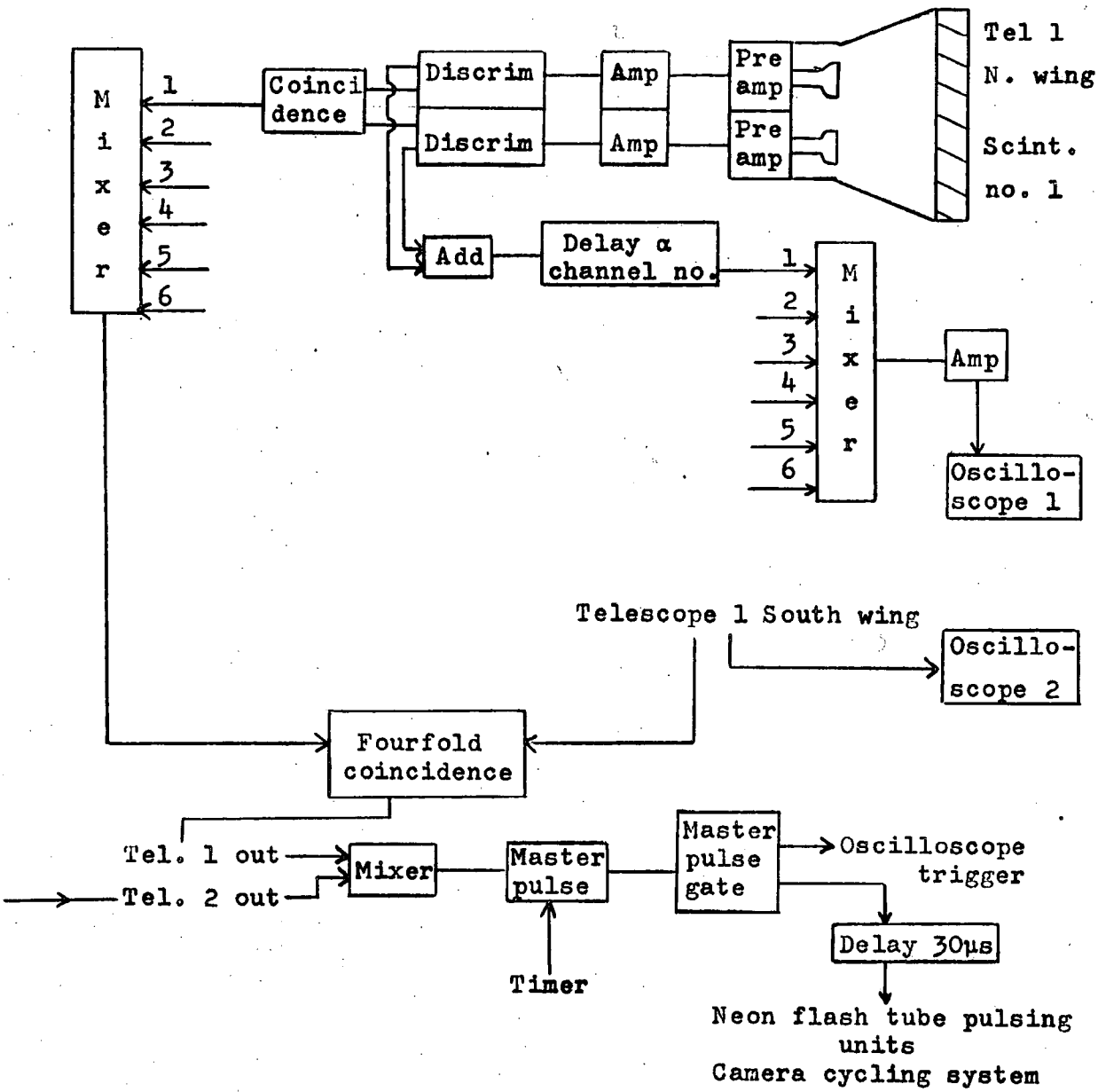

film in all the cameras and triggered the illumination of clocks and fiducial lights which marked the flash tube positions.

The neon flash tubes, filled to 60 cm Hg pressure with a mixture of 98% neon and 2% argon, were fired by a field of approximately 4 kV/cm applied 30 μs after the passage of an ionising particle. The column efficiency was observed on surface to be in the region 75 - 80%, making the probability that two or more tubes would fire per tray greater than 92% even for a perpendicular traversal. In general particle traversals were not perpendicular to the broad face of the tray and the tray efficiency when in use underground (gauged as the probability that two or more flashes per tray would define a particle track) was close to 100%.

The angle made by the camera lens with the axis of any flash tube in its field of view was kept to a minimum, usually less than 7° and never greater than 10°. By using 35 mm Ilford HPS film (800 a.s.a.) and optimum development conditions, the reduction of light emission at 10° by a factor of five from that at 0° could be tolerated.

The flash tubes were triggered by the discharge of a 0.04 μF condenser at about 13 kV on to the central aluminium electrodes of not more than four trays. This was initiated by the master pulse, which after amplification drove the grid of a high voltage thyratron (XH 16-200) positive, causing the completion of the discharge circuit. The high voltage condenser was charged by a conventional U.H.T. supply giving a rectified 13 kV, the charging time being

about one minute.

As a check on the stability of the photomultipliers and coincidence circuits the twofold coincidences from each pair of photomultipliers were monitored by a counter and printing register. The 24 channels were monitored in turn for approximately 9 min each, after which the mixed twofold coincidence outputs from each of the four scintillator walls were similarly counted. The recording cycle was terminated by a timer pulse triggering the master pulse circuit. The cycling system, initiated by the master pulse, wound on the camera films preventing fogging by an overlong open-shutter exposure. The monitoring system is shown in figure 3.8. The printed record of the rates was inspected daily for any unusual fluctuations as a check on the system stability.

Following the initial results from the first two telescopes, it was decided to build three telescopes of a more sophisticated design. They were primarily planned to increase the total detecting area at the experimental site, but interest was also centered on the simultaneous detection of two penetrating particles travelling close to the horizontal, as had been observed in event number four. If the particle tracks could be completely defined, and any common origin within the surrounding rock wall fixed unambiguously, it would enable the distinction to be made between pions and muons traversing the telescope, and would throw light on the type of neutrino interaction giving rise to the observed event.

As a result of these considerations telescopes numbers

Figure 3.8

Block Diagram of Monitoring System.

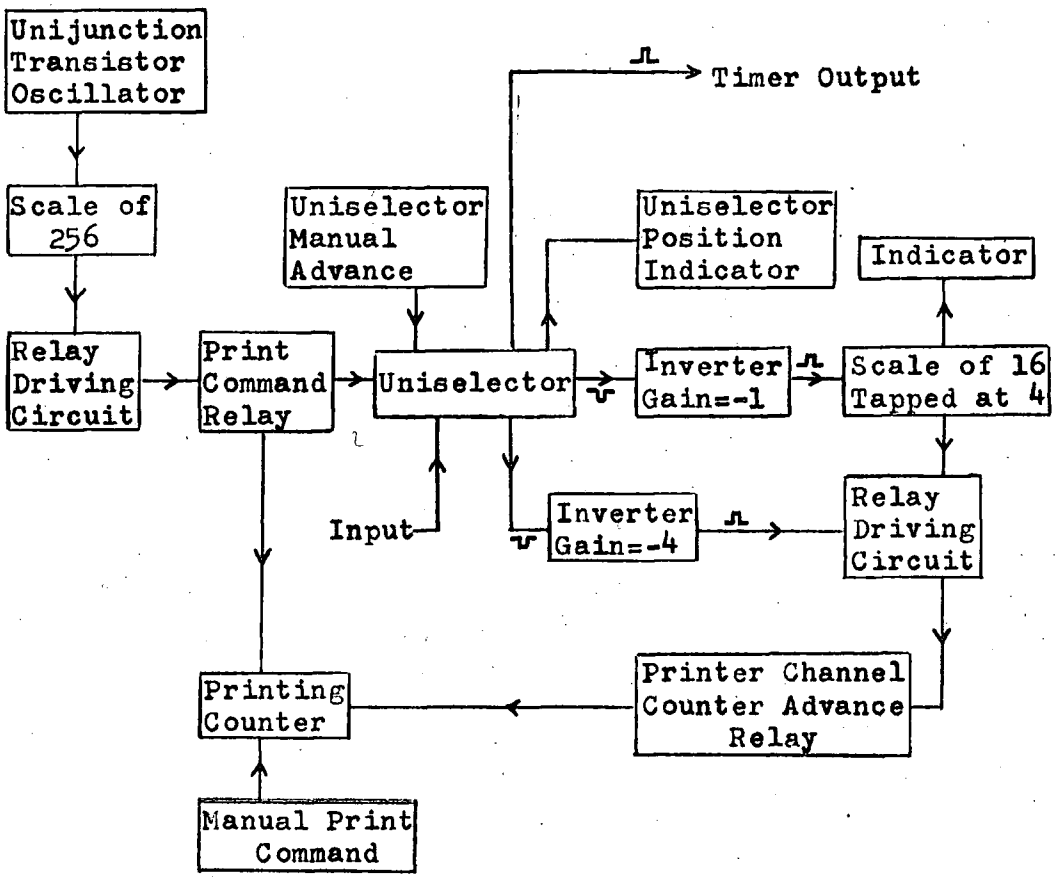

Input: 24 channels containing twofold outputs of each scintillator element, plus 4 channels containing the mixed twofold coincidence outputs of the 4 wings.

3, 4 and 5 were built in early 1966. Identical in construction, they contained three flash tube arrays as in telescopes 1 and 2 as well as two further arrays sited with the flash tubes in a vertical position; the crossed system giving complete definition of the paths of any penetrating particles. Four layers of iron, each 7.5 cm thick, were interposed between arrays to give a total thickness of absorber of 30 cm of iron (equivalent to 2.1 interaction lengths for perpendicular traversals) to aid the distinction between pions and muons. Separated by 130 cm, the scintillator walls were each 2 m square and were made up of four scintillator elements each viewed by two five inch photomultipliers. A diagrammatic representation of one of the telescopes is given in figure 3.9. Telescopes 4 and 5 were positioned with a back to back separation of 30 cm to increase the aperture for a muon to pass through a scintillator wall and then through the opposite wall of the adjacent telescope. The combination was treated as a single telescope for coincidence requirements. The disposition of the five telescopes is shown in figure 3.10. The coincidence and monitoring circuitry was similar in design to that for telescopes 1 and 2. Six oscilloscopes viewed by one camera recorded the display pulses from the mixed twofold outputs.

The neon flash tubes in each telescope were viewed through a mirror system by a single camera linked to the cycling system driven by the master pulse gate circuit. As with telescopes 1 and 2, regular checks were made on the flash tube efficiency by

Telescopes 3,4 & 5.

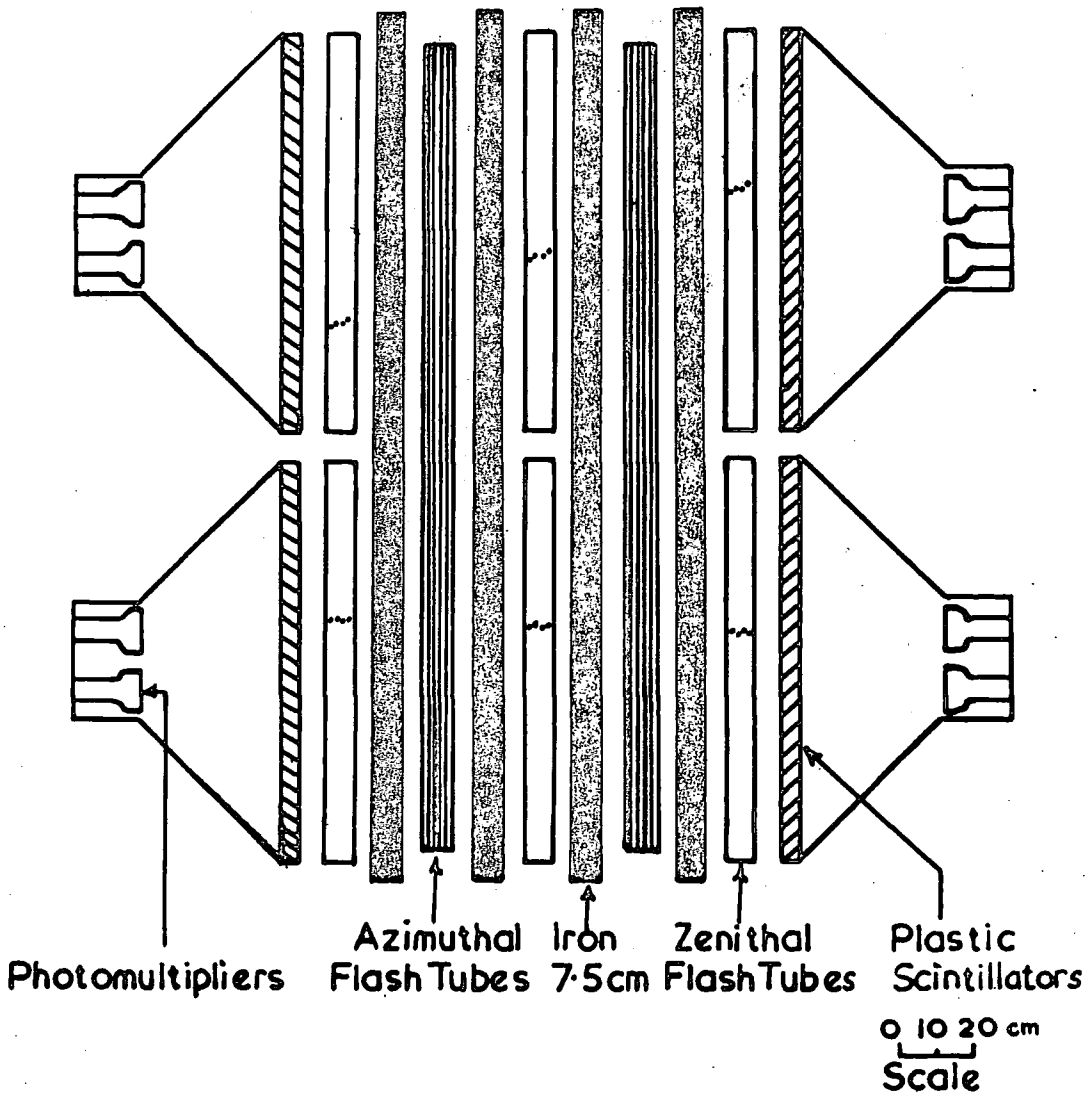

Figure 3.9

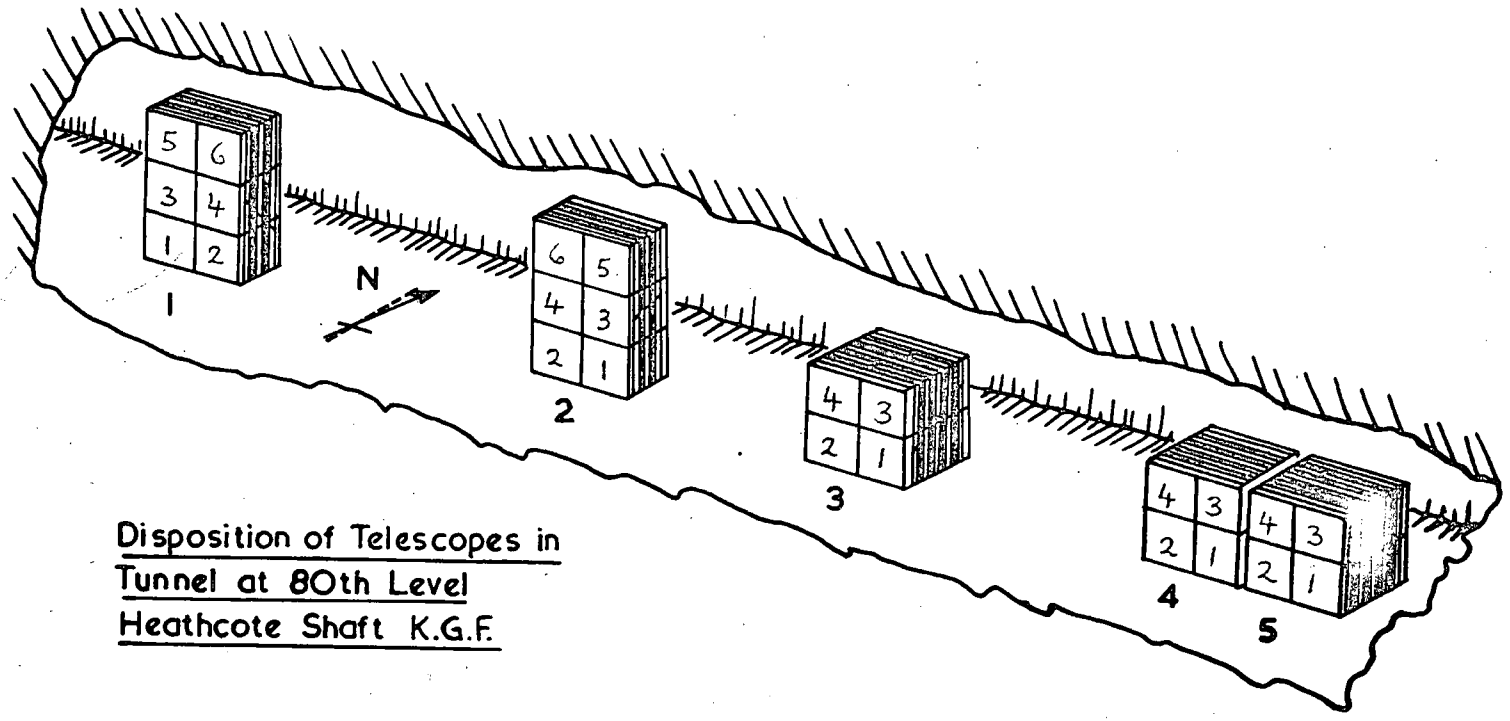

Disposition of Telescopes in Tunnel at 80th Level Heathcote Shaft K.G.F.

Figure 3.10

tests using a 1 millicurie Co^{60} radioactive source and by an analysis of the spurious flashes in each tray on frames triggered by the timing circuit. A full account of the determination of pre-amplifier and amplifier gains and biases by pilot experiments at 824 m.w.e. and 7500 m.w.e., the day to day running of the five telescopes and the checking methods used is given by Narasimham (1967).

3.3.2 The Experimental Results

Telescopes 1 and 2 became operational in the Spring of 1965. The results presented here are from 1st. April 1965 until 1st. June 1967. During this time telescopes 1 and 2 ran for a total of 24273 telescope-hours and recorded 40 events, not all of which were due to a muon traversing a telescope. Telescopes 3, 4 and 5 commenced running approximately a year later and until 1st. June 1967 had logged 22510 telescope-hours between them, registering 6 events. A complete table of events, with comments, is given in appendix A. Events were displayed on analysis sheets which gave the complete data for each event. A typical shower of electrons coming from a lead layer is shown by event 14 and a single knock-on electron from a lead layer by event 20. (Figures 3.11 and 3.12). In some cases a fourfold coincidence was triggered by the soft component, (which was generated in the rock wall by a muon), depositing energy in one or more scintillator elements. If the muon did not pass through the acceptance of the

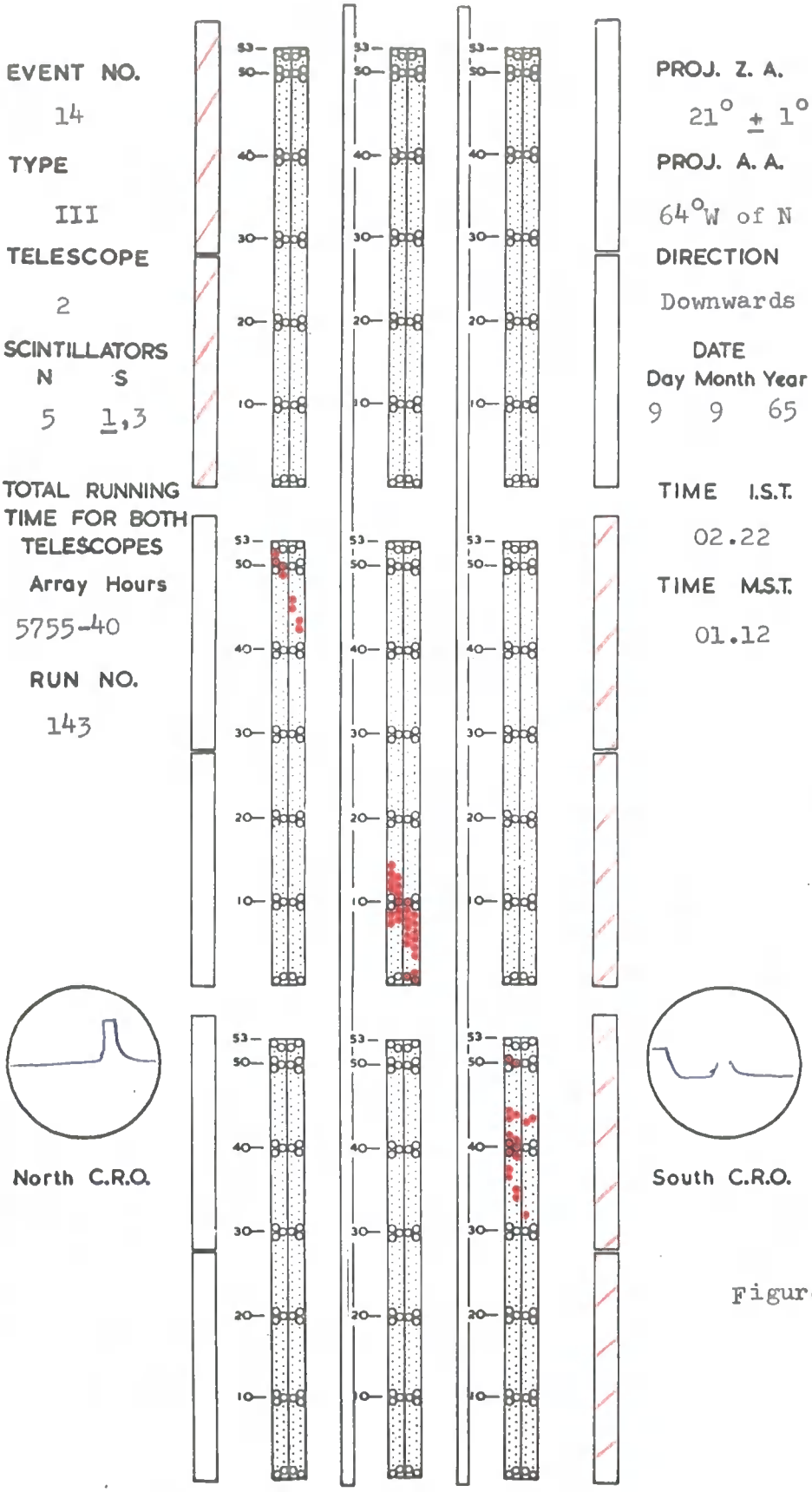
EVENT NO.
14
TYPE
III
TELESCOPE
2
SCINTILLATORS
N S
5 1,3
TOTAL RUNNING TIME FOR BOTH TELESCOPES
Array Hours
5755-40
RUN NO.
143
PROJ. Z. A.
21° ± 1°
PROJ. A. A.
64°W of N to 30°E of N
DIRECTION
Downwards
DATE
Day Month Year
9 9 65
TIME I.S.T.
02.22
TIME M.S.T.
01.12
North C.R.O.
South C.R.O.
N
S

Figure 3.11

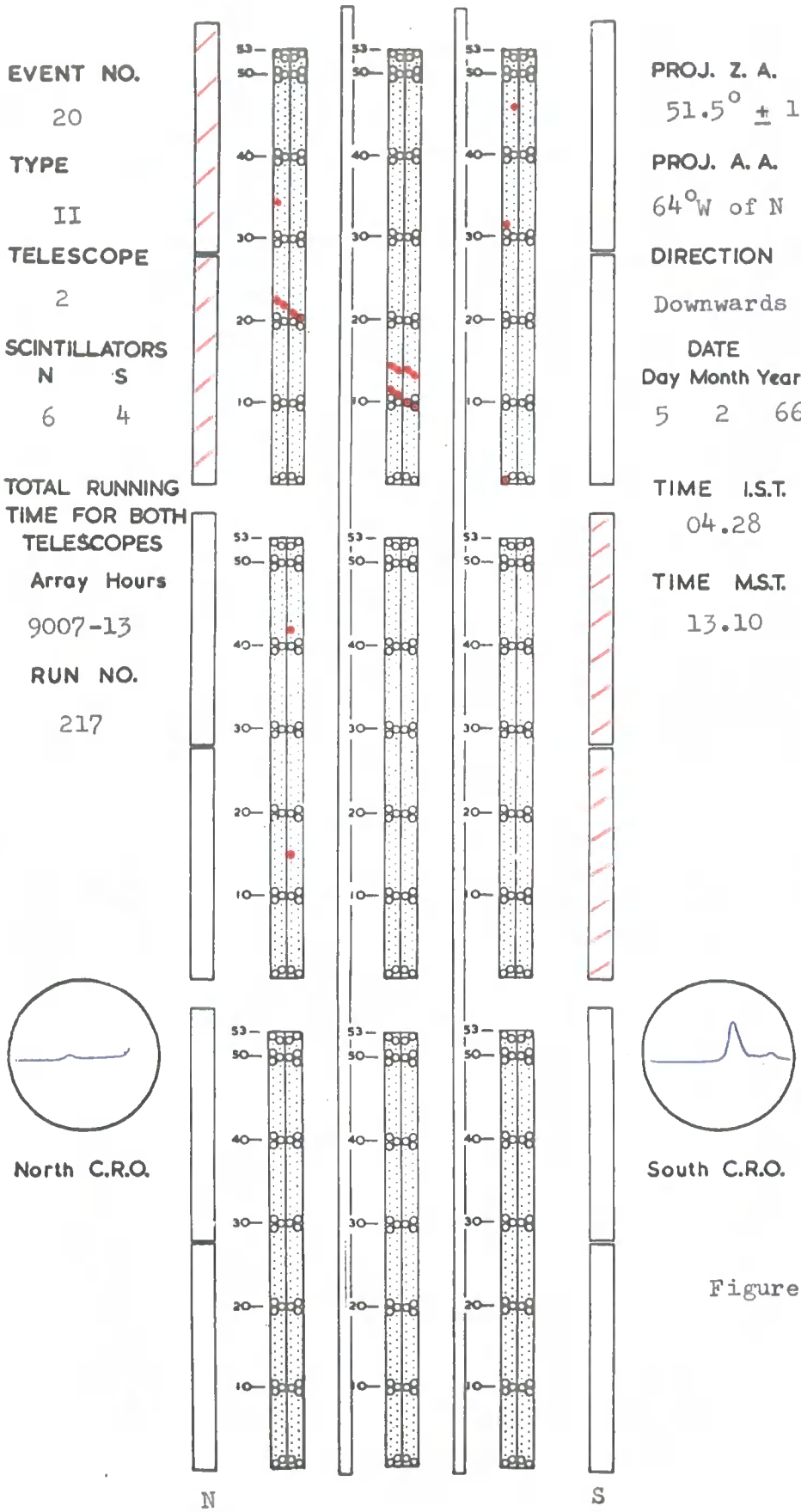
EVENT NO.
20
TYPE
II
TELESCOPE
2
SCINTILLATORS
N S
6 4
TOTAL RUNNING TIME FOR BOTH TELESCOPES
Array Hours
9007-13
RUN NO.
217
PROJ. Z. A.
51.5° ± 1°
PROJ. A. A.
64°W of N to 30°E of N
DIRECTION
Downwards
DATE
Day Month Year
5 2 66
TIME I.S.T.
04.28
TIME M.S.T.
13.10
North C.R.O.
South C.R.O.
N
S

Figure 3.12

telescope, defined by the scintillator geometry, it was termed an out of geometry (OG) event. Several large electromagnetic showers were observed with no associated penetrating particle, these are discussed in section 5.8.

3.4 Analysis of the Electromagnetic Interactions

The discussion in section 3.2.2 showed that the results of the TIFR-Durham experiment were reasonably well understood in qualitative terms. However, a glance at the table of events in appendix A reveals that the degree of accompaniment observed at a depth of 7500 m.w.e. is considerably greater than that recorded at shallower depths. With identical experimental configurations there should be a direct correlation between the degree of electromagnetic accompaniment and the mean energy of the muons and it is possible, in theory, to give an estimate of the mean muon energy of the events observed at 7500 m.w.e.

Unfortunately no work with an identical experimental arrangement has been performed where both the muon energy and the degree of accompaniment were known, but the work of Said (1966) with the Durham horizontal spectrograph allows a comparison to be made. Cosmic ray muons, with an energy known up to about 1000 GeV, produced electron showers, single knock-on electrons and δ-rays within a 60 cm thick iron magnet and an eight layer neon flash tube tray. His results are displayed as percentage probabilities for the three types of accompaniment in figure 3.13.

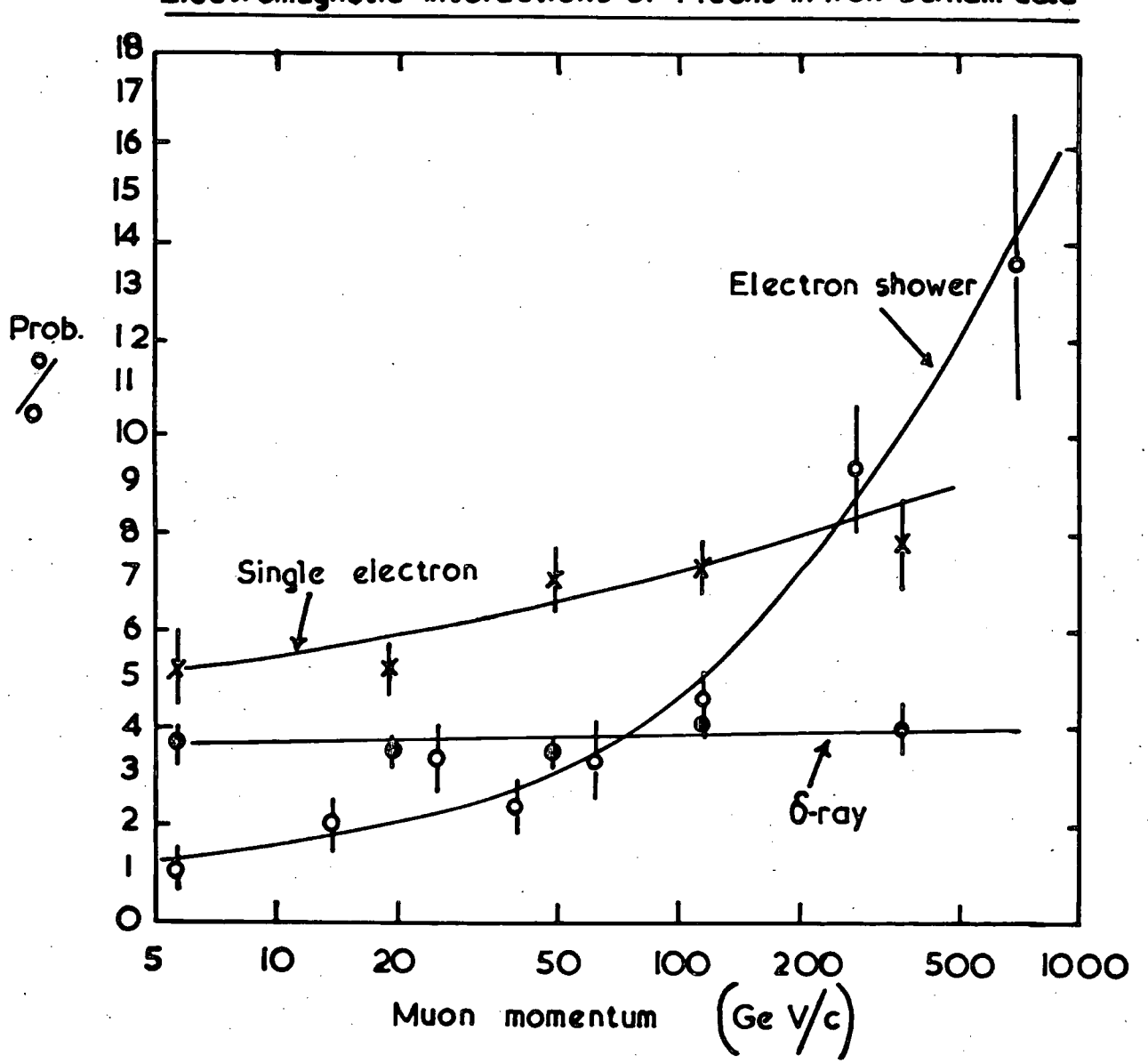
Electromagnetic Interactions of Muons in Iron Durham-data
Prob. %
Electron shower
Single electron
δ-ray
Muon momentum (Ge V/c)
0
1
2
3
4
5
6
7
8
9
10
11
12
13
14
15
16
17
18
5
10
20
50
100
200
500
1000

Figure 3.13

The steeply rising contribution to the total rate from shower production is mainly due to the increasing contribution from direct electron pair production.

A more detailed analysis was made of the shower events to divide them into three size categories: those with

i) less than 25

ii) greater than 25 and less than 50

iii) greater than 50

flashes in the first four layers of neon flash tubes, corresponding to small, medium and large electron showers. A value, n, was ascribed to each of the sizes which roughly corresponded to the minimum number of electrons necessary to cause a shower of that size to be observed. The values of n were 2, 4 and 8 for the three shower sizes. The showers in each energy range were examined and the mean value, $\bar{n}$, found. As expected, the mean values increased from 2 at the lowest energies to about three at the highest energies where the medium and large showers made an appreciable contribution.

A function, R, was defined such that:

$$R(E) = 1 + 0.7f_1(E) + f_2(E) + \bar{n}(E)f_3(E) \qquad 3.4.1$$

where $f_1(E)$, $f_2(E)$ and $f_3(E)$ were the probabilities of the three types of accompaniment, δ-rays, single knock-on electrons and electron showers, and were a function of the muon energy. The value of 0.7 was given to δ-rays, since in general they travelled only 2 to 3 flash tube

diameters within the neon flash tube trays. Single knock-on electrons had an effective value of unity.

The function R(E) provides a good measure for the degree of accompaniment within the Durham spectrograph, but has to be modified for it to be applicable to the TIFR-Durham and KGF neutrino experiments. The modification for the shorter path length within the neon flash tube tray (four layers compared with eight), effective in δ-ray production, is easily made and if it is assumed that the single knock-on and shower production in a material at any given energy is proportional to the rate of energy loss of muons at that energy, then the relative contributions from iron and lead can be estimated assuming an infinitely thick absorber. The main difficulty is in estimating the effective thickness of absorber contributing to the observed accompaniment as a function of the muon energy. Clearly at low energies only the last few millimetres of absorber will be effective, but as the energy increases more absorber is brought into play, and the whole thickness is eventually contributing to the rate, a situation that will occur at a lower energy in the 5 cm lead absorber than in the 60 cm thick iron magnet.

Some help in this problem is given by figure 3.5. The shower probability rises with increasing projected zenith angle and flattens at high energies to a plateau. Two effects cause this; the rising mean muon energy and the increased path length taken through the absorber by the muon. At a depth of about

2000 m.w.e. the mean energy is not increasing quickly with depth, the difference in expected mean muon energy between those arriving from the vertical direction and from an angle of about 35° where the plateau starts is less than 10%. A comparison of the total shower probability (3.6%) which is the value at the median projected zenith angle of 15° and the probability at 35° (5.0%), shows an increase by a factor of 1.4. This is some indication of the increase with path length through the absorber and the figure is supported by a similar result from an analysis of the data at 816 m.w.e. of both single knock-on electrons and showers. In the limit, the correction factor will be the ratio of the amount of matter in $g.cm^{-2}$ in the two absorbers, a value of 8.3, but the muon energy necessary to reach this limit would be very high, and a considerable allowance should be made for the re-absorption of showers within the absorber.

An alternative approach at low energies is to establish a definite level of muon accompaniment for a lead absorber at a fixed energy. Lloyd and Wolfendale (1959) give a figure of 9.5% for the total number of electrons emerging from a 1 cm lead plate, at a muon energy of 10 GeV. If this figure is multiplied by the fractional increase or decrease in energy loss in lead for a given energy, the total accompaniment at low energies can be estimated.

From the considerations given above the expected values of R at different energies were evaluated for the configuration used in the TIFR-Durham experiment, and are plotted in figure 3.14.

Figure 3.14

The Variation of R with Muon Energy.

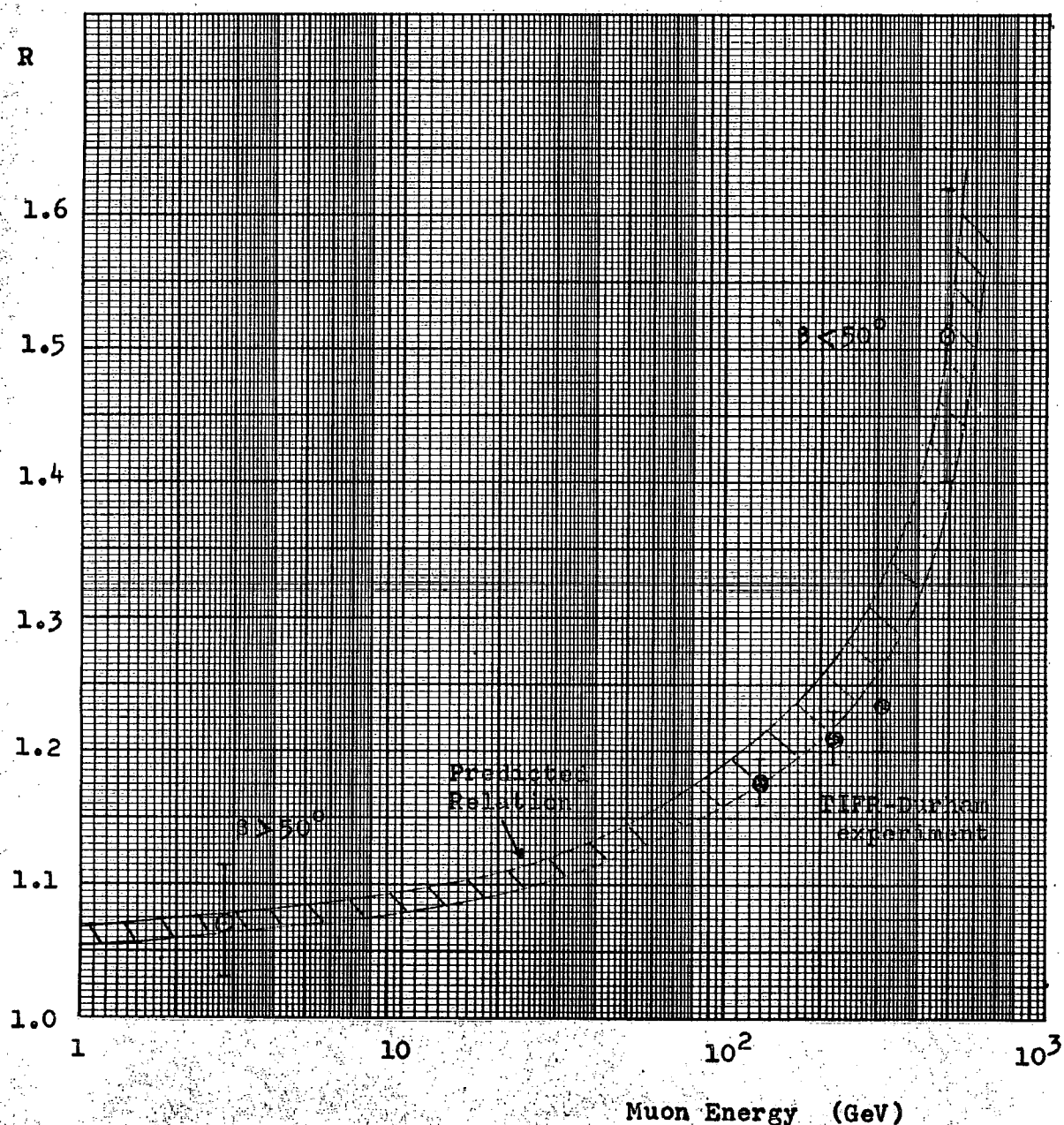

The large error on these values, especially at high energies, is reflected by the shaded area and it is emphasised that this calculation was of necessity very approximate.

The value of R was calculated for the depths of 816 m.w.e. and 1812 m.w.e. from equation 3.4.1, by substituting the total observed probabilities for the three types of accompaniment observed below the lead layer, and a value of $\bar{n}$ derived from Said's shower data at the mean muon energy for the two depths. For the greatest depth, 4100 m.w.e., all the events were analysed. The showers were divided into small, medium and large categories and the value of $\bar{n}$ found. The agreement between the points at the three depths, plotted at the relevant mean muon energies, and the expected value of R is reasonable.

At the depth of the KGF neutrino experiment the residual atmospheric muons are expected to have a projected zenith angle of less than about 50°, whilst the neutrino-induced muons will be peaked at an angle of 90°. For this reason the analysis of the electromagnetic accompaniment is divided into two categories, those events above and below a projected zenith angle of 50°. The events at low angles have a mean angle of about 35°, as can be seen from figure 4.5, and at this angle the path length through the 2.5 cm thick lead layer will be approximately 5 cm, a thickness equivalent to that used in the analysis given above. However, the path length through the four layers of flash tubes will be increased, giving an increased probability for δ-ray production,

and a larger number of flashes observed for a shower of given energy content.

Each event with a projected zenith angle (p.z.a.) of less than 50° was examined for interactions within the first and second lead layers, and for δ-rays within the second and third neon flash tube arrays. After a reduction for the increased path length of the muons through the trays the mean value of R, plotted in figure 3.14, was calculated.

Events with a p.z.a. greater than 50° show few or no electromagnetic interactions and the thickness of the absorber is therefore relatively unimportant. Events in this category were considered from all five telescopes and the value of R calculated in each case. The mean value of R is plotted in figure 3.14 at the energy for which it best fits the 'theoretical' curve.

Before any conclusions can be drawn from these results it is necessary to examine the derivation and variation of the mean muon energies to be expected at various depths underground.

3.5 The Mean Muon Energy Underground

A full discussion of this subject has been given by Craig et al. (1967). At energies less than about 1000 GeV the sea level muon spectrum has been accurately obtained from spectrograph measurements. By adopting a particular range-energy relation for muons in rock the mean muon energy at shallow depths can be calculated quite accurately. At energies above 1000 GeV the sea

level muon spectrum has to be estimated either from an assumed primary cosmic ray spectrum and a mode of propagation in the atmosphere, or from the measured underground depth-intensity relation by using the adopted range-energy curve with allowances made for fluctuations in the range of muons of given energy. A discussion of fluctuations in energy loss is given in section 4.2.5.

Craig et al. considered four different sea level spectra, two derived from the primary spectrum, and two from the underground depth-intensity relationship. At 7500 m.w.e. they obtained mean muon energies ranging from 286 to 393 GeV. The highest value came from an assumption that the angular distribution of atmospheric muons underground followed the relation:

$$I_\theta = I_o \cos^n \theta$$

where I_θ and I_o are the muon intensities at zero and θ degrees, spatial zenith angle, and n is an exponent that varies with depth. At 7500 m.w.e. they took n = 8. In fact, the events recorded in the KGF experiment are peaked at a p.z.a. of 35°, corresponding to a depth of the order of 10,000 m.w.e. The expected mean muon energy of the events is thus greater than 393 GeV, and on calculation proves to be 490 GeV. (E.C.M. Young: private communication.)

At shallower depths the uncertainties are less, and following the treatments of Hayman et al. (1963) and Osborne et al. (1964) for the range-energy relation and sea level muon spectrum respectively, the expected mean muon energies for the

three depths of observation in the TIFR-Durham experiment are approximately 130, 220 and 310 GeV.

3.6 Conclusions

As explained in section 3.2.2 the results of the TIFR-Durham experiment are fairly well understood in qualitative terms. The analysis given in section 3.4 shows that if a mean muon energy is assigned to the muon flux at various depths the results are in quantitative agreement with other experiments giving results on muon accompaniment.

The events recorded in the KGF neutrino experiment, when classified on the degree of accompaniment alone, fall into two classes. These classes coincide with events having projected zenith angles above and below approximately 50°, which indicates that they probably are, respectively, neutrino and atmospheric induced muon events. From a comparison with the accompaniment probabilities predicted by other experiments it is evident that the atmospheric muons have a high mean energy consistent with the predictions of Craig et al. (1967) for a muon intensity that falls as D^{-9} (where D is the depth below ground level) for depths greater than about 7500 m.w.e. The results appear to be inconsistent with a mean energy of 287 GeV predicted by them for an exponential depth-intensity relation below this depth, especially since the figure of 287 GeV is expected to be invariant at greater depths.

The neutrino-induced muons appear, on the basis of their

apparent electromagnetic interactions, to have a very low median energy, which is between threshold and about 30 GeV. However, conclusions based on this method of analysis must be regarded as tentative, although it will be shown later that they are consistent with other data from the KGF neutrino experiment.

Chapter 4

THE INTENSITY OF ATMOSPHERIC MUONS UNDERGROUND

4.1 Introduction

In this chapter the mechanisms responsible for the loss of energy of relativistic muons are considered and it is shown that theory and experiment are in good agreement down to depths of the order of 1500 m.w.e. whether the absorber be rock or water. Below this depth it is suggested that comparable experiments performed under the two types of absorber could help to determine the degree and character of the energy loss mechanisms that dominate at high energies, where there is a difference of theoretical opinion.

An examination is made of the results from the KGF experiment to give the vertical muon intensity at 7500 m.w.e. and this figure is combined with those of recent workers to obtain a best estimate depth-intensity curve in the region below 4000 m.w.e.

Finally there is a discussion of the relationship between the vertical intensity of muons at various depths and their distribution in zenith angle.

4.2 The Energy Loss Mechanisms for Relativistic Muons

It is known that relativistic muons lose energy through collision, pair production, bremsstrahlung and nuclear interactions. A theoretical evaluation of these losses enables a muon range-energy relation to be calculated for a given medium. When the effect of fluctuations in the energy loss has been added to the range-energy relation, the relation can be applied to experimental observations of muons at various depths under various types of overburden and the sea level energy spectrum of muons can be estimated.

4.2.1 Collision Losses

A muon penetrating an absorber loses energy by inelastic collisions with atomic electrons causing excitation and ionisation of the atoms. This process was first studied by Bethe and Bloch in the early 1930s and it is now well understood.

The method of calculation of the average energy loss considers close and distant collisions separately. In a close collision an electron of high energy is ejected, the impact parameter is small and the atomic electrons are regarded as free. In distant collisions the muons are treated as point charges and the system formed by each atom and muon is examined using a knowledge of the probabilities of the allowed transitions leading to excitation or ionisation. This introduces the effective mean ionisation potential, I, which is taken as the minimum energy

transfer. I is approximately equal to 13Z eV where Z is the atomic number of the absorber. The exact value of I is usually found experimentally. The average rate of energy loss for distant collisions was given by Bethe (1932) and that for close collisions by Bhabha (1938) and Massey and Corben (1939). For a particle of $\frac{1}{2}$ spin the total rate of energy loss from the combined equations is:

$$-\left(\frac{dE}{dx}\right)_{coll} = \frac{2\pi NZmc^2}{A\beta^2} r_o^2 \left[\ln \frac{2m\beta^2c^2T}{(1-\beta^2)I^2} - 2\beta^2 + \frac{1}{4}\left(\frac{T}{E+\mu c^2}\right)^2\right] \qquad 4.2.1$$

where A is the atomic weight of the medium, N is Avogadro's number and $r_o = e^2/mc^2$, the classical radius of the electron of mass m and charge e. T is the maximum energy transferred to the electron and is given by

$$T = \frac{E^2 - \mu^2c^4}{\mu c^2\left[\frac{\mu}{2m} + \frac{m}{2\mu} + \frac{E}{\mu c^2}\right]} \qquad 4.2.2$$

where E is the energy and μ the mass of the muon and dx is expressed in $g.cm^{-2}$.

The last term in equation 4.2.1 involves the spin of the muon and this contributes less than 1% to the energy loss at any muon energy. Since T approaches the value $E - \mu^2c^2/2m$ asymptotically with increasing energy, the energy loss depends mainly on the logarithmic term showing that the loss of relativistic particles increases logarithmically with momentum. The logarithmic form is

explained by the character of the relativistic deformation of the coulomb field of the incident muon which allows the muon to affect atoms at larger distances from its geometrical path. At energies from 1 to 100 GeV the main form of energy loss by a muon is through collision.

In the late 1930s it was realised that for distant collisions the atoms of the absorber close to the path of the muon screened the muon's electric field from the atoms further away, reducing the interaction and therefore decreasing the energy loss. Fermi (1940) was the first to treat this polarisation of the medium quantitatively by considering the electrons of the medium as having a single characteristic oscillation. Later other workers extended the treatment to consider the behaviour of the electrons belonging to the various atomic shells independently. In particular, Sternheimer (1952, 1956) gives a very full treatment. This reduction of the energy loss, known as the density effect, has been carefully studied experimentally and the results have been found to be in good agreement with the theoretical treatment of Sternheimer, who introduces a term $-\delta$ inside the square brackets in equation 3.2.1 such that:

$$\begin{aligned} \delta &= 4.606X + C + a(X_1 - X)^{m'} && X_o < X < X_1 \\ \delta &= 4.606X && X > X_1 \end{aligned} \qquad 4.2.3$$

where $X = \log_{10}(P/\mu c)$, with P the momentum of the muon and X_o, X_1, a, m' constants of the medium. C is defined by:

$$C = -2\ln(I/h\nu_p) - 1 \qquad 4.2.4$$

where $\nu_p = \left(\frac{N\rho Ze^2}{m\pi A}\right)^{\frac{1}{2}}$ the plasma frequency of the medium, with ρ the density of the absorber and h Planck's constant.

Constants for many media derived from theoretical treatments are given by Sternheimer (1956) and it is these figures which are taken for the calculations in section 4.3.

With this reduction in energy loss the most probable loss tends towards a constant level, with increasing energy, known as the Fermi plateau. In the early 1950s several theoreticians pointed out that part of the energy dissipated by high energy muons will appear as Cerenkov radiation and that most of the increase in loss above the ionisation minimum, where the logarithmic increase becomes dominant, should appear as Cerenkov radiation. This prediction has not yet been fully verified.

Including the $-\delta$ term in the expression 4.2.1 results in an equation which has been found to accurately represent the energy loss of muons through collision to an energy where other forms of loss, mentioned later, become dominant. A second order radiative supression effect suggested by Zhdanov et al. (1963) which introduces a further negative term into equation 4.2.1 has not found general acceptance amongst theoreticians, and confirmatory experimental evidence is ambiguous. If included it roughly negates the relativistic logarithmic rise, introducing an error of about 10% at an energy of 20 GeV which decreases with increasing energy.

4.2.2 Direct Pair Production Losses

When passing through a nuclear coulomb field a high energy muon may lose energy by the creation of an electron pair. This effect has been studied since the mid 1930s when Bhabha and Racah, working independently, made theoretical predictions that differed by a factor of two. The process is known to be almost independent of the spin and magnetic moment of the particle, but the effect of screening introduces uncertainties into the predictions. A treatment by Mando and Ronchi (1952), based on the work by Racah, gives:

$$-\frac{dE}{dx}_p = \frac{Nm(\alpha Z r_0)^2}{A\mu\pi} E\left[19.3 \ln\left(\frac{E}{\mu c^2}\right) - 53.7\right] \qquad 4.2.5$$

with $\alpha = 1/137$, the fine structure constant. The factor by which the energy loss is reduced by the screening effect of the atomic electrons is:

$$f = \left[\frac{16}{9}\ln(183Z^{-1/3}) + 1\right]\left[\frac{16}{9}\ln\left(\frac{E}{\mu c^2}\right) - \frac{14}{9} + \ln 2\right]^{-1} \qquad 4.2.6$$

The energy lost by pair production is given by multiplying equations 4.2.5 by 4.2.6 for E greater than 30 GeV and by writing f=1 for E less than 30 GeV. The contribution from pair production is significant at energies above 500 GeV and the energy loss is approximated by :

$$-\frac{dE}{dx} = 1.6 \times 10^{-6} E \quad \text{MeV.g}^{-1}\text{.cm}^2$$

at very high energies for standard rock with Z=11, A=22 and ρ=2.65 g.cm^{-3}. Hayman et al.

(1963) adopted the treatment of Mando and Ronchi and their results are shown in table 4.1.

Recently, Erlykin (1965) made a reassessment of the energy losses of muons by pair production and bremsstrahlung. Using the cross-sections given by Ternovski (1959), who took into account the asymmetric energy distribution between pair components more accurately than before, Erlykin obtained energy loss values from 10 to 10^4 GeV, some of which are shown below.

Table 4.1 Values of $b_p \times 10^6$ ($g^{-1}cm^2$) for Standard Rock

Energy (GeV)	Castagnoli et al.	Hayman et al.	Erlykin
10^2	0.91	1.32	1.95
10^3	0.95	1.52	2.21
10^4	0.97	1.64	2.24

From these figures there is clearly a wide range of uncertainty in the value to be ascribed to b_p the pair production energy loss parameter, which is defined by:

$$-\frac{dE}{dx}_p = b_p E \ ,$$

an uncertainty caused both by the cross-section used and by the screening factor applied. Experimental observations underground on the production of electron pairs give weight to the theory of Mando and Ronchi, though the evidence is by no means conclusive.

4.2.3 Bremsstrahlung Losses

The acceleration or deceleration of a muon passing through the coulomb field of a nucleus or an electron results in the emission of electromagnetic radiation known as bremsstrahlung. The first accurate quantitative treatment of the process was made by Christy and Kusaka (1941) who allowed for the finite size of the nucleus, but not for the effect of electron screening. It was shown by Rossi (1952) that screening is effective for energies above E_o where

$$E_o = \frac{2\pi(\mu c^2)^2}{\alpha Z^{1/3} mc^2} v$$

v being the fraction of the energy lost by the muon in the collision.

If v is taken as $\frac{1}{2}$, the most effective region of energy transfer, then E_o = 4300 GeV for standard rock. For E less than E_o the average rate of energy loss by the Christy-Kusaka theory is:

$$-\frac{dE}{dx}_{brems} = 4\alpha N r_o^2 \cdot \frac{Z^2}{A} \left(\frac{m}{\mu}\right)^2 E \left[\ln \frac{12EZ^{-1/3}}{5\mu c^2} - \frac{1}{3}\right] \qquad 4.2.7$$

Many other workers have made theoretical studies of bremsstrahlung, in particular Rozental and Streltsov (1959), following the method of Bethe and Heitler (1934) in the region for complete screening, give:

$$-\frac{dE}{dx}_{brems} = 4\alpha N r_o^2 \cdot \frac{Z^2}{A} \left(\frac{m}{\mu}\right)^2 E \left[\ln \frac{\mu 183 Z^{-1/3}}{m} + \frac{1}{18}\right] \qquad 4.2.8$$

Erlykin considered a new nuclear form factor and arrived

at a value for the correction for the finite dimensions of the nucleus that was lower than that of Christy and Kusaka. He also took into account muon bremsstrahlung in the field of an electron, finding a higher energy loss than other workers through this mechanism. Bremsstrahlung and pair production are major contributors to the total rate of energy loss of a muon over the same range of energies. A comparison of values of b_b, the bremsstrahlung energy loss parameter, derived by different workers for standard rock is given in table 4.2.

Table 4.2 Values of $b_b \times 10^6$ ($g^{-1}cm^2$) for Standard Rock

Energy (GeV)	Castagnoli et al.	Hayman et al.	Erlykin
10^2	0.94	1.18	1.46
10^3	1.27	1.60	1.67
10^4	1.70	1.76	1.80

Castagnoli et al. (1964c) followed the work of Rozental and Streltsov throughout, whereas Hayman et al. adopted the Christy-Kusaka treatment at energies less than E_o and the Rozental-Streltsov treatment at higher energies, interpolating between them in the region of E_o.

The size-frequency distribution of bursts measured by Carmichael and Stelges (1957) has been shown by Gupta (1958) to be in good agreement with a refined form of the Christy-Kusaka

treatment. At CERN Backenstoss et al. (1961), who measured the spectral distribution of electron showers produced in iron by 8 GeV muons, found a result that supported the theory up to momentum transfers of about 0.3 GeV/c. From this it seems that the present experimental evidence at low energies is in closer agreement with the figures given by Hayman et al. than with those of other workers.

4.2.4 Nuclear Interaction Losses

A muon can undergo an inelastic collision with a nucleus by a discontinuous process that can be regarded as being between photons of the virtual photon cloud accompanying the muon, and the nucleus. The Williams-Weizacker method was first used on this problem by George and Evans (1950) who derived a relation for the virtual photon flux. The average rate of energy loss can then be expressed in terms of the photonuclear cross-section, if the latter remains constant with increasing energy, or if its form is known. An alternative expression for the virtual photon flux derived by Kessler and Kessler (1957) has found little support in experimental observations underground, using multiplate cloud chambers to observe nuclear interactions directly, and the semi-classical W-W method seems to be more acceptable. However, the photonuclear cross-section is known only roughly by experiment up to an energy of about 5 GeV and it may well increase at very high energies, if, as seems possible, the coupling between muon and nucleus becomes strong.

After a review of the experimental information Hayman et al. take a cross-section of $(2.6 \pm 0.3)\times10^{-28}$ cm^2/nucleon above 5 GeV from the experimental work of Higashi et al. (1962) giving:

$$-\frac{dE}{dx}_n = 7.3\times10^{-7}E \quad MeV.g^{-1}.cm^2 \qquad 4.2.9$$

Recently a new treatment by Kobayakawa (1966) using a general expression derived by Daiyasu et al. (1962) for the differential cross-section for a virtual photon being emitted by a muon and absorbed by a nucleus, combined with the assumption that the photonuclear cross-section is constant and equal to 0.72×10^{-28} cm^2/nucleon, gives a value :

$$-\frac{dE}{dx}_n = (2.86\text{-}3.20)\times10^{-7}E \quad MeV.g^{-1}.cm^2$$

The main difficulty in making an accurate theoretical treatment of nuclear interactions is the ignorance of the behaviour of the photonuclear cross-section at high energies and its absolute value at low energies.

4.2.5 Fluctuations in Energy Losses

The processes of ionisation, excitation and pair production are continuous since the muon loses energy in small amounts in frequent interactions with the atoms of the absorber, whereas the processes of bremsstrahlung and nuclear interaction are discontinuous, the muon losing a large fraction of its energy in a few widely spaced, near catastrophic impacts. Oda and Murayama (1965) have pointed out that the process of pair production may also be considered as discontinuous if the fractional energy lost is greater

than 0.05, but most theoretical analyses have not considered pair production in estimating the expected increase in intensity from fluctuations at great depths underground.

Menon and Ramana Murthy (1967) and Kobayakawa (1966) give tables of the correction ratio R, defined as $R = I_{nf}/I_f$, where I_{nf} is the underground intensity to be expected at various depths assuming that all energy losses are continuous. I_f is the expected intensity if the effect of fluctuations is taken into account, and it should equal the experimentally observed intensity. The value of R depends on the assumed exponent of the integral energy spectrum of muons incident on the Earth's surface. Table 4.3 indicates the range of estimates for R in standard rock, for an exponent of 3, made by various authors in recent years.

Table 4.3 Values for the Fluctuation Correction Factor R

Depth (km.w.e.)	Kobayakawa (1966)	Miyake et al. (1964b)	Osborne et al. (1967)
2	0.92	-	-
4	0.78	0.84	0.735
6	0.62	0.68	0.55
8	0.47	0.51	0.42
10	0.335	-	0.32

The agreement is moderate and the value of R for an exponent between 2.5 and 3.5 is probably known to an accuracy of

about 15% down to depths in the region of 8000 m.w.e.

4.3 The Comparison of Intensities under Sea Water and under Rock

In recent papers on underwater experiments, Higashi et al. (1965, 1966) pointed out that at depths shallower than 1000 m.w.e. there was a discrepancy between the experimentally determined intensities underwater and under rock. On conversion, their under water intensity measurements agreed well with the muon energy spectrum at sea level determined by the direct magnetic spectrograph measurements of Hayman and Wolfendale (1962), whereas the rock intensity measurements gave a sea level energy spectrum higher than that measured by Hayman and Wolfendale. This difference could be explained by a decrease in the mean densities of all the rock absorbers of about 10% over that assumed, or a decrease in the mean values of Z/A by a similar amount.

Their main point was that measurements under water allow the amount and nature of the absorber to be very accurately calculated, whilst measurements under rock are often limited by uncertainty in the geological nature of the overburden and by irregularities in the surface topography. Additionally, the measured intensities under rock could contain some soft component, the true muon intensities being approximately 10% lower than those measured. This contamination would not be as severe in water since the production of knock-on electrons is a function of Z^2/A.

The validity of these findings is examined in the subsequent

sections of this chapter.

4.3.1 Derivation of the Range-Energy Relation for Muons in Standard Rock and Sea Water

A re-examination of the figures of Higashi et al. was made by Creed and Wolfendale (1967). The problem of energy loss was reconsidered, and the range-energy relation calculated for sea water and standard rock ($Z^2/A = 5.5$) assuming three expressions for the total energy loss designated C, H and E.

The first, C, was based on the work of Castagnoli et al. (1964a, b, c and 1965a) who used the work of Sternheimer (1956) for collision losses, of Murota et al. (1956) for pair production losses and of Rozental and Streltsov (1959) for bremsstrahlung losses. They considered both the W-W and K-K treatments for nuclear interactions, concluding that the former was the most reliable theory, taking a value for the energy loss of:

$$-\frac{dE}{dx}_n = 1.05\times10^{-6}E \quad MeV.g^{-1}.cm^2$$

The second, H, was based on the work of Hayman et al. (1963). The collision losses were carefully re-examined using the data of Sternheimer given in equations 4.2.1 - 4.2.4. The analysis of Mando and Ronchi (equations 4.2.5 and 4.2.6) was used for pair production losses, whilst equations 4.2.7 to 4.2.9 were used for bremsstrahlung and nuclear interaction losses.

The final expression, E, was derived using the same figures as H for collision and nuclear interaction losses, and

followed the work of Erlykin (1965) for bremsstrahlung and pair production.

The details of the absorbers considered are listed in table 4.4.

Table 4.4 The Composition of Some Overburdens

Overburden	Z	A	Z/A	Z^2/A	Density ($g.cm^{-3}$)
Standard rock	11	22	0.5	5.5	2.65
K.G.F. rock	12.8	26.1	0.494	6.29	3.02
Mt. Blanc rock	10.3	20.9	0.494	5.11	2.6
Johannesburg rock	-	-	-	5.0	2.75
Sea water	7.433	14.79	0.553	3.76	1.027

The range of a muon of initial energy E is given by:

$$R(E) = R(E_o) + \int_{E_o}^{E} \left(\frac{dE}{dx}\right)_{tot}^{-1} dE \qquad 4.3.1$$

if the effect of fluctuations is ignored. It is convenient to take E_o = 1 GeV, at which energy the range $R(E_o)$ has been evaluated from the data of Sternheimer (1959) as 5.45 m.w.e. in rock of $Z^2/A = 5.5$. For sea water $R(E_o)$ is approximately 4.7 m.w.e.

The range-energy relations for muons in standard rock and sea water were obtained directly from equation 4.3.1 using energy loss expressions H and E. The relation using C was taken

directly from the figures of Castagnoli et al. (1965a), who calculated the range-energy curves for muons traversing pure water, Mt. Blanc rock and KGF rock, with an adjustment for the different values of Z/A (effective in collision losses), and Z^2/A (effective in bremsstrahlung and pair production losses), since the exact form of energy loss for each process was not clear from their publication. No account was taken of fluctuations, but in the initial consideration of muon intensities down to a depth of 1500 m.w.e. the intensity is affected by less than 2% through this omission. Figures 4.1 and 4.2 give the range-energy relations derived from E, H and C for standard rock and sea water.

4.3.2 The Sea Level Muon Energy Spectrum at Low Energies

It has been known for some time that discrepancies exist between muon intensity measurements underground that are outside the quoted statistical errors. These discrepancies arise from the difficulty in making absolute measurements, (often a normalisation procedure is necessary,) and from the assumed angular distribution of the muons, a knowledge of which is essential in calculating the vertical intensity. To obtain the precise rate of muons passing through a detector the geometrical acceptance must be accurately known, and to avoid counting the accompanying soft component a suitable thickness of absorber must be placed between two detecting planes.

An attempt was made by Hayman et al. (1963) to allow

Figure 4.1

Muon Range-Energy Relation for Standard Rock Assuming Three Forms of Energy Loss.

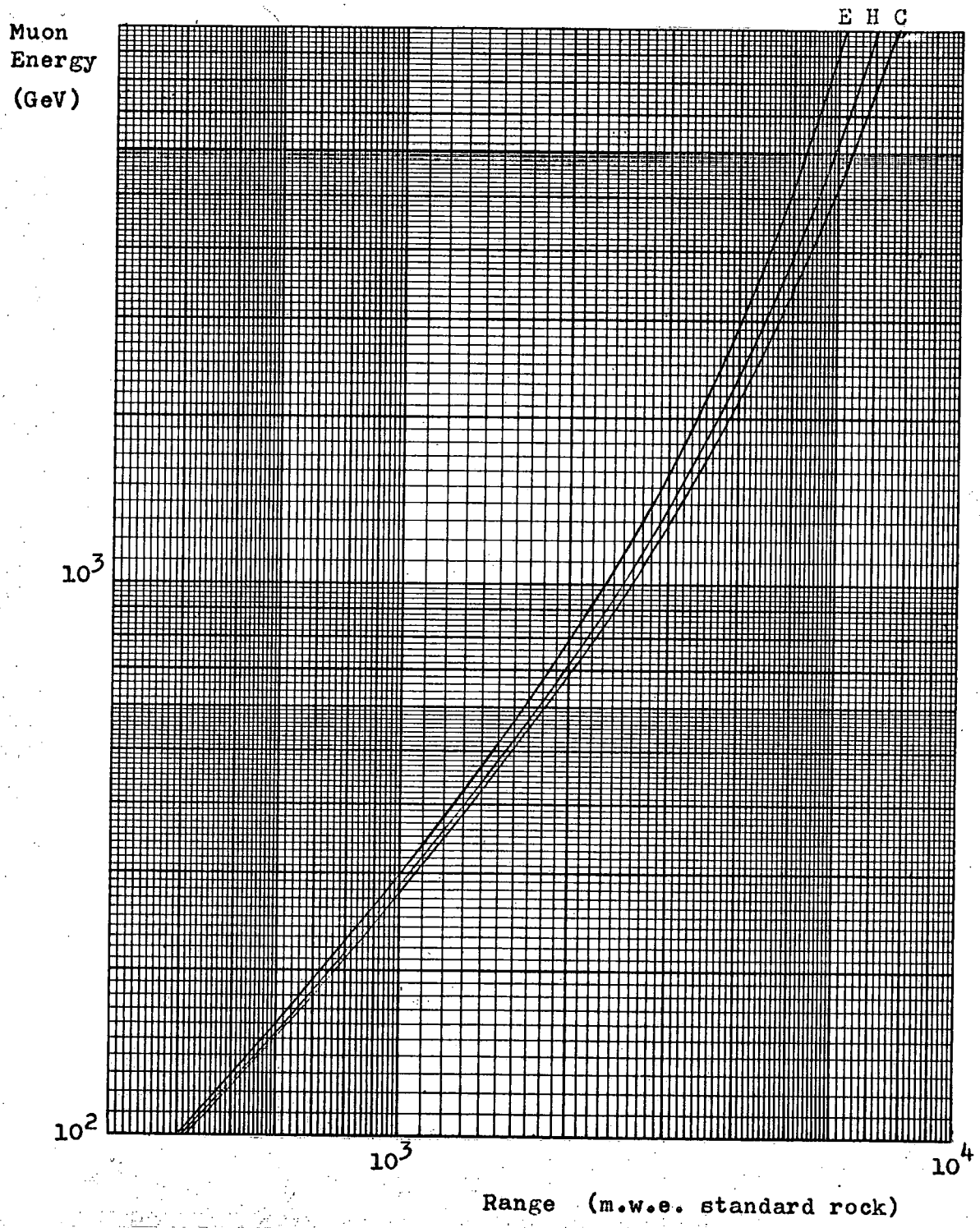

Figure 4.2

Muon Range-Energy Relation for Sea Water Assuming Three Forms of Energy Loss.

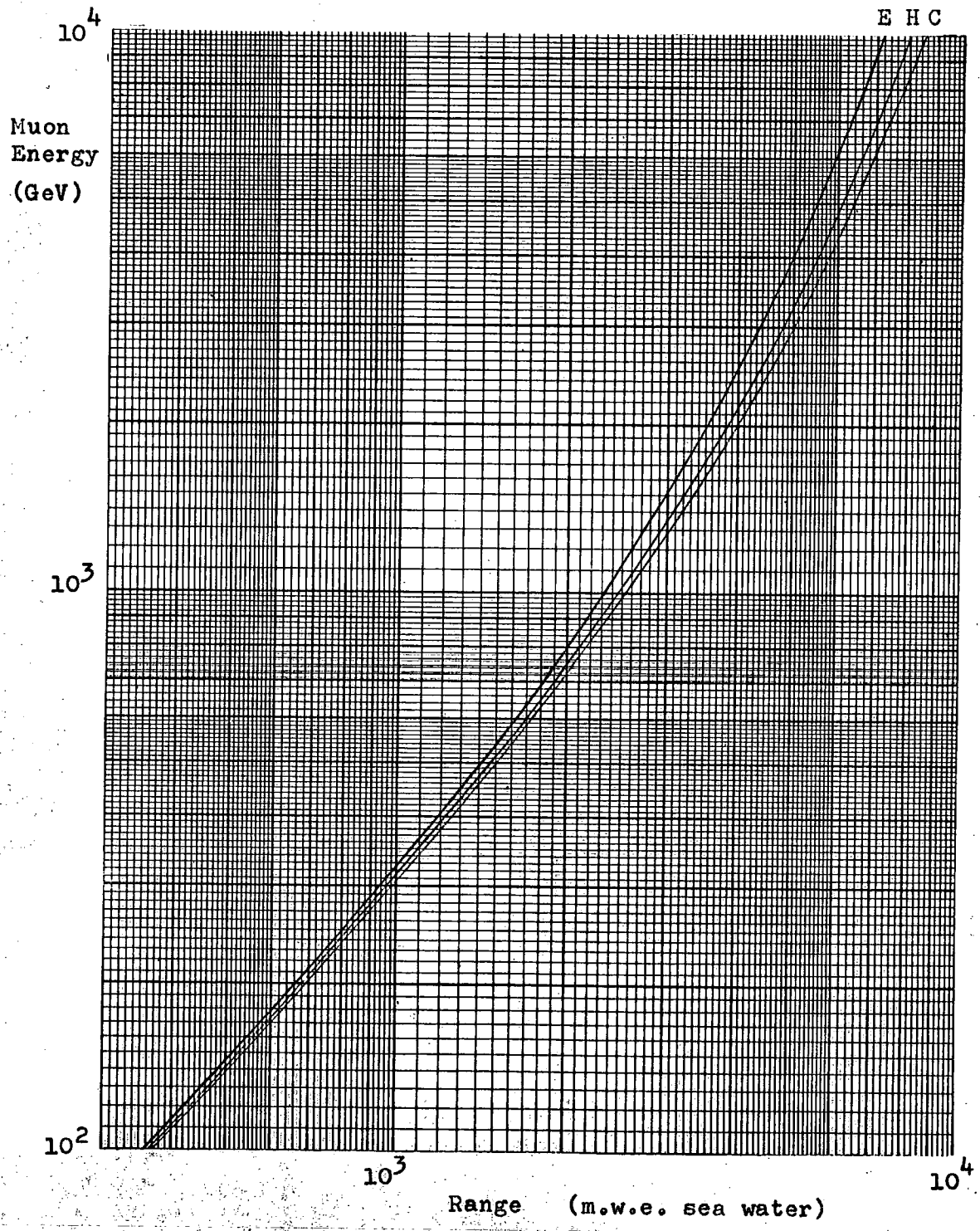

for these uncertainties and to derive a best estimate for the depth-intensity relation down to 7000 m.w.e. An improved version was derived by Osborne et al. (1964) and they obtained a sea level energy spectrum that took into account a correction for shower rejection bias in the magnetic spectrograph results of Hayman and Wolfendale. In the range 20 to 200 GeV they found a discrepancy between the spectrum obtained from the corrected spectrograph measurements and that obtained directly from shallow underground measurements, the latter being rather higher with a maximum difference of about 25% at 100 GeV.

The reason for this discrepancy is not clear, but some of it is undoubtedly due to inaccurate measurements made several decades ago that did not fully exclude the accompanying soft component, or did not have a detector with an accurately known geometry. There is also a possibility that the shower rejection bias factor was underestimated slightly. Osborne et al. concluded that a good estimate of the sea level spectrum of vertical muons follows the corrected intensities of Hayman and Wolfendale up to 200 GeV and follows the intensity-depth spectrum to 7000 GeV. It is this spectrum (OPW) that is plotted in figure 4.3.

As Higashi et al. (1966) have pointed out, sea water has an accurately known composition and a low value of Z^2/A making the effect of fluctuations in energy loss less serious and the transition to the sea level energy spectrum easier. However, it is technically difficult to operate a muon detector of the

necessary large area and high degree of sophistication at great depths under the sea.

The apparatus used by Higashi et al. did not contain visual detectors to give the necessary angular distribution of the particles, nor did it have absorber to eliminate counts from muon produced secondary particles and hence the conclusions of these authors cannot be accepted.

The discrepancies noted by Higashi et al. arose from two causes:

1) As mentioned above, shallow underground measurements carried out many years ago are subject to criticism, for example:

Wilson (1938) did not eliminate local radioactivity or the accompanying soft component associated with the muon flux to the degree now known to be necessary.

Clay and van Gemert (1939) measured the muon intensity under water and then converted to measurements under rock by the crude assumption of a 1.19 ratio between intensities under rock and under water. A similar criticism applies to Ehmert (1937). Generally, a normalisation procedure was used by these early workers, which clearly resulted in large errors if an incorrect normalisation point was assumed.

2) The measurements of Higashi et al. were not absolute, but were normalised at a depth of 20 m (20.54 m.w.e. in sea water) to a value of 1.90×10^{-3} $cm^{-2} sec^{-1} sterad^{-1}$, the Hayman and Wolfendale best estimate value. This best estimate curve has

been superseded by the Osborne et al. (OPW) energy spectrum which gives an intensity of 2.04×10^{-3} $cm^{-2} sec^{-1} sterad^{-1}$, an increase of 7% over the original estimate. If this new normalisation is adopted, together with the three treatments of energy loss E, H and C, the vertical intensity figures of Higashi et al. for vertical and oblique incidence give the points shown in figure 4.3. For muons that only penetrate to shallow depths, less than about 1000 m.w.e., the energy loss is mainly through collision and thus these three treatments, which commonly adopt the analysis of Sternheimer, give nearly identical values with the result that the spread of points resulting from E, H and C is only shown for the greatest energy. At lesser energies the points from E and C approximate very closely to that from H, which is plotted.

In order to plot other experimental points obtained by workers under Kolar rock and standard rock, the energy loss and range-energy curves for muons were calculated with the KGF rock values given in table 4.4, following the treatment H. The points plotted are those of Sreekantan et al. (1956), Randall and Hazen (1951), Bollinger (1951), (only absolute measurements in the vertical direction), Miyake et al. (1964a), Barrett et al. (1952) and Achar et al. (1965a). These workers obtained absolute values for the muon intensity with carefully controlled conditions under rock of accurately known composition. Recently, measurements have been made under Mt. Blanc by Castagnoli et al. (1965b). Using the data shown in table 4.4 and the energy loss treatment C, they

Figure 4.3

The Sea Level Muon Energy Spectrum Derived from Measurements Made under Water and Rock

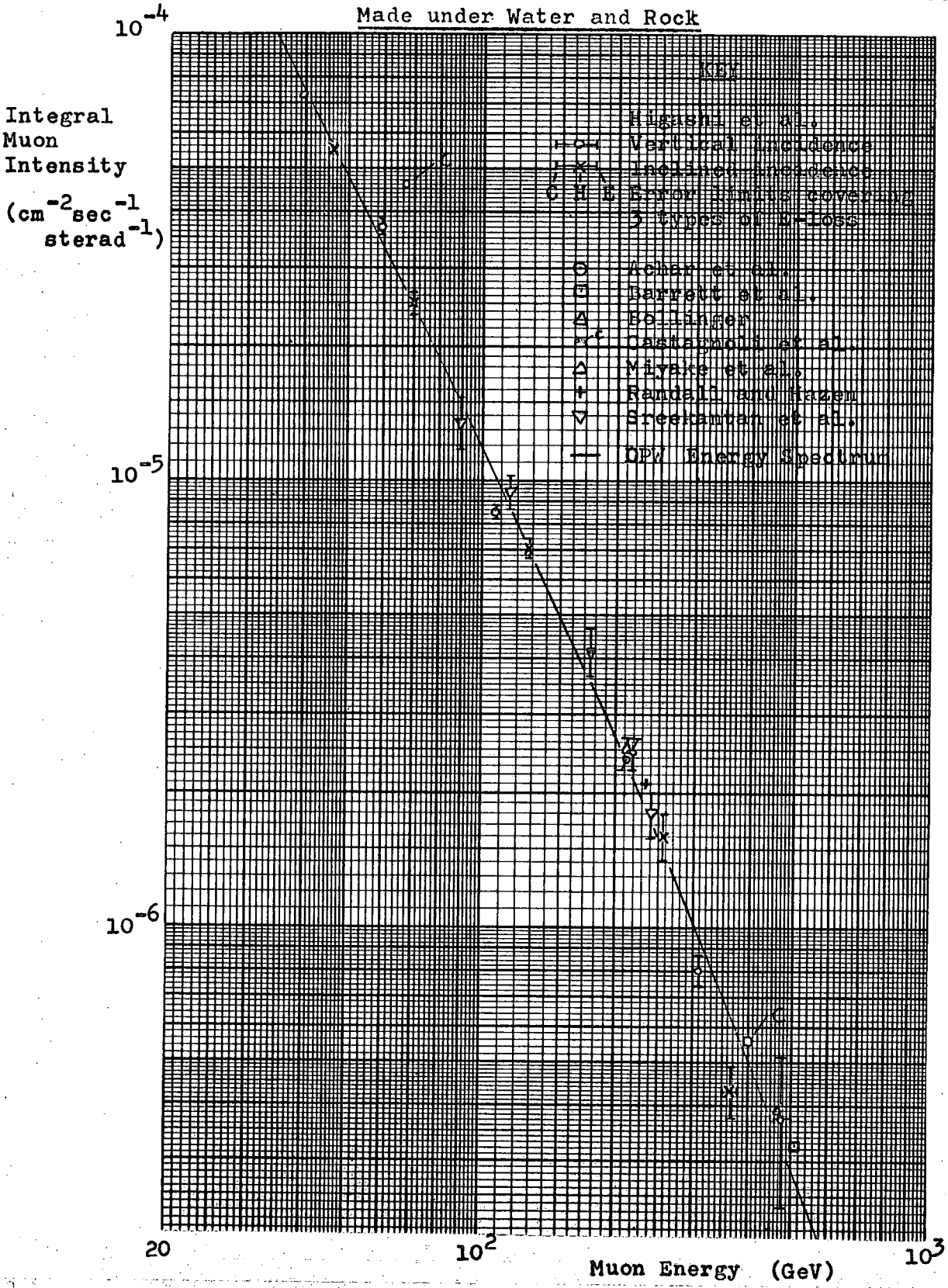

obtained the points shown on figure 4.3, which are at variance with other experimental results. Certainly the vertical intensities that they quote are much higher than those observed by Higashi et al., working at similar depths, when allowances are made for the difference in Z/A. A possible explanation is that they assumed an incorrect value for the exponent of the angular distribution, n, since they used non-visual detectors, but the most likely explanation is that they made a mis-estimation of the amount of overburden when they were working at shallow depths. The point at 400 GeV is in reasonable agreement with the OPW curve, since the corresponding intensity was measured at a site 880 m inside the Mt. Blanc road tunnel, (not very close to the tunnel entrance as had been the case when obtaining muon intensities at very shallow depths), where the effect of the complicated surface topography could be calculated more accurately.

From figure 4.3 it is clear that underwater and under rock measurements are in good agreement with each other and with the directly measured energy spectrum up to 500 GeV, equivalent to a depth of about 1500 m.w.e. It is also apparent that at such low energies, where collision losses dominate, the comparison of underwater and under rock measurements cannot throw light upon the exact form of the energy loss parameters b_p, b_b and b_n, the sum of which are referred to as b_{tot}.

4.3.3 The Comparison of Submarine and Subterranean Muon Intensities at Great Depths

If an experiment to measure the total intensity of muons at a great depth, say 4000 m.w.e., under water and under rock could be completed to yield intensities accurate to a few percent, a limitation could be placed on the possible range of values of b_{tot}. From figures 4.1 and 4.2 for measurements under sea water the average sea level energies corresponding to a depth of 4000 m.w.e. would be 2.53×10^3 GeV, 2.17×10^3 GeV and 2.03×10^3 GeV for the energy loss treatments E, H and C respectively. For a similar measurement at 4000 m.w.e. under standard rock the corresponding figures would be 2.98×10^3 GeV, 2.35×10^3 GeV and 2.16×10^3 GeV. The effective values of b_{tot} for energy loss in standard rock in the three cases are 5.0×10^{-6} $g^{-1}cm^2$, 4.1×10^{-6} $g^{-1}cm^2$ and 3.5×10^{-6} $g^{-1}cm^2$, giving a range of b_{tot} of 1.5×10^{-6} $g^{-1}cm^2$, showing that the value of b_{tot} is quite sensitive to the energy loss treatment adopted. Analysis of the ratios of the expected sea level energies quoted above, with reference to the depth-intensity relation, shows that if the ratio of measured underwater and under rock intensities is known to 5% the value of b_{tot} can be inferred to $\pm$ 0.25×10^{-6} $g^{-1}cm^2$. The absolute accuracy of an intensity measurement at this depth would need to be $\pm$ 3.5%, not an impossible figure, but one that would be very difficult to achieve under water.

It must be noted that in this analysis the effect of

fluctuations has been ignored. As explained in section 4.2.5, there is no precise agreement on the absolute values of R and consequently the inferred accuracy given to b_{tot} would be lower. However, if the experiment under rock were carried out in the KGF mine where $Z^2/A = 6.3$, as opposed to that of 5.5 for standard rock, the range of values of b_{tot} would be greater than 1.5×10^{-6} $g^{-1}cm^2$ and the accuracy necessary in the vertical intensity for a given accuracy in b_{tot} would be less.

There is clearly a need for more underwater experiments with, if possible, identical experiments under rock since an accurate knowledge of b_{tot} at various depths would enable the dominant character of its components to be elucidated, particularly that of b_n, over which there is considerable doubt.

4.4 The Angular Distribution of Atmospheric Muons Underground

At any depth underground muons are observed to arrive chiefly from the vertical direction and with a decreasing intensity at increasing angles to the vertical. The form of the distribution of muon intensity with spatial zenith angle is determined by the increased path length through the atmosphere of the parent pions, allowing an enhancement of π-μ decay, and the muon intensity at the vertical depth equal to the inclined depth of ground traversed by the muons. If the vertical muon intensity follows a power law:

$$I_v(D) = C.D^{-(n+1)}$$

then the angular distribution is

of the form:

$$I(\theta) = I_v \cos^n\theta$$

where θ is the spatial zenith angle, since the π-μ decay enhancement is approximately proportional to $\sec\theta$. The value of n is a slowly changing function of the vertical depth D, and thus a more accurate treatment to determine n than taking the slope of the depth-intensity curve on a logarithmic plot at a particular depth, is to use the relation:

$$I(\theta,D) = I(0,D\sec\theta)\sec\theta.$$

The values of $I(\theta)$ obtained for a given depth can be fitted to a $\cos^n\theta$ distribution and the best value of n obtained by a chi-squared test. Because the value of n changes slowly with depth, the best value of n obtained will depend on θ_{max}, the maximum angle to which the fit is made. Most experiments that have been carried out underground and that have investigated the angular distribution have measured the projected rather than the spatial zenith angle. Experimentally determined values of n have been controlled by the geometry of the apparatus which usually allowed β, the projected zenith angle, to be measured out to the region of 40°- 60°.

Figure 4.4 shows the values of n determined experimentally down to 7500 m.w.e. It is considered that the effective θ_{max} will lie in the range 40°- 60°. In addition, the values of n expected from the observed depth-intensity relation for $\theta_{max} = 40^\circ$, 50° and 60° have been plotted to a depth of 6000 m.w.e. Below this depth

Figure 4.4

Exponents of the Angular Distribution of Underground Muons as a Function of Depth.

Curve A: $\theta_{max} = 60^{\circ}$. Curve B: $\theta_{max} = 50^{\circ}$. Curve C: $\theta_{max} = 40^{\circ}$

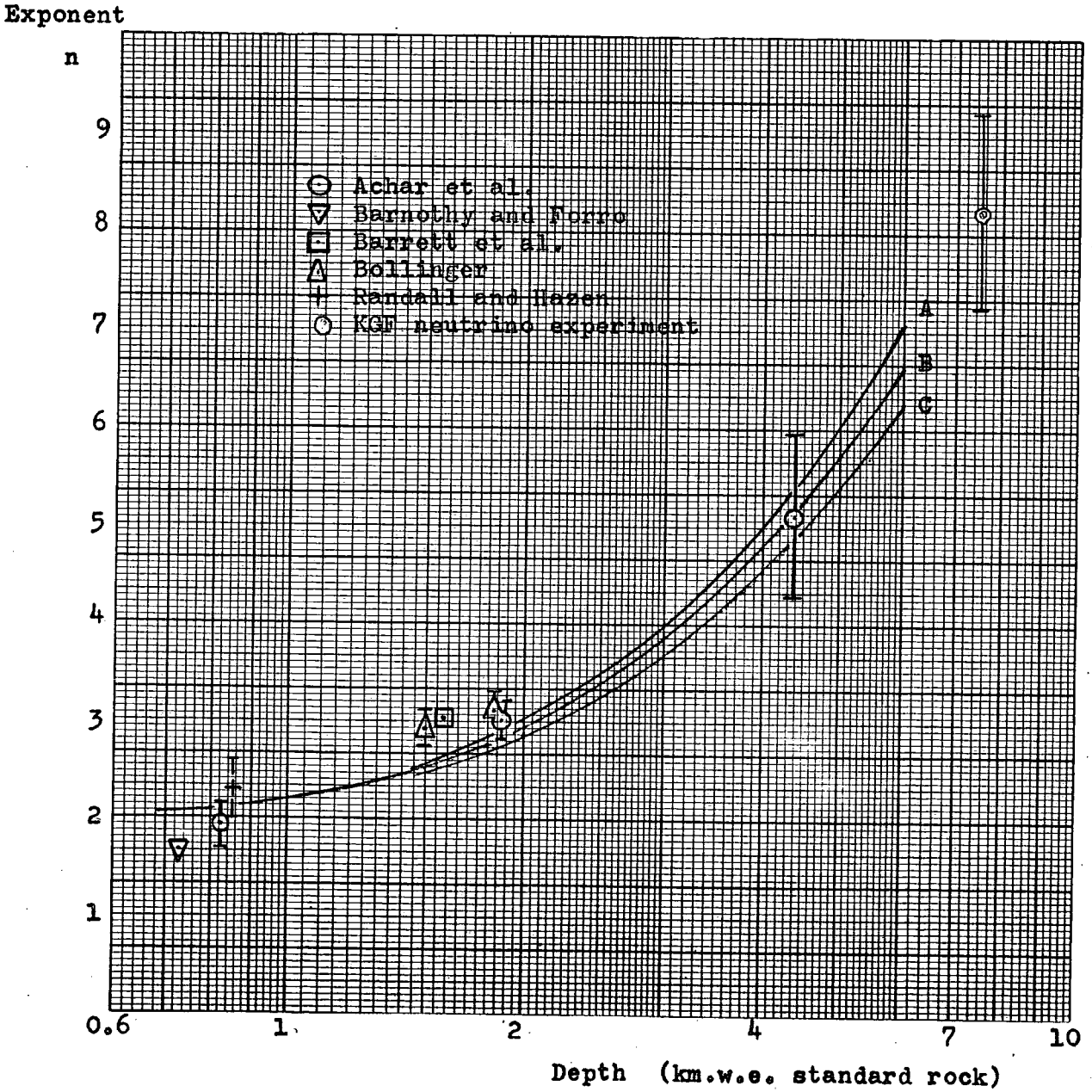

it is not possible to estimate n accurately since the behaviour of the depth-intensity curve is not known at very great depths. The work of Barnothy and Forro (1948) is known to be inaccurate since insufficient absorber was used to reduce the effect of the electromagnetic accompaniment of the muons. The excess of the observed over the expected values in the region of 1800 m.w.e. cannot be explained simply.

4.4.1 The Angular Distribution at 7500 m.w.e.

The observed angular distribution of the 31 'in geometry' events through telescopes 1 and 2 (T(1,2)) is shown in figure 4.5. Events with $\beta > 60^{\circ}$ are expected to be neutrino-induced events, and for reasons explained in section 5.6 it is expected that approximately two events with $\beta < 60^{\circ}$ will be neutrino-induced also, and that the two events are most likely to fall in the range $35^{\circ} \lesssim \beta \lesssim 50^{\circ}$. The differential apertures for all the telescopes have been calculated by J.L. Osborne. (Table 4.5 and figures 4.6 and 4.7) The apertures for telescopes 1 and 2, together with an angular distribution of the form $\cos^{n}\theta$ have been used to compute the best value of n to fit the data, with a β_{max} of 60°. The best fit was obtained using a maximum likelihood function:

$$L(N) = \frac{N^{N_o}}{N_o!} e^{-N}$$

where N_o = no. observed
and N^o = no. expected.

Since the events in each 5° cell are expected to fall in a Poissonian distribution about the expected number, this is

Figure 4.5

Observed and Expected Muon Angular Distributions in the KGF Neutrino Telescopes.

A: Expected distribution following a $\cos^{8.25}\theta$ relation

B: Expected distribution following a $\sec\theta.\exp(-9.26(\sec\theta-1))$ rel^{n}.

C: Expected neutrino-induced muon relation.

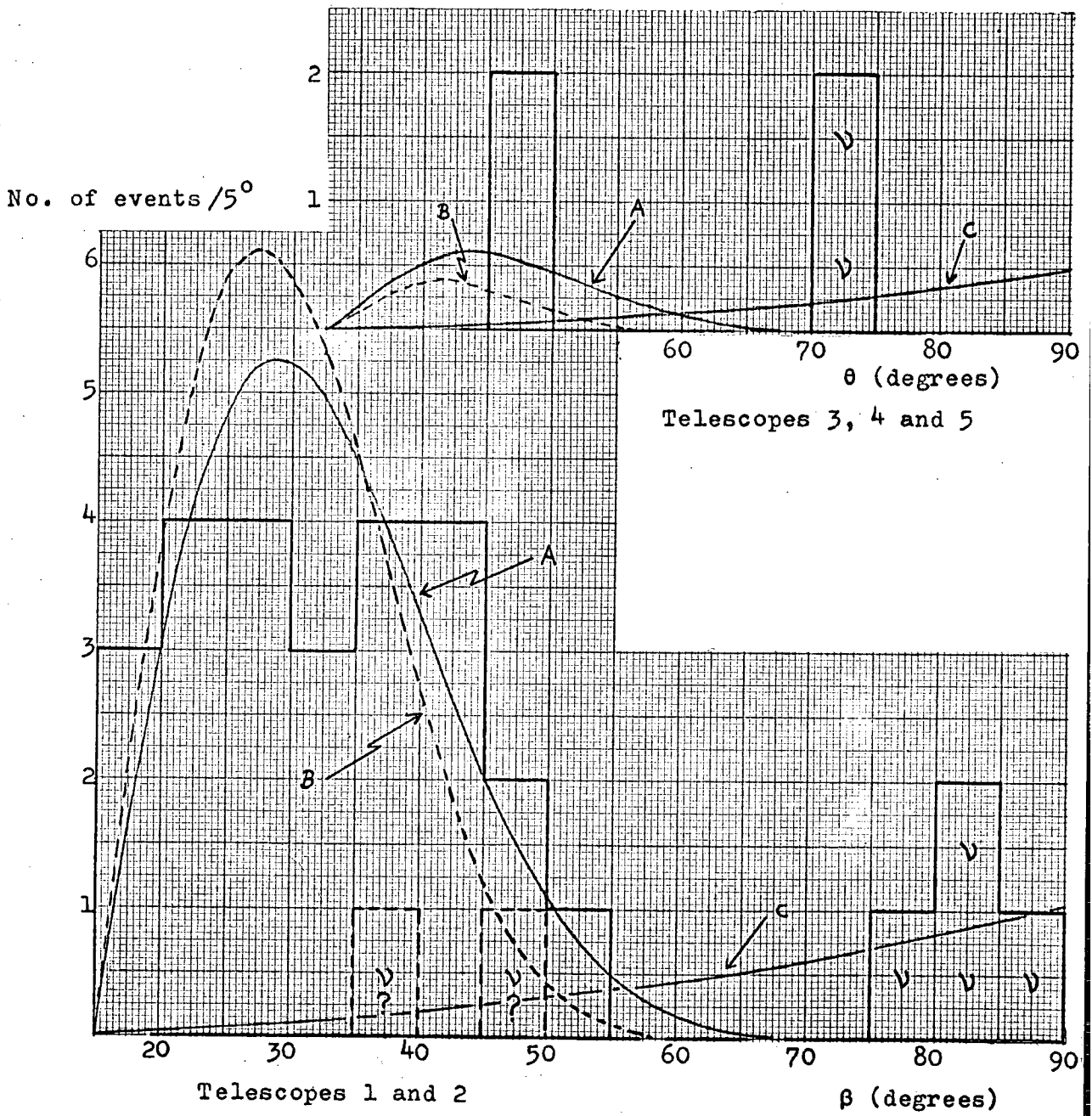

Figure 4.6

Differential Aperture of Telescope 1 or 2 with respect to β the Projected Zenith Angle.

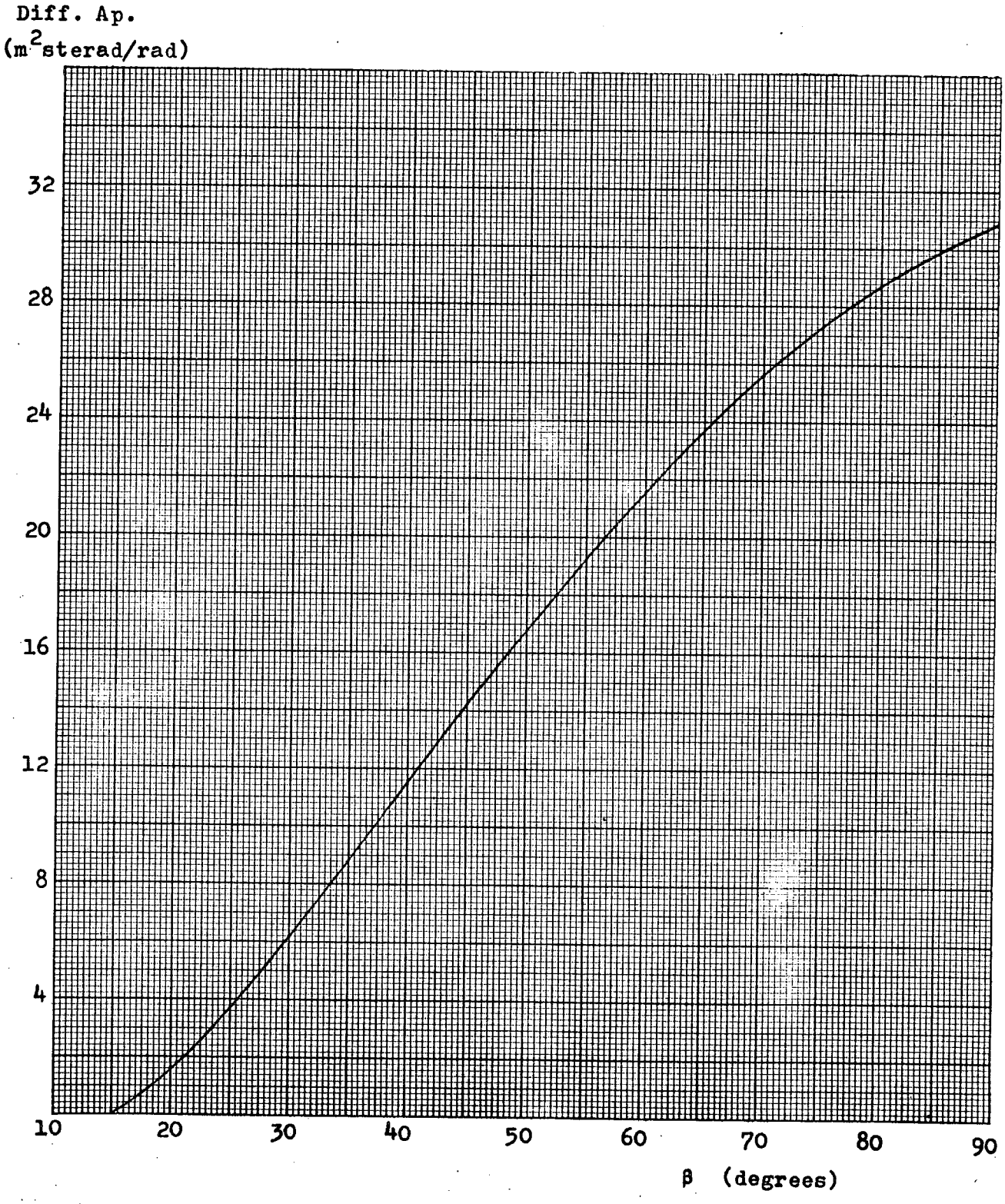

Figure 4.7

Differential Apertures of Telescopes 3-5 with respect to θ the Spatial Zenith Angle.

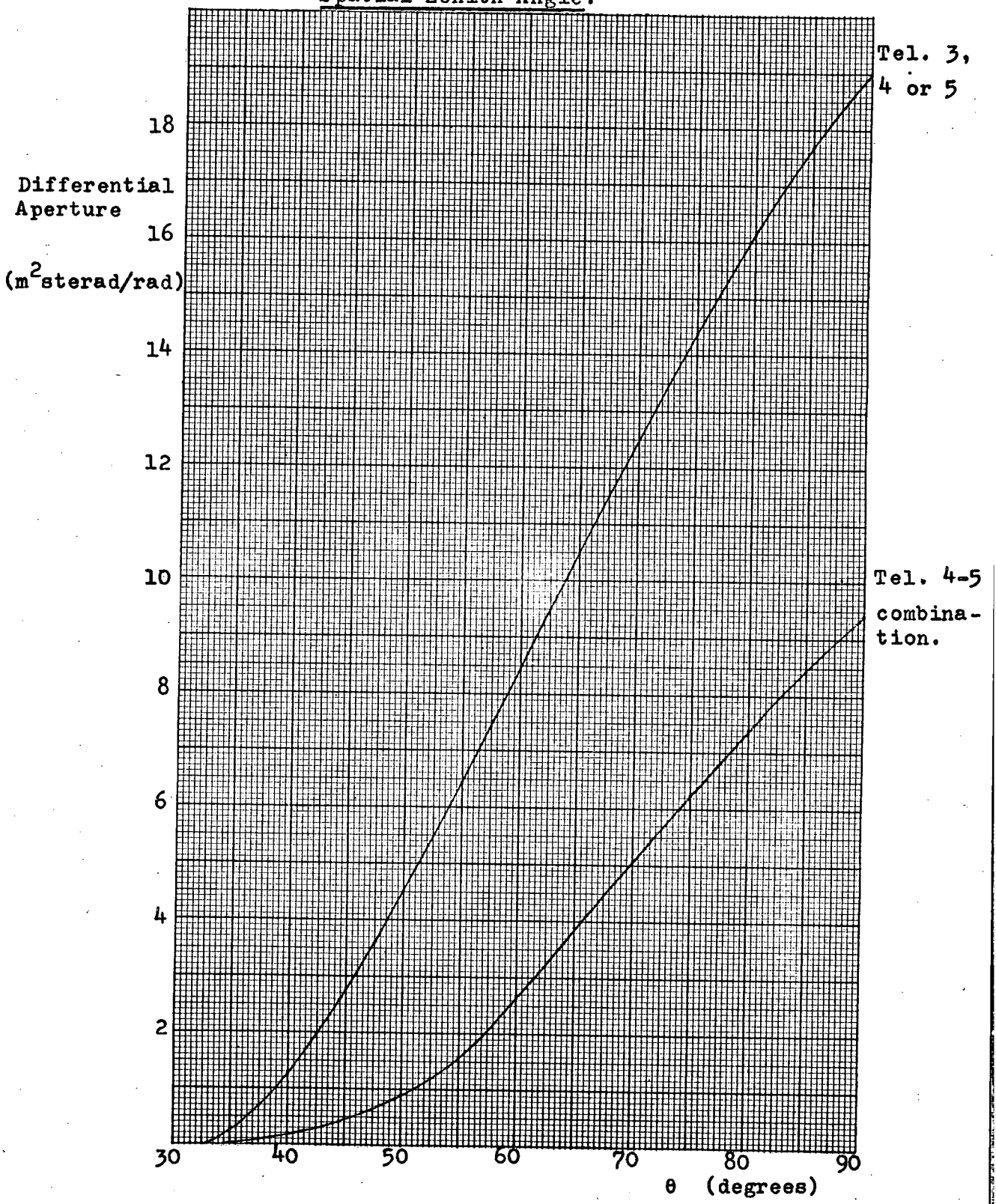

the best method. The result was confirmed with a chi-squared test.

The best value of n = 8.25 $\pm$ 1.0, the error limits being for best fits with β_{max}= 52.5° and 67.5°. The expected distribution following a $\cos^{8.25}\theta$ relation is shown in figure 4.5 normalised to the total number of in geometry atmospheric muon events whose angles are known. (25).

Table 4.5 Characteristics of the KGF Telescopes

	Telescope 1 or 2	3, 4 or 5
Scintillator block dimensions (cm^3)	49.6 x 49.6 x 5.0	as T(1 or 2)
Scintillator wall		
length (cm)	207	207
height (cm)	314	208.7
separation (cm) (centre to centre)	84.5	132.8
Telescope		
Geometrical aperture (m^2sterad) (no gap allowance)	22.4	9.08
Orientation (° West of North) (perp. through both scint. walls)	17.3	11.3
Geographical location		
Latitude (°N)	12.9	as T(1 or 2)
Longitude (°E)	78.3	as T(1 or 2)

In a paper by Menon et al. (1967a) it is suggested that below a depth of about 4000 m.w.e. the intensity follows an exponential decrease with depth given by:

$$I(0,D) = 9.8\times10^{-7}\exp(-D/\lambda) \quad cm^{-2}sec^{-1}sterad^{-1} \qquad 4.4.1.1$$

where $\lambda = 810 \pm 50$ m.w.e. This would predict:

$$I(\theta,D) = I(0,D)\sec\theta\exp(-m(\sec\theta-1)) \qquad 4.4.1.2$$

where $m = D/\lambda = 9.26$ at 7500 m.w.e. At small values of θ equation 4.4.1.2 approximates to :

$$I(\theta,D) = I(0,D)\cos^{m-1}\theta, \text{ or } I(\theta) = I(0)\cos^{8.26}\theta$$

at 7500 m.w.e. This is in excellent agreement with the experimentally determined value of n, but at large values of β it is clear from figure 4.5 (where the expected angular variation using relation 4.4.1.2 with $m = 9.26$ is plotted normalised to 25 events) that the depth-intensity curve does not follow an exponential decrease, but rather a power law decrease, below about 7500 m.w.e.

Implicit in the derivation of the angular distribution from the vertical intensity variation is the assumption that the effect of Coulomb scattering is negligible. This is in fact justified since the energies of the muons reaching a depth of 7500 m.w.e. are very high during most of their passage through the Earth. It is estimated that the mean muon energy of atmospheric muons arriving from the vertical at 7500 m.w.e. is about 400 GeV on arrival, resulting in a very small broadening in the angular distribution observed.

From the vertical intensity derived from the events in T(1,2) in section 4.5, a $\cos^{8.25}\theta$ distribution and the differential apertures given in figure 4.7, the expected angular distribution of atmospheric muons in T(3-5) has been calculated

and is shown in figure 4.5, together with the observed distribution, as a function of spatial zenith angle.

4.5 The Vertical Intensity of Atmospheric Muons at Great Depths Underground

4.5.1 The Intensity at 7500 m.w.e.

Of the 46 events listed in appendix A, 40 were observed in T(1,2) and 6 in T(3-5). In the former category, 7 events are either shower events or are definitely out of geometry, event no. 17 is discarded as having a $\leq 40\%$ chance of being a genuine event and events nos. 9, 16 and 31 could be out of geometry. Additionally 6 events are thought to be of neutrino interaction origin for reasons explained in section 5.6. Thus 26 (-3?) events are thought to be in geometry, atmospheric muon events in either telescopes 1 or 2 (T(1 or 2)) occurring in a running time of 24273 telescope-hours.

If an angular distribution of $I_\theta = I_v \cos^{8.25}\theta$ is assumed, the effective aperture in the vertical direction for T(1 or 2) is 0.267 m^2sterad. This must be reduced by about 5% to allow for gaps between scintillator elements. The vertical intensity is found to be $(1.13 \begin{smallmatrix} + 0.41 \\ - 0.31 \end{smallmatrix}) 10^{-10}$ $cm^{-2} sec^{-1} sterad^{-1}$.

Two of the four events in T(3-5) that are in geometry are thought to be neutrino-induced events, leaving two events attributable to atmospheric muons. The effective aperture in

the vertical direction for T(3, 4 or 5) is calculated to be 0.0248 m^2sterad and the additional effective aperture through the operation of telescopes 4 and 5 as one telescope is 0.0048 m^2sterad. The total effective vertical aperture for T(3-5) is thus 0.079 m^2sterad which must be reduced by about 5% to allow for gaps. The running time for T(3-5) is equivalent to 7471 hours, giving a vertical intensity of $(1.0 \begin{smallmatrix} + 1.3 \\ - 0.6 \end{smallmatrix}) 10^{-10}$ $cm^{-2}sec^{-1}sterad^{-1}$, in good agreement with the value from T(1,2). The errors quoted on the vertical intensities include an estimate for the error of $\pm$ 1.0 on the value of n.

4.5.2 The Best Estimate of the Depth-Intensity Relation at Great Depths

In recent years a number of authors have considered the data available from underground experiments and have given estimates of the best line through the experimental points, notably Osborne et al. (1964), Menon and Ramana Murthy (1967), Pattison (1965) and Menon et al. (1967a). In so far as the present experiment gives information only on intensities at depths below 7500 m.w.e., it is proposed to examine the depth-intensity relation at depths greater than 4000 m.w.e., as was done by Menon et al. (1967a). For shallower depths the best estimate is probably that of Pattison (1965) who gives a curve that lies between those of Menon and Ramana Murthy and Osborne et al.

If the experimental points in figure 4.4 are plotted on

a linear graph, it is found that the value of the exponent n at any depth D may be given approximately by the relation:

$$n(D) = 1.47 + 0.885D \qquad 4.5.2.1$$

where D is in km.w.e., if the best straight line is put through the experimental points for values of D greater than 1 km.w.e. From the observed angular distribution at 7500 m.w.e., and the lack of any other accurate information at a greater depth, it can be assumed that the relation 4.5.2.1 holds at great depths. The value of n at any depth is then the effective value for a detector at that depth with a cut off, θ_{max}, of about 60°. It is clear, however, that the true value of n at small values of θ will be less than at large θ, the effective value being the best estimate for the region about 30°, and hence for the entire angular range of the detector.

In figure 4.8 experimental data from Miyake et al. (1964a), Achar et al. (1965a), Castagnoli et al. (1965b) and the present experiment are plotted normalised to standard rock and, where the value of n was not directly measured, corrected to the value of n predicted by relation 4.5.2.1. The vertical intensity derived from the Johannesburg experiment (section 6.1.4) is also plotted. A consideration of these points does not give rise to a depth-intensity relation significantly different from that of Menon et al. (1967a) (see section 4.4.1) in the region from 4000 m.w.e. to 7500 m.w.e. At greater depths the adoption of relation 4.5.2.1 and the assumption that the value of n at any depth applies most

Figure 4.8

The Depth - Intensity Relation for Muons at Great Depths

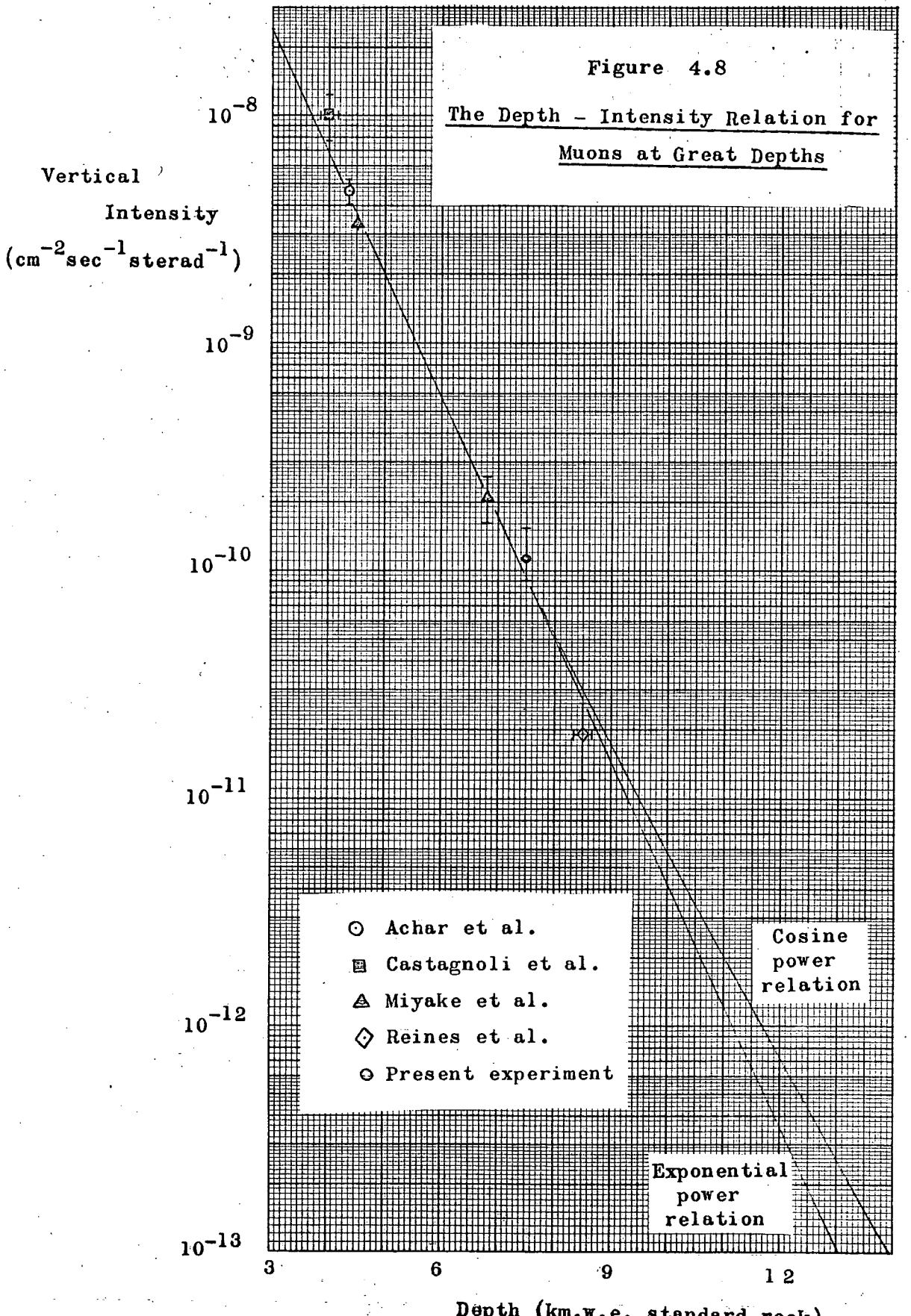

accurately to the muons arriving at about 30° to the zenith gives a depth-intensity relation that diverges from the exponential form of Menon et al. Both relations are drawn out in figure 4.8. Because of the lack of experimental observations, this approach can only be a tentative one, but it is interesting to note that the relation based on the linear increase in n is close to that predicted by Craig et al. (1967) for the depth-intensity relation derived from the primary spectrum of Greisen (1965) for the energy per nucleus, with the assumption that heavy nuclei are negligible at all energies. This tends to confirm that the assumption of a cosine power law is not an unreasonable one for the angular distributions of muons at great depths, provided that a unique value of n is not assumed to apply out to large angles.

Chapter 5

NEUTRINO INTERACTIONS UNDERGROUND

5.1 Introduction

Before the results mentioned in section 3.3.2 and appendix A can be analysed in terms of neutrino-initiated muons, the already established facts and the theoretical predictions concerning the modes of neutrino interactions at various energies must be discussed. Three basic types of neutrino interaction that produce muons are predicted. Elastic and inelastic interactions have been established with approximate cross-sections up to an energy of about 10 GeV by machine experiments, and the possible mediation by the vector boson, W, at high energies has been suggested. These three modes of interaction, together with that of the Glashow resonance which arises as a direct consequence of the postulation of the W, are considered. A total rate of neutrino-induced muons is derived from the KGF experimental data and its significance discussed. Finally the results of an analysis of the arrival directions of the muons listed in appendix A are presented.

5.2 Elastic Interactions

The interactions of the muon neutrino through:

$\bar{\nu}_\mu + p \rightarrow n + \mu^+$ and $\nu_\mu + n \rightarrow p + \mu^-$

where the charge of the lepton changes but no additional hadrons are created are termed elastic, and the predicted cross-section has been confirmed by recent experiments at CERN. Close to the threshold the cross-section increases linearly with neutrino energy, but at $E \gtrsim 1$ GeV the total cross-sections for both interactions tend to a constant value of approximately 6.10^{-39} cm^2 per nucleon. Since the present experiment does not distinguish between positive and negative muons, and the proton to neutron ratio in Kolar rock is close to unity, the cross-section for elastic interactions is taken as 6.10^{-39} cm^2/n-p pair. At machine energies the muon is found to take 0.9 of the neutrino energy, and this value is assumed to apply at higher energies.

The experimental results obtained at CERN mentioned in this and subsequent sections are given by Young (1966). The possible existence of the intermediate vector boson has very little effect on the elastic cross-section.

5.3 Inelastic Interactions

In this category are placed all neutrino interactions where one or more hadrons are produced, but where interactions are not mediated by the vector boson. Paty (1965) gives a discussion of the many theoretical treatments of the subject. In general the interaction is expected to produce pions and possibly heavier particles:

$$\nu_\mu + N \longrightarrow N' + \mu + \pi's + \ldots\ldots$$

Since the KGF apparatus cannot distinguish between the different types of inelastic interaction, and only the total rate of muons is of interest here, the best estimate for the cross-section is taken from the machine data available up to 10 GeV. Beyond the experimental limit of 10 GeV two possible limiting cases are considered:

case (a) $\sigma_{inel.} = 3.0 \times 10^{-39} E_\nu$ cm^2/nucleon for all E_ν where E_ν is in GeV, and

case (b) $\sigma_{inel.} = 3.0 \times 10^{-39} E_\nu$ cm^2/ nucleon for $E_\nu < 10$ GeV

and $\sigma_{inel.} = 3.0 \times 10^{-38}$ cm^2/nucleon for $E_\nu > 10$ GeV; although the present experimental data obtained in the CERN heavy liquid bubble chamber are not incompatible with the cross-section rising faster than E_ν. For the energy region where the cross-section is increasing it seems most likely that the muon will take 2/3 rds of the neutrino energy, and that it will take all the energy in the region where the cross-section is limited by a restriction on the momentum transfer.

5.4 Boson Mediated Interactions

The intermediate boson hypothesis was first suggested by Yukawa and developed by Lee and Yang (1960) as an explanation of the high energy behaviour of weak interactions. It is presumed to exist in both positive and negative charge states, (though it is thought unlikely that a W° exists) and to mediate weak interactions. It must be massive since the weak interactions are of short range,

the lowest possible mass consistent with machine data being 1.8 GeV (Bernardini et al. 1965). The boson would have a lepton number and a baryon number of zero, a spin of one and a magnetic moment of $\frac{e}{2m_W}(1+k)$, the anomalous magnetic moment, k, being unknown, but usually taken as zero. The W is created through:

$$\nu_\mu \rightarrow \mu^- + W^+ \quad \text{or} \quad \bar{\nu}_\mu \rightarrow \mu^+ + W^- \qquad 5.4.1$$

in the Coulomb field of a nucleus. The minimum momentum transfer to the nucleus by the neutrino is $m_W^2/2E_\nu$ and this momentum transfer, necessary to conserve momentum in the interaction 5.4.1, becomes smaller for higher neutrino energies.

If the momentum transfer in the impact is small and the neutrino makes only a peripheral collision, the nucleus recoils as a whole giving a coherent collision. At low neutrino energies the momentum transfer increases and the collision is incoherent, the scattering taking place at a single nucleon.

A full discussion of the calculation of both coherent and incoherent cross-sections has been given by Osborne (1966). He adopts the cross-sections of Wu et al. (as quoted by Burns et al. 1965) for both types of interaction up to an energy of 20 GeV. The figures of von Gehlen (1963), who gives the asymptotic limit to the cross-sections valid above 100 GeV, are taken for the coherent cross-section and an interpolation procedure is used for intermediate energies. At energies near threshold the incoherent process dominates the coherent interaction and at higher energies ($E_\nu \gtrsim 50$ GeV) the situation is reversed.

The W is expected to decay with a lifetime of less than 10^{-17} sec in either a leptonic or non-leptonic mode. In the leptonic mode two decays are possible:

$$W \longrightarrow \mu + \nu_\mu \quad \text{or} \quad W \longrightarrow e + \nu_e . \qquad 5.4.2$$

In his analysis Osborne assumes the muonic branching ratio to be 0.4 since the most recent theoretical treatments indicate that leptonic decays will predominate for $m_w \lesssim 3$ GeV and that the leptonic decays will be equally divided between the two modes of 5.4.2.

Neutrino interactions via the W therefore produce two muons: the 'interaction muon' and subsequently the 'decay muon' emitted by the boson. It is thought that the energy spectrum of the muons produced in 5.4.1 will be strongly peaked at an energy $E_\nu m_\mu/(m_\mu+m_w)$ corresponding to the minimum momentum transfer to the nucleus of $m_w^2/2E_\nu$. For a value of m_w = 1.8 GeV this results in the muon taking 1/20 of the neutrino energy at 10 GeV. However at high energies the asymptotic formula given by Lee et al. (1961) indicates that the muon takes half the neutrino energy, though this limit is only reached at energies of the order of 10^4 GeV.

If the intermediate boson exists, then it will allow the resonance interaction:

$$\bar{\nu}_e + e^- \longrightarrow \mu^- + \bar{\nu}_\mu \qquad 5.4.3$$

to occur at a threshold laboratory energy of $E_t = m_w^2/2m_e$ with a cross-section of approximately 10^{-31} cm^2 and a resonance width of $E_t/10$ GeV. This fact was first published by Glashow (1960).

Zagrebin and Zheleznykh (1964) have calculated the flux and angular distribution of muons produced through 5.4.3 and their figures have been used to estimate the number of events expected from this mechanism.

There have been a number of theories of weak interactions involving bosons other than the one mentioned above, each with different characteristics. However, the boson of Lee and Yang is the generally accepted mediator of weak interactions at high energies, if such a mediator exists.

5.5 The Flux of Neutrinos Underground

It is expected that above the threshold energies of the telescopes, 100-200 MeV for telescopes 1 and 2 and 400-800 MeV for telescopes 3, 4 and 5, depending on the angle of inclination of the muon, the predominant contribution to the neutrino flux comes from the decays of muons, pions and kaons in the atmosphere. A very much smaller flux is expected from extra-terrestial sources, a subject that is discussed in section 5.7. The energy spectrum of atmospheric neutrinos has been estimated by a number of authors in recent years. The most comprehensive reports have been given by Cowsik et al. (1966) and Osborne et al. (1965) and when allowance is made for the different assumptions adopted by these authors, their values agree to within 5% at most energies.

The figures of Osborne et al. are those taken here for the estimate of the total underground rate of neutrino-induced

muons. The angular distribution of all types of neutrinos was found to be peaked towards the horizontal direction, the ratios of horizontal to vertical intensities increasing from 1.43 to 3.70 at 1 GeV and 10^3 GeV respectively. They assumed a K/π ratio (ratio of all kaons to all pions at production in the atmosphere) of 20%. Uncertainty in this value was reflected by an uncertainty of up to 20% in the intensities quoted. Figure 5.1 illustrates the variation of intensity with energy for the various modes of production. At energies less than about 50 GeV the bulk of muon neutrinos come from μ-e decay, since there is an enhanced probability of μ-e decay in the long path length encountered between the production levels and ground level.

5.6 The Rate of Neutrino-Induced Muons in the KGF Experiment

Using the cross-sections and energy distributions mentioned above together with the neutrino fluxes calculated by Osborne et al., the range-energy relation for muons and the differential apertures of the five telescopes, Menon et al. (1966b) have calculated the numbers of events due to neutrino interactions expected to be observed under different assumptions in the period 1st April 1965 to 1st October 1966. The predictions have been brought up to date, (1st June 1967) and are given in table 5.1 together with the expected median neutrino energies for each process.

Figure 5.1

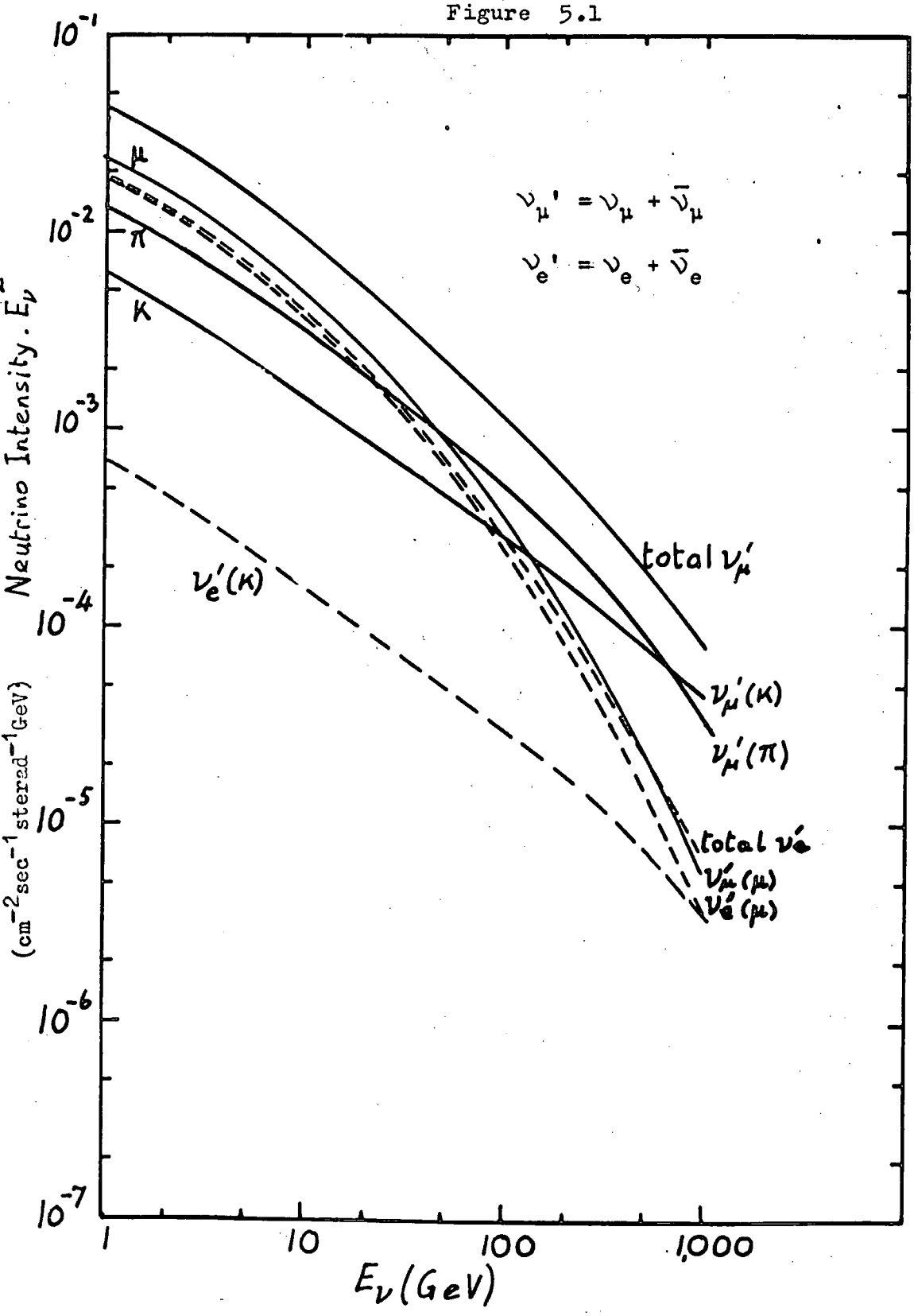

Muon-neutrino and Electron-neutrino Intensities in the Horizontal Direction.

Table 5.1 Neutrino Cross-sections and Expected Numbers of Events in the Period 1st April 1965 to 1st June 1967

Interaction	Cross-section (cm^2)	Fraction of Energy taken by Muon	No. of events	Approx. median neutrino energy (GeV)
Elastic	0.6×10^{-38}/n-p pair	0.9	1.2	2.5
Inelastic				
E_ν <10 GeV	$0.3E_\nu \times 10^{-38}$/nucleon	0.67	1.8	
E_ν >10 GeV	Case (a) $0.3E_\nu \times 10^{-38}$ for all E_ν	0.67	4.5	25
	Case (b) 3.0×10^{-38}	0.67	1.5	9
Boson production	m_W = 1.8 GeV near threshold		7.0	100
	asymptotic		(25)	
	m_W = 2.5 GeV near threshold		3.1	200
	asymptotic		(11.4)	
Glashow resonance	m_W = 1.8 GeV	0.25	2.2	3000
	m_W = 2.5 GeV	0.25	0.5	6000

Upper limit: m_W = 1.8 GeV and case (a) 16.7

Lower limit: $m_W \gg$ 1.8 GeV and case (b) 4.5

The angular distribution of events observed in all telescopes has been displayed in figure 4.5. From the expected distribution of atmospheric events it is clear that all events with zenith angles above about 60° are most probably due to neutrino-induced muons, μ_ν. The angular distribution expected for the μ_νs can be estimated from a knowledge of the telescope

differential apertures and the distribution of parent neutrinos, if it is assumed that the μ_ν is emitted with the same direction of flight as the neutrino. This angular distribution was estimated and normalised, for angles above 60°, to the number of events (4) at angles $>60^\circ$ p.z.a. observed in telescopes 1 and 2. This indicated that approximately 2 events could be expected to have been observed at angles $<60^\circ$ p.z.a. Inspection of the observed angular distribution of all events and comparison with the expected μ_ν distribution showed that the two events were most likely to have fallen in the range of β from 35° to 50°.

Careful analysis of the accompaniment of all muons observed revealed only one event that showed more than a slight possibility that the muon could have been upward moving. This event, no. 18, was assumed to be a μ_ν. Additionally one event in the angular range 45°- 50° was similarly ascribed to the observation of a μ_ν, on the grounds of probability.

The expected μ_ν angular distributions, normalised to six events for T(1,2) and two events for T(3-5), are plotted in figure 4.5.

The aperture for T(1 or 2) for an isotropic distribution (the instrumental aperture) is 22.4 m^2sterad or 19.5 m^2sterad after a 13% reduction to allow for scintillator gaps. For T(3, 4 or 5) the instrumental aperture is 9.08 m^2sterad, or 7.90 m^2sterad after gap reduction. The extra instrumental aperture gained by placing telescopes 4 and 5 close together is

3.64 m^2sterad. Based on a running time of 24273 tel-hrs for T(1,2), 22510 tel-hrs for T(3-5) and 6988 tel-hrs for the T(4-5) combination, the instrumental intensities of μ_νs are:

T(1,2) $(3.5 \,^{+\,2.8}_{-\,1.7})10^{-13}$ $cm^{-2}sec^{-1}sterad^{-1}$

and T(3-5) $(2.7 \,^{+\,3.7}_{-\,1.8})10^{-13}$ $cm^{-2}sec^{-1}sterad^{-1}$, giving a weighted mean of $(3.2 \,^{+\,1.9}_{-\,1.3})10^{-13}$ $cm^{-2}sec^{-1}sterad^{-1}$.

These intensities assume the neutrino flux to be isotropic. A more accurate comparison can be made between different telescope geometries by allowing for the expected peaking in the horizontal direction and deriving a value for I_h, the horizontal μ_ν intensity. In order to do this a median neutrino energy must be assumed for the majority of events, and a choice must be made of the type of interaction giving rise to the greater part of the μ_ν flux. Here it is assumed that the parent neutrinos of the events have an energy of 10 GeV. This assumption gives an effective aperture in the horizontal direction of 13.4 m^2sterad for T(1 or 2) and 6.7 m^2sterad for T(3, 4 or 5) including the T(4-5) combination, after allowing for gaps. The horizontal μ_ν intensities are estimated to be:

T(1,2) $(5.1 \,^{+\,4.0}_{-\,2.5})10^{-13}$ $cm^{-2}sec^{-1}sterad^{-1}$

and T(3-5) $(3.7 \,^{+\,4.9}_{-\,2.4})10^{-13}$ $cm^{-2}sec^{-1}sterad^{-1}$, giving a weighted mean of $(4.6 \,^{+\,2.7}_{-\,1.8})10^{-13}$ $cm^{-2}sec^{-1}sterad^{-1}$.

The number of events thought to have been observed, $8 \,^{+\,4.8}_{-\,2.0}$, is within the expected range. The significance of the result is discussed in section 5.9.

5.7 The Celestial Co-ordinates of the KGF Experiment Events

The sidereal time, the projected zenith angle and the range of permitted azimuth angles for any events in T(1,2), and the telescope orientation, can be used to give the arrival direction of the muon as an arc on the celestial sphere. Results from T(3-5) can be similarly combined to give a unique point on the same plot for each event, since the azimuth angles are known to about one degree accuracy. The events are divided into four categories, those with β above and below 60° coming from the North and South hemispheres. The event arrival directions are plotted in figures 5.2 and 5.3. Where the values are known, out of geometry events are plotted. Event no. 13 is included on the assumption that $\beta = 90^{\circ}$, and allowance has been made for the uncertainty in the value of β for event no. 3. Where the sense of travel of a muon with $\beta > 60^{\circ}$ is at all uncertain it is plotted twice to include both directions of travel.

An analysis of the running times of T(1,2) shows that they have been operational throughout the sidereal day with a deviation from uniformity of less than $\pm$ 17%. The sidereal time of an event is approximately equivalent to its Right Ascension if the zenith angle is small, and thus it is expected that the events in figure 5.2 should be nearly uniform in Right Ascension if the muon flux is isotropic. The expected and observed distributions for downward moving muons, plotted as histograms for North and South hemispheres for events with $\beta < 60^{\circ}$ are given in figure 5.4. A chi-squared test shows that observation is significantly different from expectation,

Figure 5.2a

Celestial Co-ordinates of Events with $\beta < 60^{\circ}$.

Northern Hemisphere.

---- limit of sensitive region

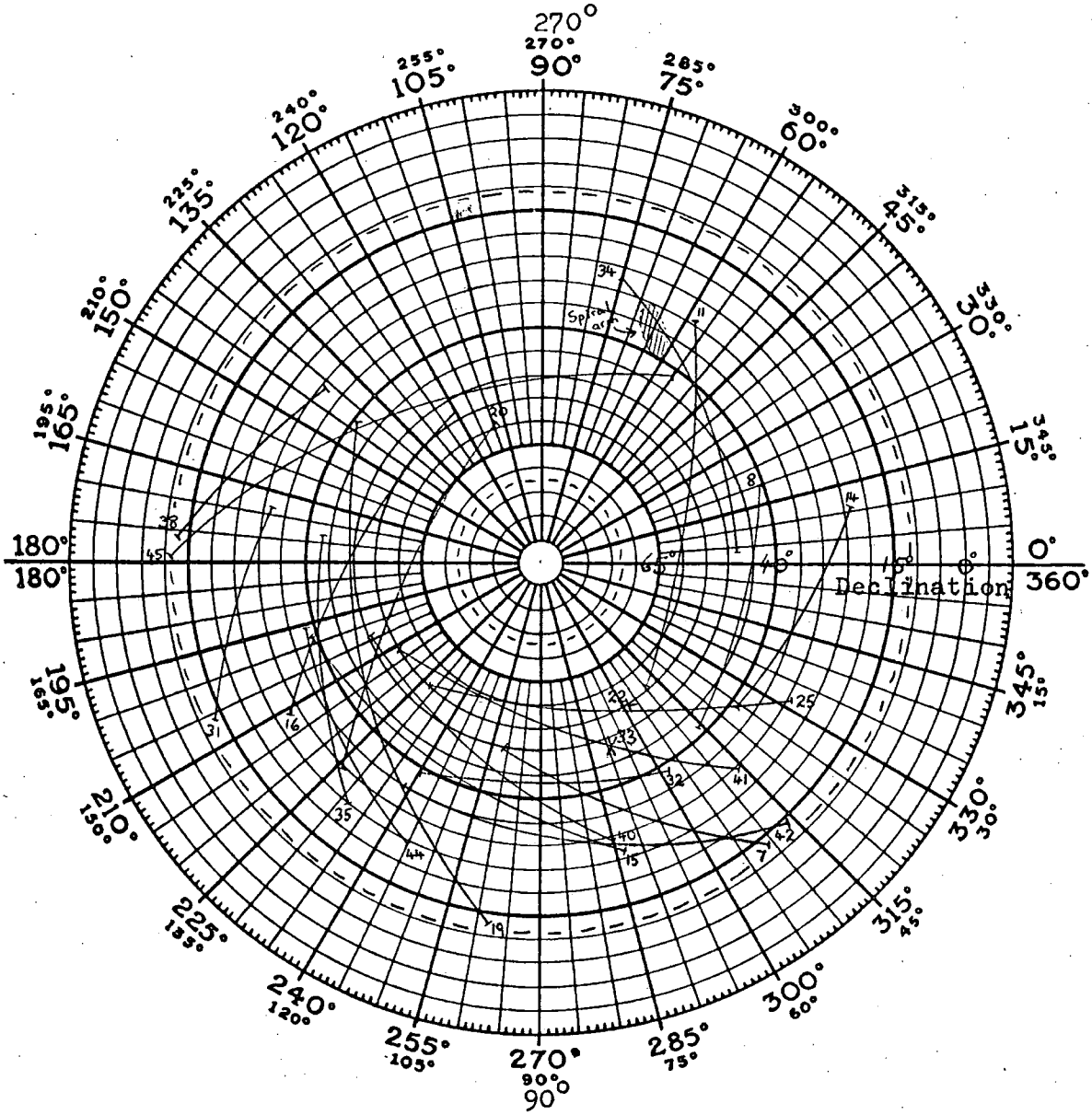

Figure 5.2b

Celestial Co-ordinates of Events with $\beta < 60^{\circ}$.

Southern Hemisphere.

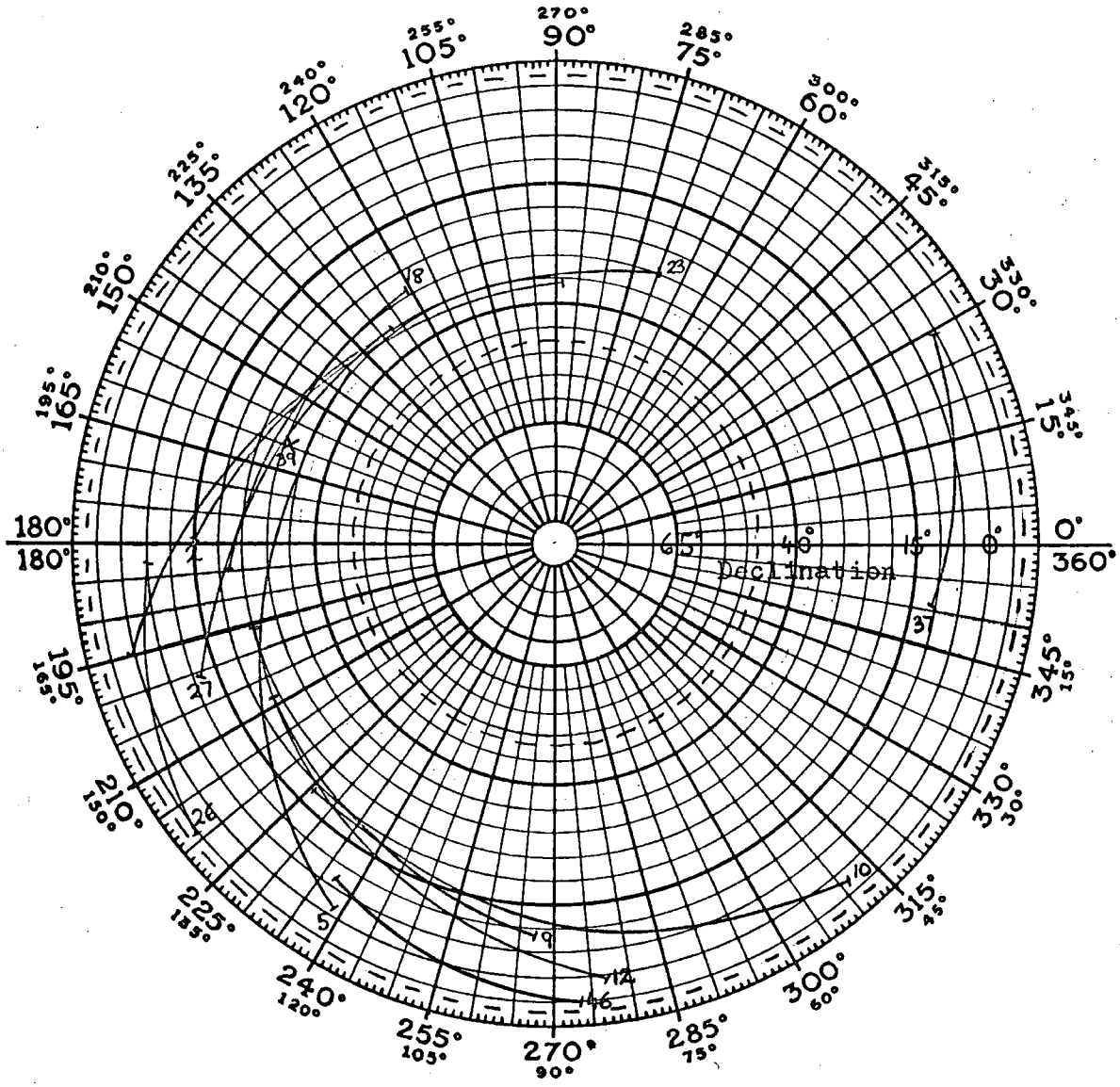

Figure 5.3a

Celestial Co-ordinates of Events with $\beta > 60^{\circ}$.

Northern Hemisphere.

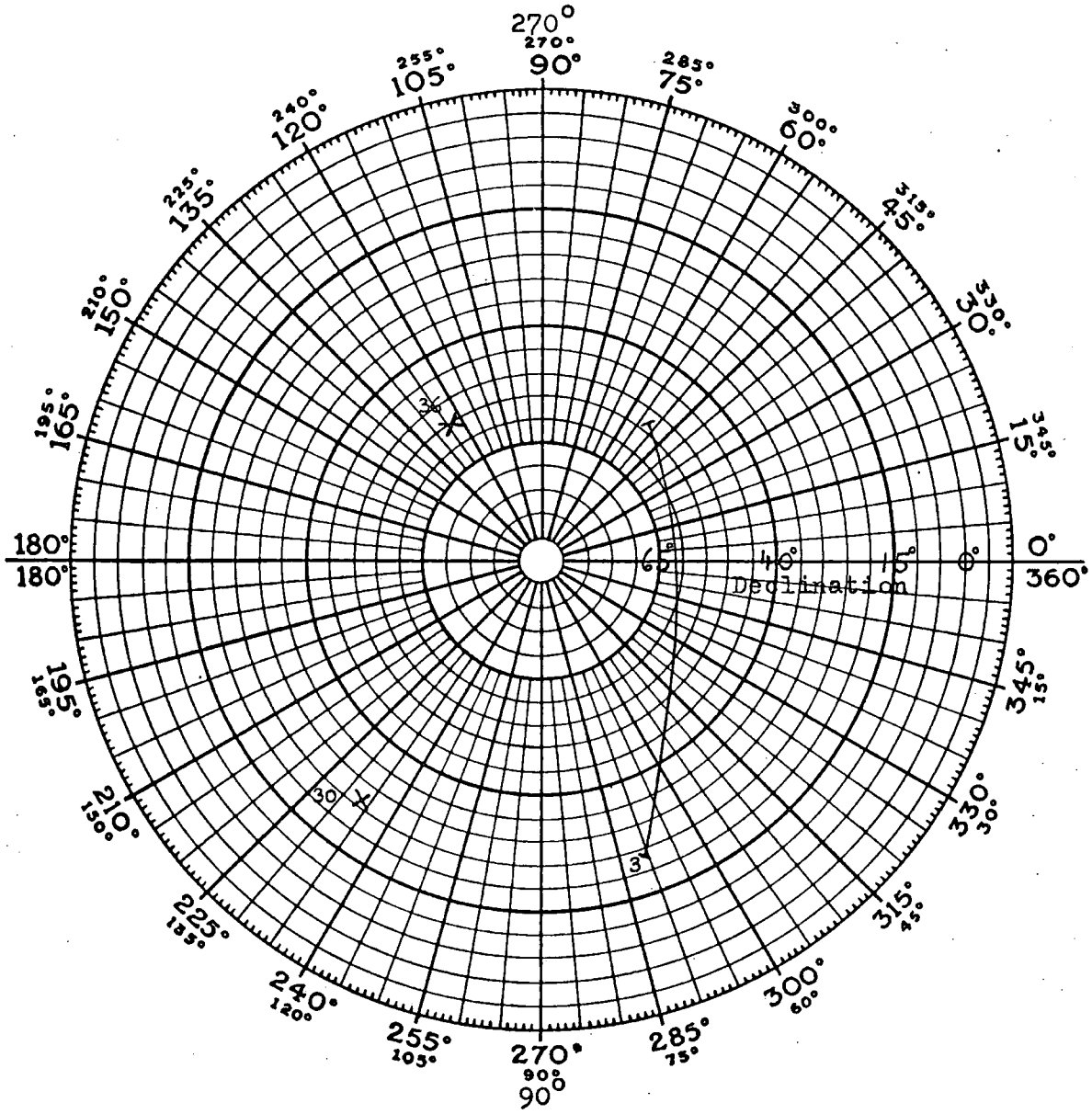

Figure 5.3b

Celestial Co-ordinates of Events with $\beta > 60^{\circ}$.

Southern Hemisphere.

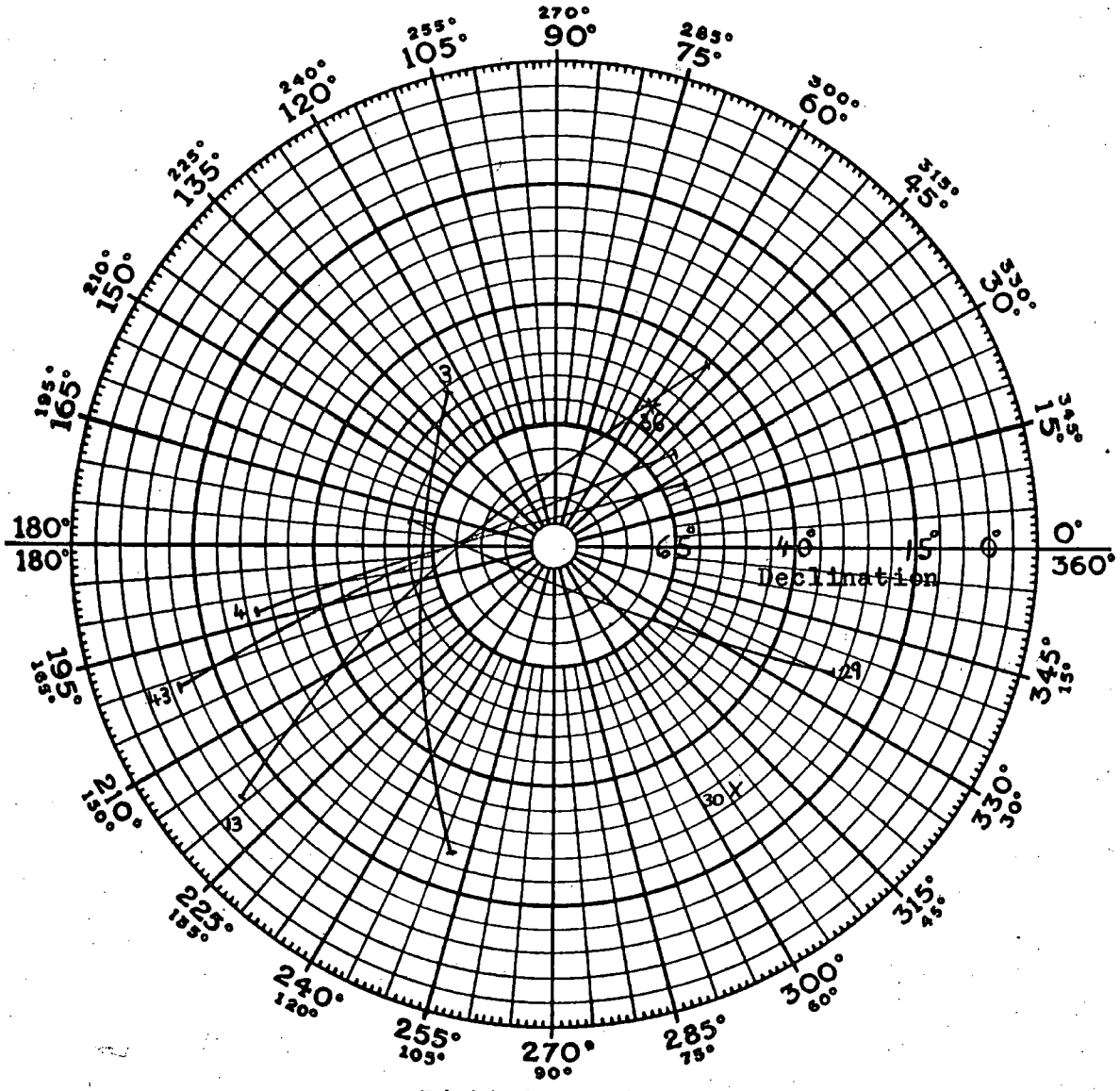

Figure 5.4

Expected and Observed Distributions in Right Ascension for Events with $\beta < 60^{\circ}$.

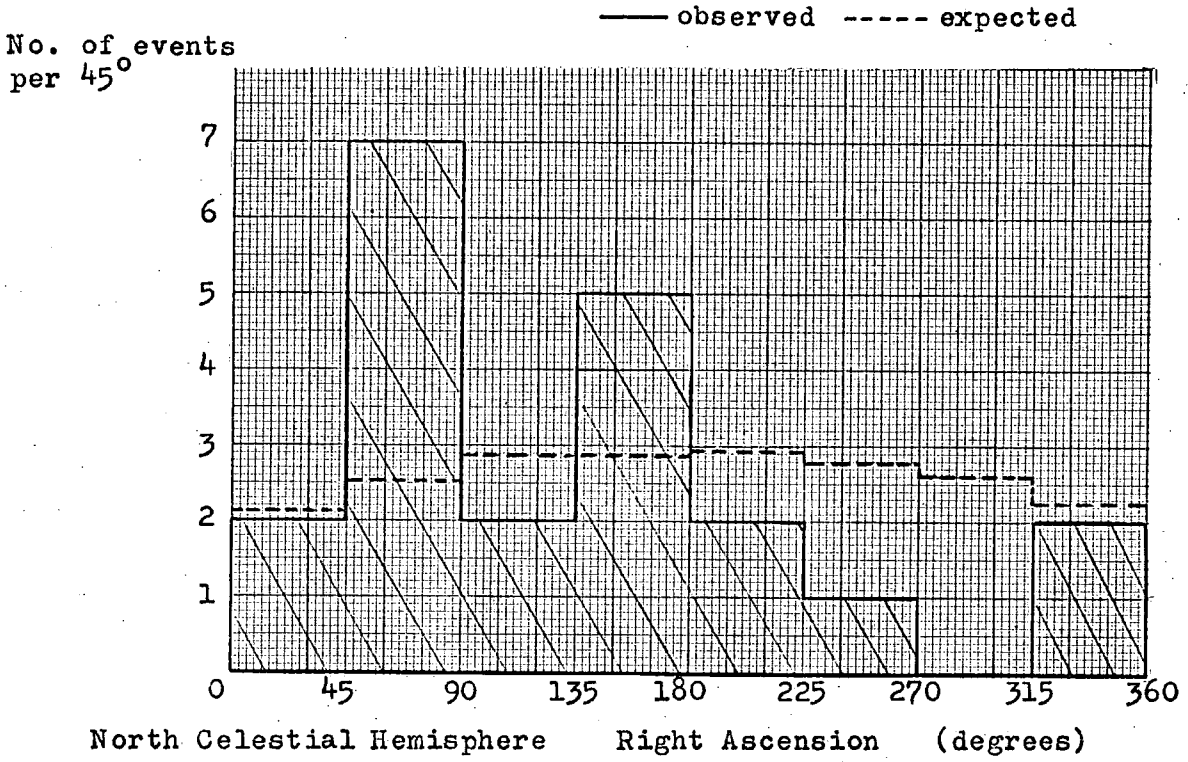

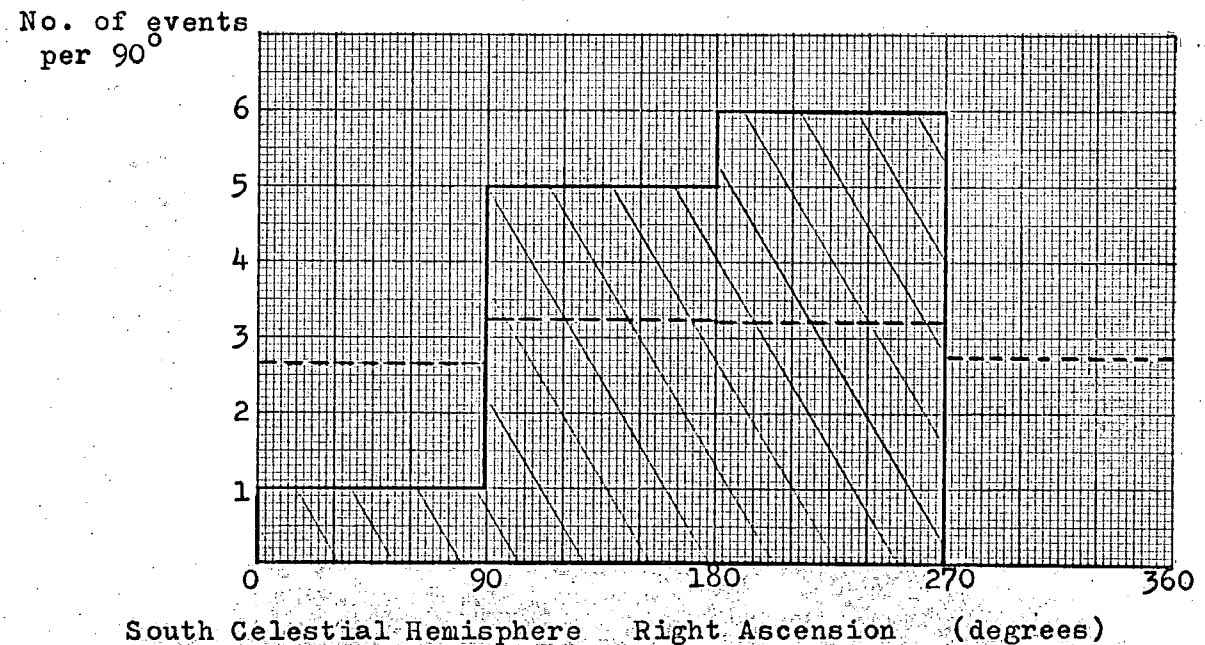

the degree of anisotropy being 95% and 93% for North and South hemispheres respectively.

The chief features are the enhancement of events between 45° and 90° R.A. and the 'dark area' between 225° and 315° R.A. in the Northern hemisphere, and an approximately corresponding enhancement from 135° to 270° R.A. and dark areas from 45° to 90° and from 315° to 0° R.A. in the Southern hemisphere. It must be emphasised that the statistics are poor, especially in the Southern hemisphere and that even with only four 90° cells, the chi-squared test is near the limit of applicability. However, some support for the existence of the dark area comes from the work of Matano et al. (1965) on muon rich EAS having an electron number of approximately 10^{6}. They found an anisotropy in Right Ascension of 97%, the most noticeable feature being a dark area from 225° to 315°. This suggests that the two observations of a deficiency of events in this region may be connected, and that the heavy primary cosmic rays, assumed to be the parents of the majority of the muon rich air showers observed by the Tokyo group, may also be responsible for some of the events observed at great depths underground. A primary cosmic ray which will produce a pion in its first interaction energetic enough to decay to a muon that will penetrate to the depth of the KGF experiment is estimated to have a mean energy of a few times 10^{14} eV, whereas the energy of the primaries of the EAS observed by the Tokyo group were an order of magnitude higher than this.

Observations of muons at shallower depths, notably 4360 m.w.e. (Achar et al. 1965a) have failed to reveal any anisotropy, even when events at high angles to the vertical are examined. This would appear to indicate that the anisotropy, if it is indeed statistically significant, only appears in underground muon directions at depths greater than about 7000 m.w.e. corresponding to muon sea level energies of about 10^4 GeV. The dark area does not appear to lie in the direction of any obvious galactic feature, though the local spiral arm is at 296° R.A. in the Northern hemisphere.

The most recent survey of the galactic magnetic fields shows a field minimum in the line of sight in the direction of the dark area. If the minimum in the line of sight corresponds to a maximum normal to the line of sight, the cosmic rays arriving from that direction would suffer a maximum deflection which would show up as a deficit in the intensity in that direction. However it is difficult to see why such an effect would be constricted to primary energies greater than $\sim 10^{14}$ eV.

The co-ordinates of the probable neutrino-induced muons are shown in figure 5.3. It is apparent that the arcs of events numbers 4, 29 and 43 intersect at a single point, and that if event 13 is assumed to be caused by a particle travelling at 90° to the zenith, an estimate made before any intersection was found, a fourth arc lies within the intersection area. Additionally, the zenith angular range of event number 3, $75^\circ \pm 15^\circ$, gives a region

on the Southern celestial hemisphere that overlaps the apparent intersection. From this it can be seen that the evidence is not inconsistent with those events observed in telescopes 1 and 2 with $\beta > 60^\circ$ having come from a small area between R.A. $180^\circ \pm 4^\circ$ and Dec. $70^\circ \pm 3^\circ$ South. It has been estimated that the probability of the arcs of the three events with clearly defined values of β intersecting within an area of this size is about 1:1200. Because of the uncertainty in the range of β for the remaining two events, the observation that they could also be due to muons arriving from the same direction does not reduce this probability much further.

The apparent intersection area can be explained as being due to chance, or by the neutrino parents of the events arriving from a definite extra-terrestial origin, since the muons are expected to maintain the direction of the initiating neutrino to within a few degrees.

A survey of the sky has been made in the region mentioned. There are no interesting visual objects, and there are no radio sources of appreciable intensity recorded near the position. In a recent 11 cm scan by Day and Thomas over the area R.A. 179°- 180°, Dec. 69°- 72.5° no source greater than the limiting intensity of $\sim 0.5 \times 10^{-26} \omega m^{-2} (c/s)^{-1}$ was found. (E.G. Bowen, private communication). However, a new X-ray source was reported by Harries et al. at the Calgary Cosmic Ray Conference to be located at R.A. $204^\circ \pm 5^\circ$, Dec. $64^\circ \pm 4^\circ$, which is near enough to the apparent intersection to warrant further investigation should

future observations confirm the existence of a point source.

Any apparent origin point of the parent neutrinos would imply that they were extra-terrestial in nature, since the primary nuclear active cosmic ray flux is known to be roughly isotropic at the primary energies giving the greatest contribution to the neutrino flux effective in producing the muons observed underground. The problem of extra-terrestial neutrinos has been reviewed by Osborne (1966). It is expected that the interaction of the nuclear component of cosmic rays with inter-stellar or inter-galactic matter will produce pions and kaons which will subsequently decay producing both ν_e, ν_μ and γ-rays. However this neutrino flux is expected to be isotropic in arrival direction if the primary cosmic rays are isotropic, and from the associated γ-ray production the muon neutrino flux has been estimated to be more than two orders of magnitude less than the atmospheric muon neutrino flux, even at energies in the region of 10^4 GeV.

The alternative possibility is that some neutrinos are themselves primary cosmic rays coming from discrete sources. It is expected that there will be a large flux of thermal electron neutrinos from the Sun and other stars, but because of their low energy they will not be detected in the KGF experiment. Calculations show that supernovae might be expected to give out very large numbers of energetic neutrinos over a very short period, much less than the 18 months separating event numbers 4 and 43, though a series of supernovae type explosions within a massive celestial

object like a quasar could produce the necessary long term flux, and the very great distances at which these objects are thought to lie could result in an attenuation of the γ-ray flux from these bodies by interactions with optical photons.

Measurements on γ-ray emission from discrete sources indicate that at low energies the discrete neutrino flux will be two orders of magnitude less than the atmospheric neutrino flux, but at energies in the region of 5000 GeV the extra-terrestial flux could equal the atmospheric flux. This immediately suggests that the Glashow resonance interaction, which presumes the existence of the intermediate boson, might produce a significant flux of muons at the resonant energy which is about 6000 GeV for $m_W = 2.5$ GeV. It can be seen from table 5.1 that the expected number of events from the Glashow resonance interaction with atmospheric neutrinos is an order of magnitude less than that observed, which would seem to rule out this mechanism, although as explained in the previous paragraph, the estimate of the upper limit of the γ-ray flux could be in error for very distant objects. A further difficulty is that four of the five interactions have been observed to be close to the telescopes, whereas the high energies effective in the Glashow resonance should mean that the average interaction point within the rock wall will be well away from the detectors.

If further observation reveals that there is an apparent discrete source of muons observed to have values of $\beta > 60^{\circ}$, it will probably be necessary to postulate a new mechanism of neutrino

production unassociated with γ-ray production, which will of necessity mean that it will be unassociated with pion production in nuclear active collisions. For the rest of the analysis of this experiment it will be assumed that no extra-terrestial neutrino-induced muons have been observed, and that the arrangement of arrival directions in figure 5.3b is due to chance.

5.8 Shower Events

In the breakdown of events listed in table A.2 there are several categories of event that are not classified as 'in geometry' muon events. The way in which a muon can be out of geometry (part of the electromagnetic accompaniment triggering the fourfold coincidence) has been discussed. In some of these events the muon track is clearly visible, and often the electrons causing the fourfold coincidence can be seen in the flash tube record.

Occasionally a fourfold coincidence is generated by what appears to be a shower of electrons, no clear muon track standing out on the record. A typical shower event is illustrated in figure 5.5 (event no. 24). An electron shower is visible in the south nft array, and the oscilloscope trace for the same wing shows saturated pulses indicating a large energy deposition in the south scintillator wall. The shower does not seem to traverse the telescope, the twofold north wing pulse being small, probably being caused by chance, or by a low energy electron from outside the telescope that failed to penetrate to the north nft array.

EVENT NO.

24

TYPE

shower

TELESCOPE

1

SCINTILLATORS

N S

4 1,3,5

TOTAL RUNNING TIME FOR BOTH TELESCOPES

Array Hours

11786-47

RUN NO.

302

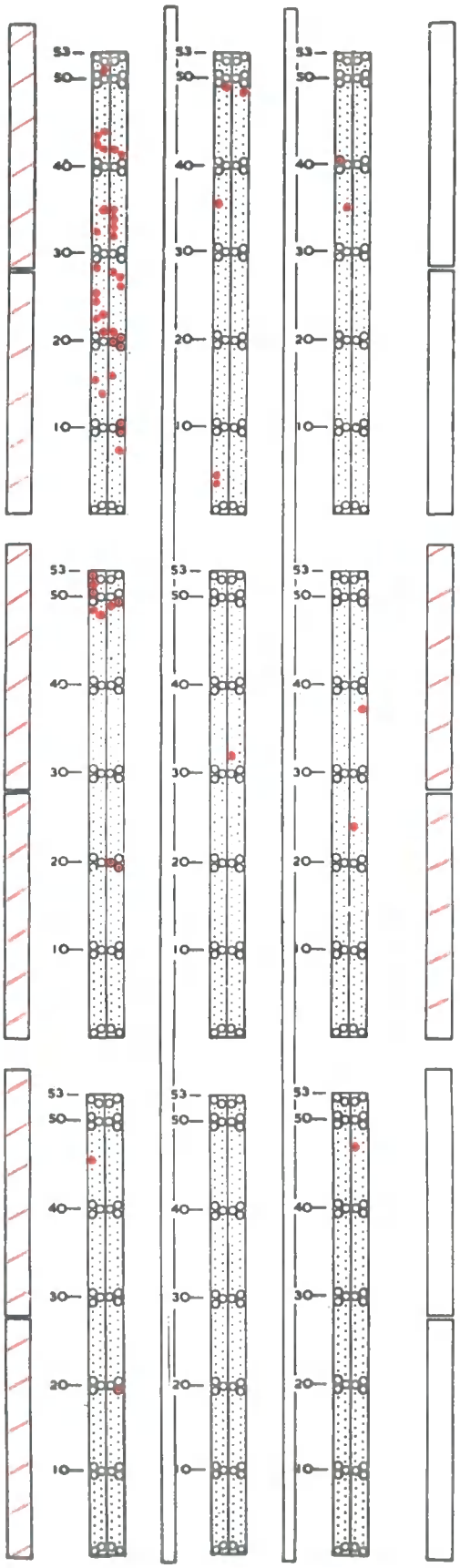

S N

PROJ. Z. A.

about 50°?

PROJ. A. A.

?

DIRECTION

Downwards?

DATE

Day Month Year

25 5 66

TIME I.S.T.

00.01

TIME M.S.T.

15.52

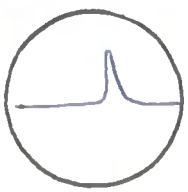

North C.R.O.

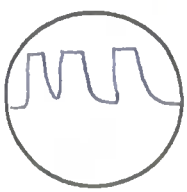

South C.R.O.

Figure 5.5

For the majority of the telescope running time the chance twofold coincidence rate for any pair of photomultipliers was a few hundred per hour, making the former explanation quite possible.

The two other events in this category were similar in nature. Event 13, discussed in appendix A, was a very large shower, though there tracks could be seen in all three nft arrays, the shower apparently penetrating telescope 2 and travelling in a near horizontal direction. Event 21 was a near vertical shower with tracks visible in the top three nft trays, different parts of the same development of the shower being absorbed in the N6 and S5 scintillators. This event is most likely to have been caused by an electromagnetic shower being generated in the rock ceiling by a muon travelling downwards in a near vertical direction, the muon missing the telescope altogether, or its track being hidden by the shower. Event 24 is probably attributable to the same cause, although the shower is by no means vertical in its direction of propagation. A large photon component could give the high number of single and grouped flashes observed, by the Compton effect or by pair production.

The most difficult event to understand in this category is number 13. The very large energy content, estimated to be of the order of several hundred GeV, and the direction of propagation are inconsistent with the initiating particle being an atmospheric muon. One interaction that can give a muon with a very high energy is the Glashow resonance interaction (section 5.4) which might be

expected to produce muons with energy ~1000 GeV. A similar process discussed by Hiroshige and Matsuda (1965), also involving the intermediate boson:

$$\bar{\nu}_e + e^- \rightarrow W^- + \gamma$$

which would take place at neutrino laboratory energies above E_t, the threshold energy referred to in the Glashow resonance interaction discussion, might produce a shower directly from the interaction of the γ-ray, although this interaction would necessarily have to take place close to a telescope for it to be detected.

Alternatively, a high energy electron, created through

$$\nu_e + N \rightarrow N' + e,$$

could cause the development of a large electromagnetic shower, if the energy of the ν_e was large.

Because the nature of the initiating particle is unknown and because any penetrating particle might be out of geometry, this event has not been included in the analysis of the total muon rates. However it appears likely that it is associated with a neutrino interaction rather than with an atmospheric muon.

Table A.2 lists the observation of two possible weak photon showers. They are discussed at the end of appendix A. These 'events' may only be an upward statistical fluctuation in the number of spurious flashes observed combined with an electron track from background radioactivity. In a number of

frames in the nft records short tracks appeared, always in outer nft arrays, that were ascribed to background β-rays because the frame advance and nft trigger was initiated by the timing unit. This unit regularly generated a master pulse to avoid fogging of the open shutter cameras through an over long exposure. However, the three 'events' mentioned in appendix A were triggered by a fourfold coincidence.

A possible interpretation of such events is in terms of weak photon showers, but until further data has been collected it is difficult to assess what significance should be attached to these observations.

It is cases such as these which make it essential to employ a visual detector underground for this type of work, since interpretation that is difficult with a visual record would become impossible without it.

5.9 Conclusion

The expected numbers of events in the KGF experiment from various modes of neutrino interaction have been given in table 5.1. These figures can be converted to expected intensities of muons in the horizontal direction. Figure 5.6 shows the observed horizontal neutrino-induced muon intensity at KGF and at Johannesburg. (The latter figure is given in section 6.1.4). The figure also shows the estimated horizontal intensities under three different assumptions.

Figure 5.6

Comparison of Experimentally Observed Horizontal Muon Intensities

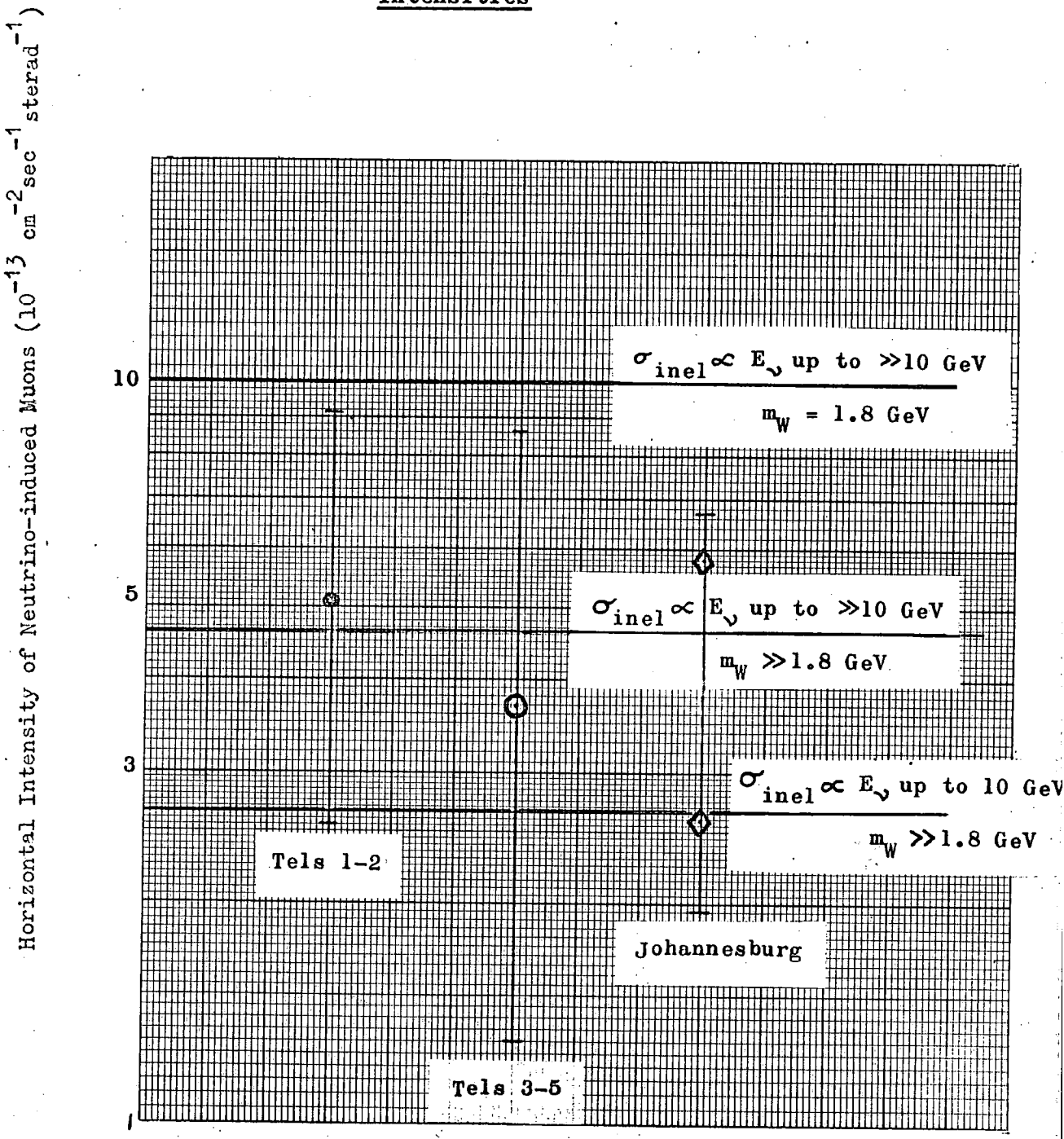

Purely on the basis of the observed rates, it is not possible to distinguish between the contribution to the rate by the presence or absence of an intermediate boson and the contribution by the rising inelastic cross-section. If it is assumed, as seems reasonable, that the inelastic cross-section does not saturate at the limit of machine energies, but continues to increase with energy up to a point controlled by the breakdown of the V-A theory of weak interactions, then it can be assumed that the contribution from a boson mediated interaction is very small, and as a consequence the boson mass, if the boson exists, must be high.

Two methods are being adopted to resolve this dilemma. The first, which was embodied in the design of telescopes 3-5, was to attempt to observe simultaneously two penetrating tracks whose directions were unambiguously defined. The unequivocal pin-pointing of the apparent origin of the tracks, and their passage through 30 cm of iron would enable a firm conclusion to be drawn about the nature of the particles causing the tracks. If two muons were simultaneously observed this would constitute strong evidence for the existence of the intermediate boson.

In chapter 7 the design and recent construction of two magnetic spectrographs is discussed. It is hoped that the elucidation of the energy of a sufficient number of neutrino-induced muons will enable a decision to be made on the type of interaction in which they were produced.

Chapter 6

OTHER NEUTRINO EXPERIMENTS UNDERGROUND

At present there are only two experiments, other than the one at KGF, designed to investigate the neutrino initiated muon flux underground. Chronologically the first of these was the Johannesburg experiment, mentioned in chapter 2, which is now discussed.

6.1 The Johannesburg Experiment

As explained in section 2.2, this experiment is basically very similar to the KGF arrangement. Located in the East Rand Proprietary Mines near Johannesburg, (the only other mine in the world comparable in depth with the Champion Reef Mine, KGF) at a site 3200 m below surface, the overburden is roughly equivalent to 8800 m.w.e. local rock, ($Z^2/A = 5.0$ and $\rho = 2.75$ g.cm^{-3}) or approximately 8500 m.w.e. standard rock. The characteristics of the overburden have not been published, making the conversion to standard rock only an approximate one, the absolute depth in standard rock may be in error by $\pm$ 150 m.w.e. since no great emphasis has been placed on accurately measuring the equivalent depth below surface, the experiment being primarily concerned with measuring the horizontal muon flux.

6.1.1 Description of the Apparatus

The detector array, shown schematically in figure 6.1, consists of two parallel vertical walls made up of 36 detector elements. The array is grouped into 6 'bays' of 6 elements each. Each element is a rectangular box of Lucite of sensitive dimensions 547x56x12.7 cm^3 containing 380 litres of a mineral oil based liquid scintillator and is viewed by two 5 in photomultipliers at each end. Later three further bays were added (nos 7-9), each containing 6 elements of sensitive dimensions 473x56x12.7 cm^3, increasing the detecting area to approximately 165 m^2. The array constitutes a hodoscope giving a rough measurement of the zenith angle of a charged particle passing through it. Additionally, the event is located along the detector axis by the ratio of the photomultiplier responses from the two ends of each element traversed. The sum of the responses indicates the total energy deposited and hence the track length in the scintillator. The energy deposited by a minimum ionising particle traversing the scintillator should be greater than about 20 MeV, well above the energies characteristic of natural or induced radioactivity. The triggering requirement was a fourfold coincidence between any four photomultipliers on one wing of the array.

It is unnecessary to discuss the detail of the experimental arrangement and checking system here, a full account can be found in the literature. (Reines et al 1965a, b, 1967, Reines 1966, Crouch et al. 1966a, b, Gurr 1966.)

Figure 6.1

The Johannesburg Neutrino Detector.

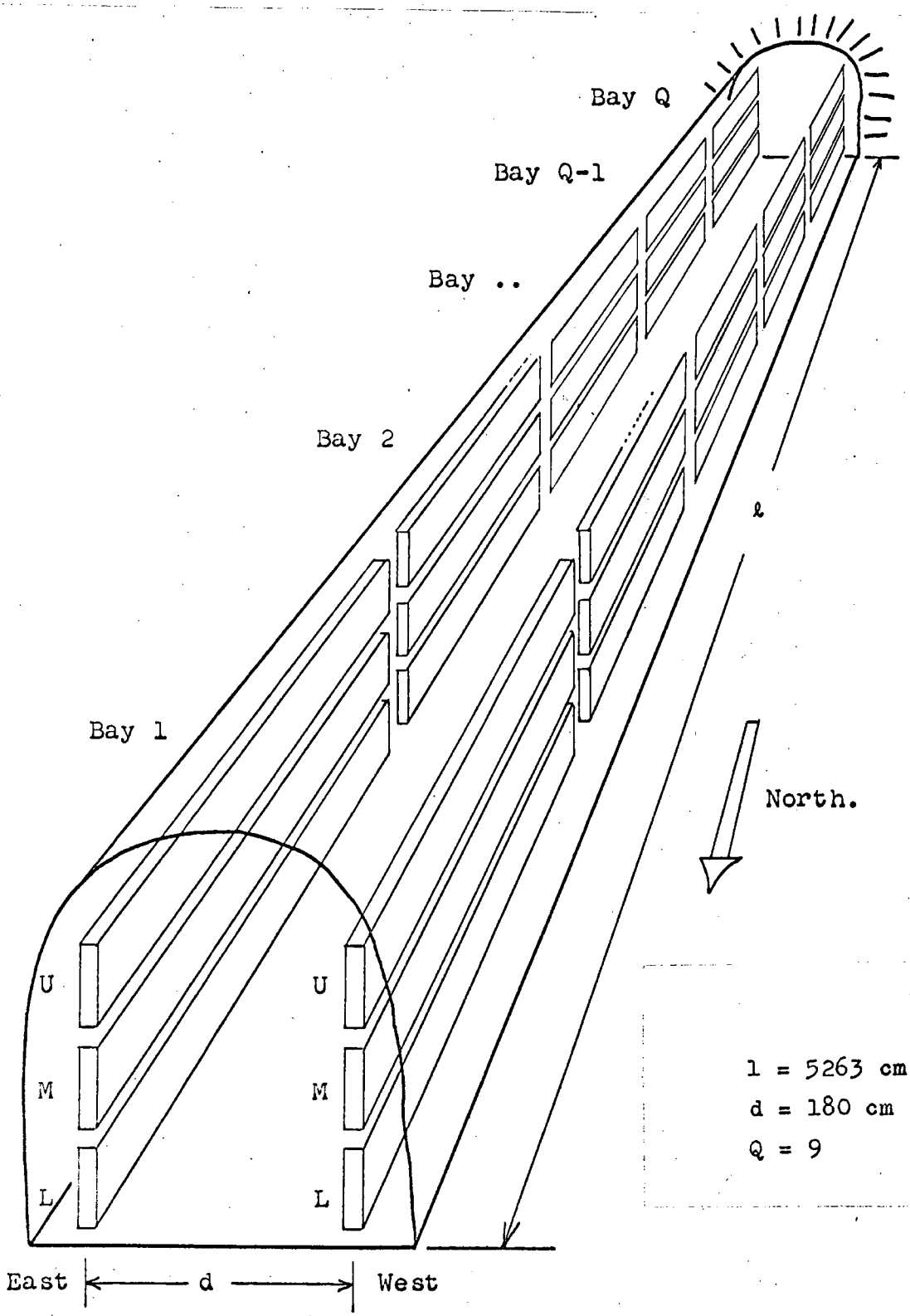

6.1.2 The Results and their Interpretation

With the array illustrated in figure 6.1 several types of event can be recorded.

1) Single Wall Events

a) Single tank events. These are triggered by a fourfold coincidence from the photomultiplier tubes viewing a single tank where no other signal is recorded in any other tank. The cause is most probably a single ionising particle traversing an element and failing to pass through any further elements.

b) Double and triple tank events in a single bay. A particle travelling in a near vertical direction will possibly pass through two or three tanks in a single bay.

c) Coincidences involving more than one bay. In the light of the KGF experiment it seems likely that these events are caused by particle accompaniment, either of a soft, electromagnetic type or pionic or muonic in nature.

2) Cross Tunnel Events (Double Wall Events)

a) Single tank incidences, one tank on each wall. These events are most probably due to a single particle moving across the tunnel at an angle greater than 43° to the zenith. This category divides into three classes, (i) U-L, (ii) U-M or M-L and (iii) U-U, M-M or L-L coincidences, where U = upper, M = middle and L = lower tank in any bay.

b) Multitank incidences involving only one bay on each wall.

c) Multitank incidences involving more than two bays and both walls. In view of the results of the KGF experiment these two categories can both be explained in terms of muons accompanied by electromagnetic showers, inelastic neutrino interactions, etc.

With this complexity of events, coupled with the fact that two or more tracks in any element will make the pulse height analysis difficult if not impodsible, it can be realised that the interpretation of this experiment is not easy. This conclusion is readily confirmed by reading the most up to date report, Reines et al. (1967), where the rate of neutrino-induced muons through the apparatus is quoted as lying between

$$(2.0 \pm 0.5 \text{ and } 4.5 \pm 0.7)10^{-13} \text{ cm}^{-2}\text{sec}^{-1}\text{sterad}^{-1}.$$

There are several difficulties associated with the derivation of a rate of either neutrino-induced or atmospheric muons. First there is no exact method for determining the angle the particle trajectory makes to the vertical. When both scintillator walls are traversed the zenith angle can be gauged to approximately $\pm 19^{\circ}$ by noting which of the six tanks in each bay was triggered, although this assumes that only one tank per wall is involved. In theory the energy deposited by a particle will be a function of its path length through the scintillator and hence of its spatial zenith angle. However this picture is confused by the quoted inaccuracy of the determination of the deposited energy, $\pm$ 20% to 30%, the increasing rate of energy loss with particle energy, and by the existence of secondary particles

accompanying the parent muon into the scintillator.

This lack of resolution of the spatial zenith angle is most important for single tank events, since cross-tunnel events involving both walls require that particles have $\theta > 43^{\circ}$. Because of the depth of the experimental site and the small cross-tunnel aperture of the detector at that angle, the contribution to the observed rate of cross-tunnel events from atmospheric muons is negligible. Single tank events are thus attributable to both atmospheric and neutrino-induced muons, and since the angular distribution of the former cannot be measured the separate contributions have to be estimated from an assumed angular distribution.

Unlike the KGF experiment, events that are 'out of geometry' cannot be subtracted easily from the total number of single tank events, but the proportion of such events can be assessed from the KGF data and allowances made for them in the estimated intensities.

The multitank events constitute a separate problem. Almost certainly they are caused by muon accompaniment, though the lack of absorbing layers between the scintillators makes it difficult to assess its nature. Where the energy deposition in one or more tanks is very high it is likely that an electromagnetic shower has entered, or been produced in the scintillator, but as has been seen in the KGF experiment, it is not always necessary for a penetrating particle to be present.

In the cross-tunnel events, 2a, it was found that approximately one third of the events deposited between 5 and 10 MeV in one of the two tanks, a level well below that expected on average from a minimum ionising particle; whilst the deposition in the other tank appeared reasonable when compared with the value expected from the known azimuth angle, (the position of the track can be estimated to $\pm$ 0.6 m along the length of the tank) and an assumed average particle energy and zenith angle. It is estimated that no more than 20% of these events can be explained by assuming that the particle passed through a corner of the scintillator tank. Some of the events may be due to a low energy electron being absorbed in an element on one wall whilst the parent muon traverses the other wall, but the large fraction of these events makes it unlikely that this is the complete explanation. Particles having fractional charges, the hypothetical quarks, might be expected to deposit amounts of energy of the order of 5 - 10 MeV, but the lack of any other evidence for their existence does not allow much emphasis to be placed on an interpretation in terms of these particles.

6.1.3 The Rate of Neutrino-Induced Muons

If it is assumed that all cross-tunnel events of the type 2a are caused by neutrino-induced muons, μ_ν, and that the cross-tunnel multitank events 2b and c are attributable to the same cause, rather than showers, or pairs or 'bundles' of particles

travelling in a near vertical direction giving rise to apparent cross-tunnel coincidences, then an upper limit to the μ_ν flux is obtained. Conversely, if it is assumed that those events of type 2a with an unusually low energy deposition in one wall are not μ_νs, and that none of the complex events in 2b or c is attributable to an in geometry μ_ν, then a lower limit to the flux is obtained. The most recent estimate of the flux given by the Johannesburg group is that given above, based on almost three years of experimentation. (September 1964 to June 1967). This is the instrumental flux, which because of the geometry of the Johannesburg array can best be compared with the flux through telescopes 3-5 in KGF, with which it is in good agreement.

The horizontal flux may be obtained in the manner described in section 5.6 by assuming a median neutrino energy of 10 GeV to give the shape of the correction factor to be applied to the differential aperture of the Johannesburg array. The horizontal intensity is found to be

$$(2.6 \pm 0.65 \text{ to } 5.8 \pm 0.9)10^{-13} \text{ cm}^{-2}\text{sec}^{-1}\text{sterad}^{-1},$$

a value that agrees well with the values from the KGF experiment, plotted in figure 5.6.

6.1.4 The Rate of Atmospheric Muons

These constitute the majority of events of type 1. The latest paper available containing details of the different types of event is that of Reines (1966). The results are listed in

table 6.1.

Table 6.1 The Johannesburg Results

No. of Events	Type of Event
23	Two tank cross-tunnel single particle (2a)
189	Single tank (1a)
35	Two tank vertical (1b)
19	Three tank vertical (1b)
4	Three tank cross-tunnel (?) (2b)
14	Multitank events (>3 tanks) involving both walls or in more than one bay (1c and 2c)

The results in categories 1a and b can be expressed in terms of 'tank incidences', defined so that there are 189 + (2 x 35) + (3 x 19) = 316 tank incidences in these two categories. The differential aperture for incidences from the upper hemisphere for any one tank can easily be calculated, the resulting aperture for the sum of the 54 single tanks in the array is shown in figure 6.2. The difficulty now arises of assigning an angular distribution to the atmospheric muon events. For the lack of better data we assume that equation 4.5.2.1 holds, from which n = 9.0, with an error assumed to be $\pm$ 1.5. When the differential aperture of figure 6.2 is multiplied by $\cos^9\theta$ and integrated, it is found that the total effective aperture for the sum of all the single tanks

Figure 6.2.

The Differential Aperture of the Johannesburg Array for Downward Travelling Muons.

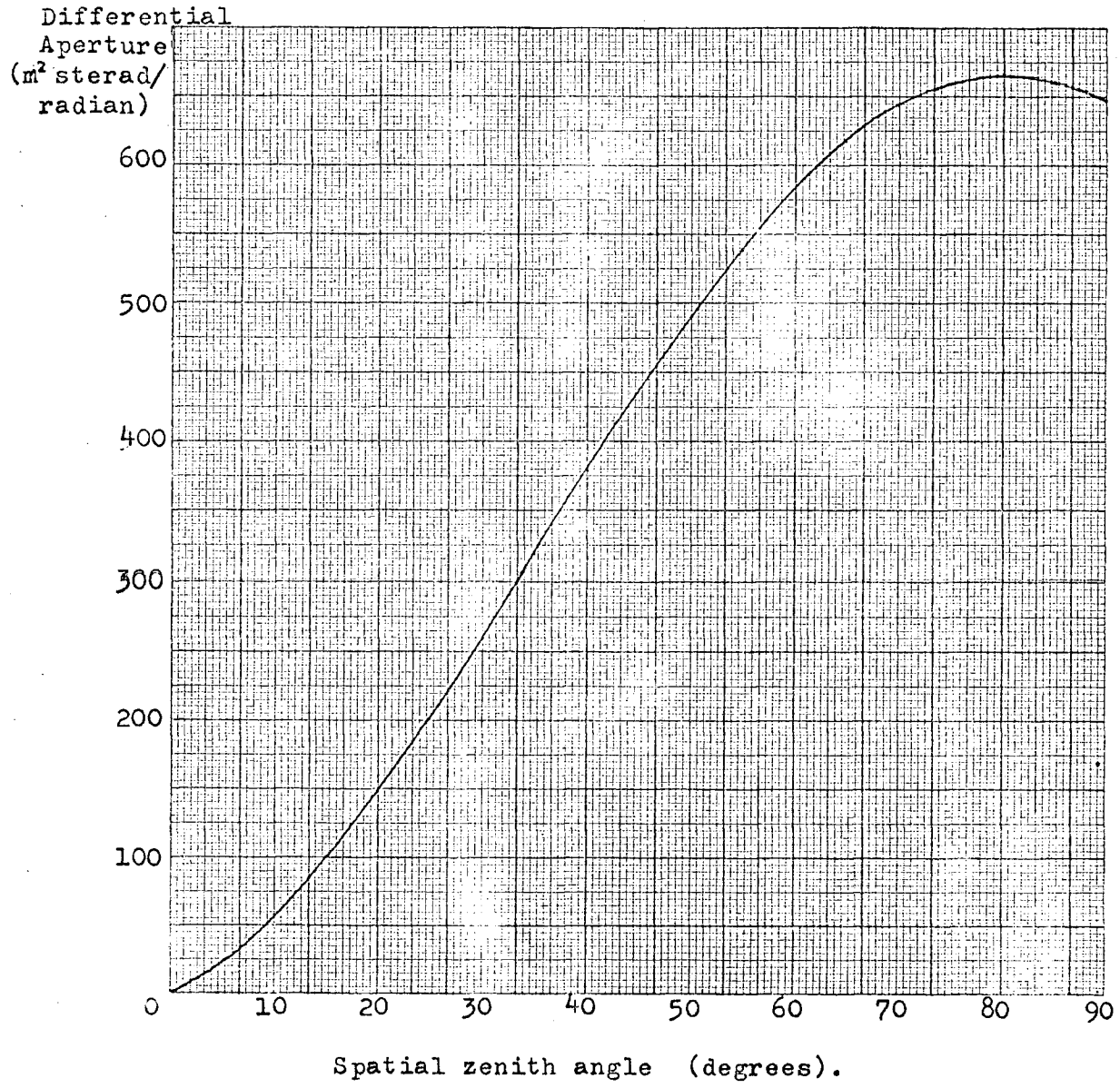

in the upper hemisphere is 44.2 m^2sterad. The effective running time for the total array was 0.93 years.

Before the vertical atmospheric intensity can be calculated the number of tank incidences caused by μ_ν must be deducted from the observed total. The total aperture in both hemispheres for the sum of the 54 tanks is 1231.1 m^2sterad (Gurr 1966) and the total aperture for cross-tunnel events is 324 m^2sterad. The aperture for μ_ν events in categories 1a and b is thus 907.1 m^2sterad, which with a running time of 0.93 y and an intensity of $(3.25 \pm^{1.95}_{1.75})10^{-13}$ $cm^{-2}sec^{-1}sterad^{-1}$ indicates that $86 \pm^{52}_{47}$ tank incidences were caused by μ_ν events, leaving $230 \pm^{52}_{47}$ attributable to atmospheric muons, μ_a. However, no account has been taken of the multitank events, type 1c. If it is assumed that half of the 14 events listed above are of type 1c and that each of them involves ~2 tank incidences, then the total number of tank incidences attributable to μ_as is $244 \pm^{52}_{47}$. This results in a vertical intensity of $(1.9 \pm 0.4)10^{-11}$ $cm^{-2}sec^{-1}sterad^{-1}$. If the inaccuracy inherent in the assumption that n = 9.0 is taken into account, a final intensity of $I_v = (1.9 \pm 0.7)10^{-11}$ $cm^{-2}sec^{-1}sterad^{-1}$ is obtained. It must be pointed out that this assumes that no events are out of geometry, i.e. that a penetrating muon was observed in each case to pass through the acceptance of the detector. However, for various reasons, the chief of which is that the accompanying particle must deposit at least 20 MeV in the scintillator, the assumption is thought to be a reasonable one.

In the paper delivered to the Calgary Cosmic Ray Conference (Reines et al. 1967) 28 events were observed to be in category 2a, of which 3 were in class (i), 12 in class (ii) and 13 in class (iii). These rates, when taken with the relevant apertures and running times, separately confirm the μ_ν intensity quoted in the paper, but more particularly it can be shown that ~3 events of μ_ν origin are expected to fall in class 2a(i), confirming that the atmospheric muon rate detected by the apparatus at $\theta > 43^\circ$ is negligible, certainly less than one event to date. Thus it is not possible to differentiate between an exponential and a cosine power law operating in the atmospheric angular distribution, from an analysis of the number of events in division 2a(i).

6.1.5 Conclusions and Future Developments of the Experiment

Summarising, the results of the Johannesburg experiment are in good agreement with those of the KGF experiment, confirming that the underground neutrino-induced muon flux exists, and has a magnitude close to that expected from an extrapolation of the machine neutrino-nucleon cross-sections. The flux observed in the near vertical direction is somewhat lower than might be expected from that observed at the KGF site, but the discrepancy, which is within the statistical limits of uncertainty, is not sufficient to determine the shape of the angular distribution of atmospheric muons at these depths. The feature of the experiment which remains partially unexplained is the apparent low energy deposition

DURHAM UNIVERSITY SCIENCE 17 JAN 1968 SECTION LIBRARY

of some of the penetrating cross-tunnel particles. It is possible that these events may be related to the weak photon showers, mentioned in section 5.8.

Since it was realised, some time ago, that the limits on the present experiment came chiefly from the lack of a visual record of the passage of a particle through the detector, plans have been made to transfer the experiment to an enlarged site slightly deeper and to install 12 layers of neon flash tubes between the two scintillator walls. With the adoption of this technique it may well be possible to interpret further the results so far obtained, as well as to acquire more precise estimates of the magnitude and direction of the muon flux.

6.2 The Utah Experiment

Although primarily designed to detect neutrino-induced muons, this experiment differs considerably from the two previously discussed. Sited at a depth of about 1500 m.w.e. standard rock in a mine near Salt Lake City, Utah, the detector relies on the unambiguous determination of the sense of direction of the muons traversing the apparatus to distinguish between atmospheric and neutrino-induced muons.

6.2.1 Description of the Apparatus

The development of a novel type of cylindrical spark counter and a large area Cerenkov counter enabled a completely

new approach to be tried. The detector is illustrated schematically in figure 6.3. The four Cerenkov counters, each consisting of a water filled concrete tank 6 x 10 x 1 m^3 provide the coincidence trigger for the banks of cylindrical spark counters. Mirrors cover the 1 x 6 m^2 and 1 x 10 m^2 surfaces of the tanks. Each 6 x 10 m^2 surface is covered by an array of light collector elements which are 6 ft long, 1.75 in diameter plastic tubes filled with mineral oil and a wave shifter. A 2 in diameter photomultiplier views one end of each tube and a mirror covers the other. The arrays, on opposite walls of each Cerenkov counter, enable the direction of traversal of a minimum ionising particle to be determined since, typically, 25 to 50 photo-electrons are produced in one array after the Cerenkov light has been trapped and wave shifted, whilst very few are produced in the opposite collectors. Data recording includes the pulse heights from each Cerenkov array as well as the relative time of the pulses, so that in the most favorable case the direction of the muon is determined by four independent Cerenkov measurements and three time of flight measurements.

The event rate, triggered on any one Cerenkov counter that indicates an energy release of about 200 MeV, (the particle travelling close to the horizontal so that most of the light strikes a single collector surface), is about 4 per minute. Specifically upward travelling muons can then be attributed to a neutrino origin.

The cylindrical spark counters fill the role occupied by

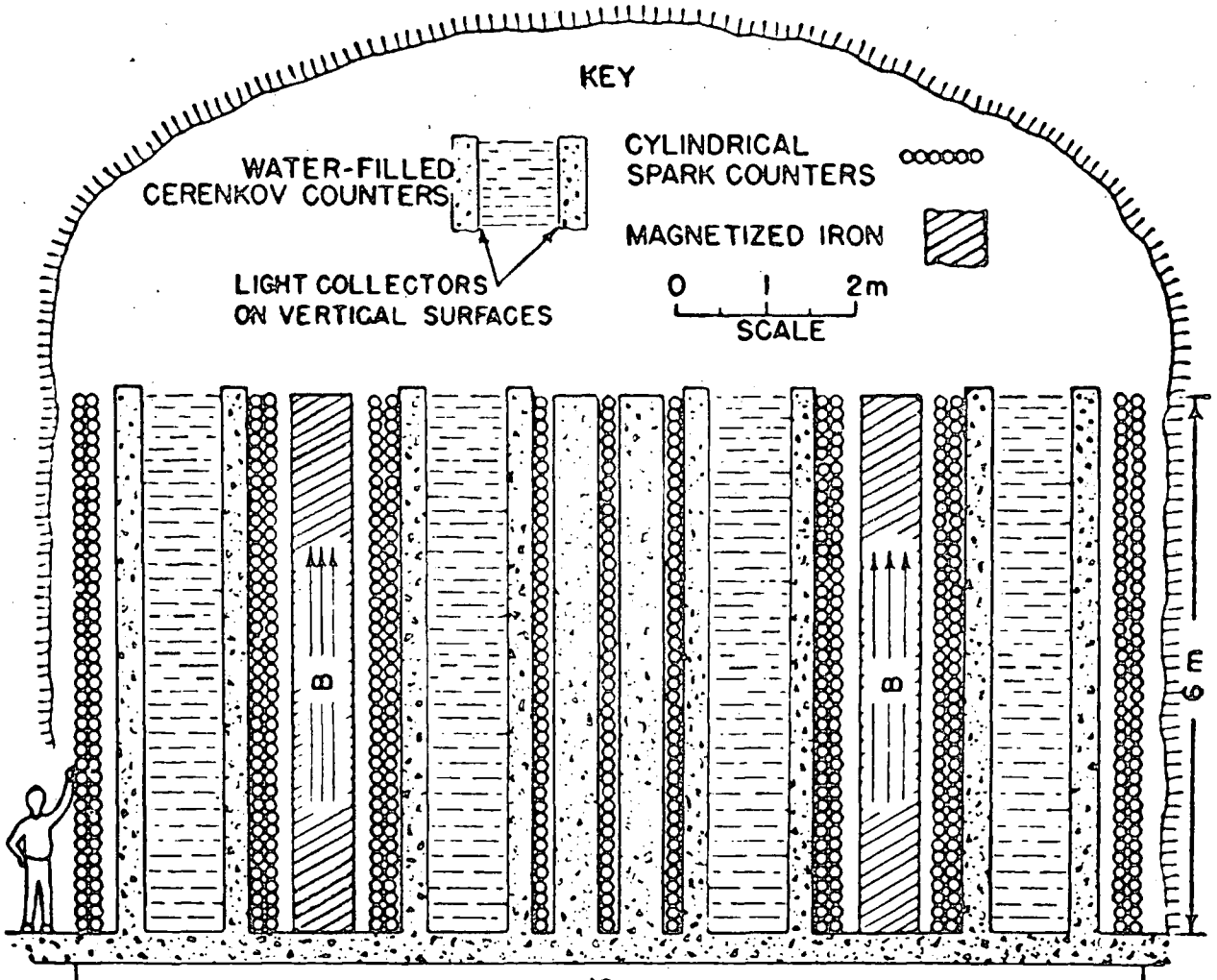

Figure 6.3. The Utah Neutrino Detector.

The dimension of the detector normal to the plane of the paper is 10 m.

the neon flash tubes in the KGF experiment. They resemble giant Geiger counters 15 cm in diameter by 10 m long. A central wire at 6 kV runs the length of the counter, which is filled with 50 cm Hg of argon and 25 cm Hg ethylene, and the application of a 1.7 μs 2 kV pulse causes a sharply localised corona spike at the point of ionisation. The streamer only builds out to about 3 mm from the centre wire before quenching takes place. Microphones mounted inside the counter at either end record the discharges, and this simple technique has been found to give a resolution of the position of the spike along the tube of about 3 mm when a single particle has penetrated the counter. Several particles can be recorded at the same time in a given counter provided that they are separated by about 15 cm. The efficiency of the counters was measured as being very close to 100%.

The two regions of magnetised iron, which are each in a field of 16 k.gauss, are expected to allow the momentum of particles to be determined up to a maximum detectable momentum of about 100 GeV/c.

The design and development of the detectors used in the experiment have been described fully by Keuffel and Parker (1967), Hilton et al. (1967) and Bergeson and Wolfson (1967). The progress of the experiment has been reported by Bergeson et al. (1965 and 1967).

6.2.2 Results and Conclusions

In order that the detectors to be used in the underground experiment might be tested, a half scale prototype was built on surface, and was successfully operated from March to August 1966, detecting more than 2.10^6 cosmic ray muons. This pilot experiment, which provided many useful results as well as testing the design for the full scale experiment, was the first in which muon pair production by muons was conclusively detected. (Morris and Stenerson 1967).

The underground detector began operating in April 1967, and until June this year had logged a number of atmospheric muons, but no upward travelling neutrino-induced muons had been detected. (Bergeson et al. 1967). The aperture of the experiment is $\sim$160 m^2sterad, which taken with a measured μ_ν intensity of $\sim 3.10^{-13}$ $cm^{-2}sec^{-1}sterad^{-1}$, indicates that about one neutrino event a fortnight might be expected to have been detected. The 'no count' result is therefore not unexpected, since the 'on time' of the detector was only three weeks.

The surprising feature of the results, as reported at the Calgary Cosmic Ray Conference in the middle of June 1967, was the angular distribution of the atmospheric muons. This distribution is reproduced in figure 6.4. The predicted number, N_μ(predicted) is based on the summary of Menon and Ramana Murthy (1967) of the depth-intensity curve. The two sets of points are obtained, with and without the secθ correction term for the enhanced π-μ decay

Figure 6.4.

Preliminary Results of the Utah Experiment.

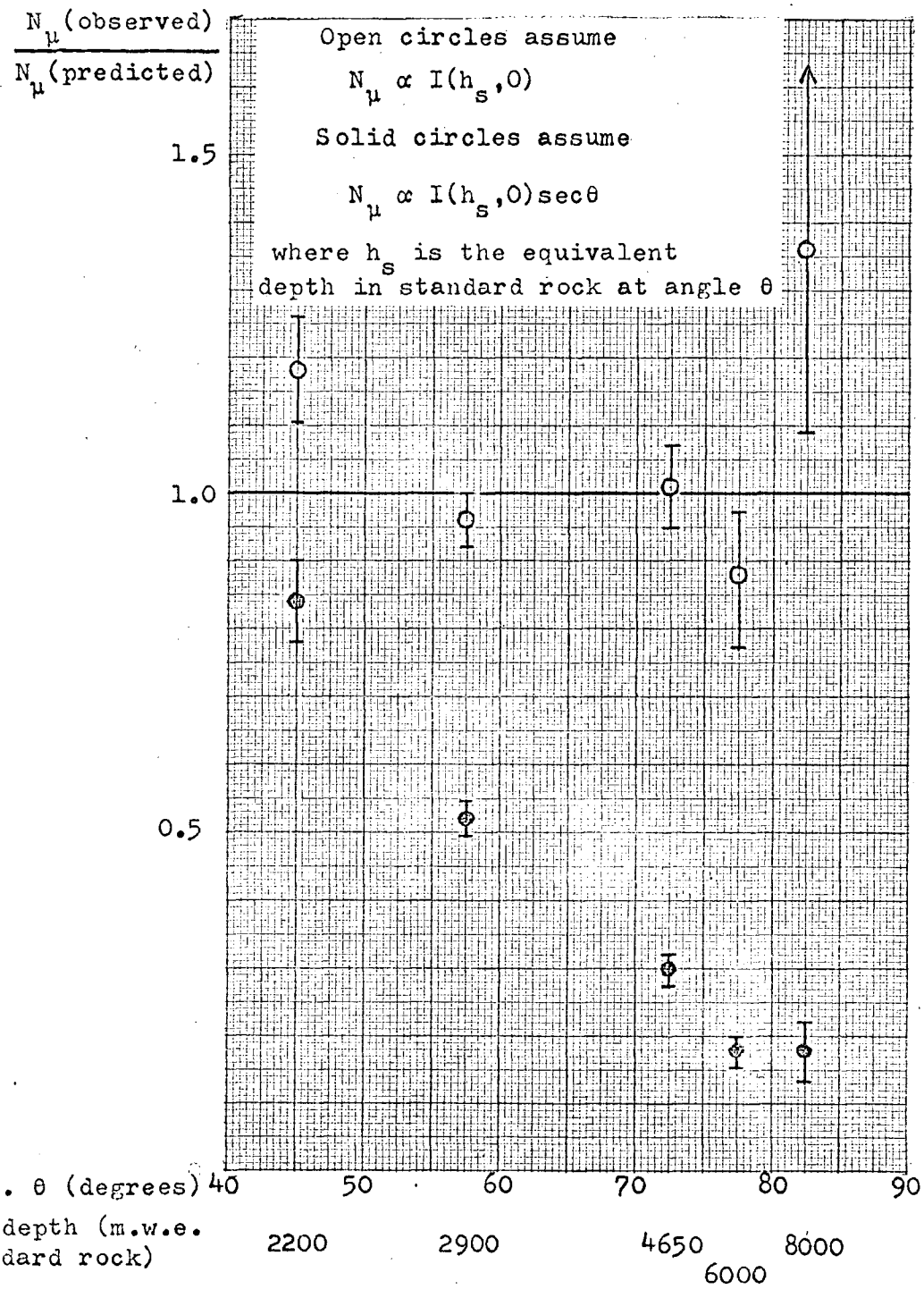

in the atmosphere, discussed in section 4.4. If correct, this graph would indicate that the secθ term did not apply at angles greater than about 45^{o}, a result only apparently explicable, according to the Utah group, by assuming that pion decay is not the production mechanism of the muons observed, but rather that they are produced either by the decay of very short lived secondaries or directly in the nuclear interactions of the primaries and their secondaries in the upper atmosphere. This result seems to be in contradiction with the predictions of quantum electrodynamics, since the cross-section for direct muon production would need to be $\sim 10^{6}$ greater than that expected on the basis of accepted theories (J. Wdowczyk: private communication).

A more likely explanation is the breakdown of the correctness of the secθ term at high angles because of the finite curvature of the atmosphere, especially if the interactions giving rise to the pions, which subsequently decay to muons, take place very high in the atmosphere. This, coupled with the survey of Menon and Ramana Murthy, (which as already noted gives, perhaps, a rather high estimate of the muon flux at great depths,) and the inaccuracies inherent in the estimation of the effective depth (and its correction to standard rock,) for a surface topography as complicated as that existing in the Utah experiment, where the experimental site is at the centre of a mountain, may account for a good deal of the effect observed. However, the result clearly needs very careful examination and it is to be hoped that the fuller analysis by the Utah group,

which is presently in hand, will clarify some of the ambiguities.

It is interesting to note that many workers have found a deficiency of events at high angles to the vertical whilst working at depths ~1500 m.w.e., resulting in the observation of a value of n, the exponent of the angular distribution, that is higher than that expected from the depth-intensity curve with the usual secθ correction. This disparity can be seen in figure 4.4.

Because the Utah experiment can potentially be triggered on events occurring within the 2000 ton bulk of the apparatus, it should be possible to register the production of secondaries of neutrino interactions very close to the point of the interaction. A knowledge of the energies and relative directions of emission of the secondaries, which should be available in the most favorable cases, will be of great use in determining the principal mode of interaction and the form of the interaction cross-section at neutrino energies higher than the 10 GeV currently available from accelerators.

The approach used by the Utah team would seem to be the most promising one devised to date, though only after an extended period of observation will it be possible to see if the particular problems that beset an underground detector have been successfully resolved.

Chapter 7

RECENT DEVELOPMENTS IN THE K.G.F. EXPERIMENTAL PROGRAMME

7.1 Introduction: The Energy Spectra of Neutrino-Induced Muons

A theoretical study of the neutrino interaction cross-sections and the production spectra of muons emerging from a neutrino-nucleus collision showed that a significant number of the neutrino-induced muons probably had an energy at the detector of less than 30 GeV. This conclusion was confirmed by the evidence from the electromagnetic accompaniment of muons coming from near horizontal directions, as has been explained in chapter 3. A very recent paper on the energy spectra of atmospheric and neutrino-induced muons at the KGF site (Craig et al. 1967) gave the theoretical estimates reproduced in table 7.1.

From these considerations it was thought worthwhile to build two spectrographs underground in the KGF laboratory with the aim of examining the momentum of the neutrino-induced muons up to a maximum of about 30 GeV/c. It was realised that even with large area detectors the rate of events whose momenta could be measured accurately would be low, so it was decided to modify the design of a conventional spectrograph to accept muons from the near vertical as well as the horizontal. A discussion of the spectrographs is given in the next section. Subsequent sections

deal with the first results from these detectors and summarise the plans for the KGF experimental programme.

Table 7.1 Mean Energies Expected at the Detector for Neutrino-Induced Muons from the Horizontal

	Processes and Cross-sections	$\bar{E}_\mu$(GeV)
i)	Elastic + $\sigma_{inel} \propto E_\nu$ to 10 GeV, then const.	8.8
ii)	Elastic + $\sigma_{inel} \propto E_\nu$ to 10^4 GeV, then const.	80
iii)	(i) + Boson production, m_W = 1.8 GeV	28
iv)	(i) + Boson production, m_W = 3.0 GeV	27
v)	(ii) + Boson production, m_W = 1.8 GeV	60
vi)	(ii) + Boson production, m_W = 3.0 GeV	76

7.2 The Magnetic Spectrographs

The gift of approximately 100 tons of soft iron from the Yawata Iron and Steel Company, Japan, made it possible to build two spectrographs, rather than the alternative proposition of a further extension of the existing array by adding more units of the telescope 1 type. After a design study a compromise between magnet area and thickness was reached so that the spectrograph magnets were identical in having a thickness of 40 cm and an area of 2 x 4 m^2. The advantage of a thick, high field magnet is that it gives a better magnetic deflection to scattering ratio than a thinner magnet would allow, although the latter has a larger

acceptance area if only a fixed weight of soft iron is available.

Between November 1966 and May 1967 two spectrographs of the type illustrated schematically in figure 7.1 were constructed. The magnets are each composed of 40 soft iron blocks 10 cm thick, and wound with 25 turns of 5 x 0.5 cm^2 cross-section aluminium belt on each of the four magnet arms. Figure 7.2 is a diagram of one of the magnets. The curved end-pieces complete the flux linkage to give an approximately uniform field in each of the four arms of 14 k.gauss when a current of 250 amps is passed through the coils.

The scintillator elements are identical to those used in telescopes 1 to 5, eight elements covering each of the 2 x 4 m^2 sides with four further elements mounted on top of the spectrographs.

A master pulse is generated by any fourfold coincidence involving two pairs of photomultipliers, each pair of tubes viewing a separate scintillator element. The coincidences thus fall into two groups, those involving top-side coincidences, almost entirely attributable to atmospheric muons and their secondaries, and those involving side-side coincidences. Muons causing side-side coincidences must have a zenith angle greater than 26.5°, because of the scintillator geometry, and are therefore likely to be a mixture, those of atmospheric origin predominating over those of a neutrino origin.

The neon flash tubes were loaded into the trays with

Figure 7.1

A Front View of one of the KGF Magnetic Spectrographs

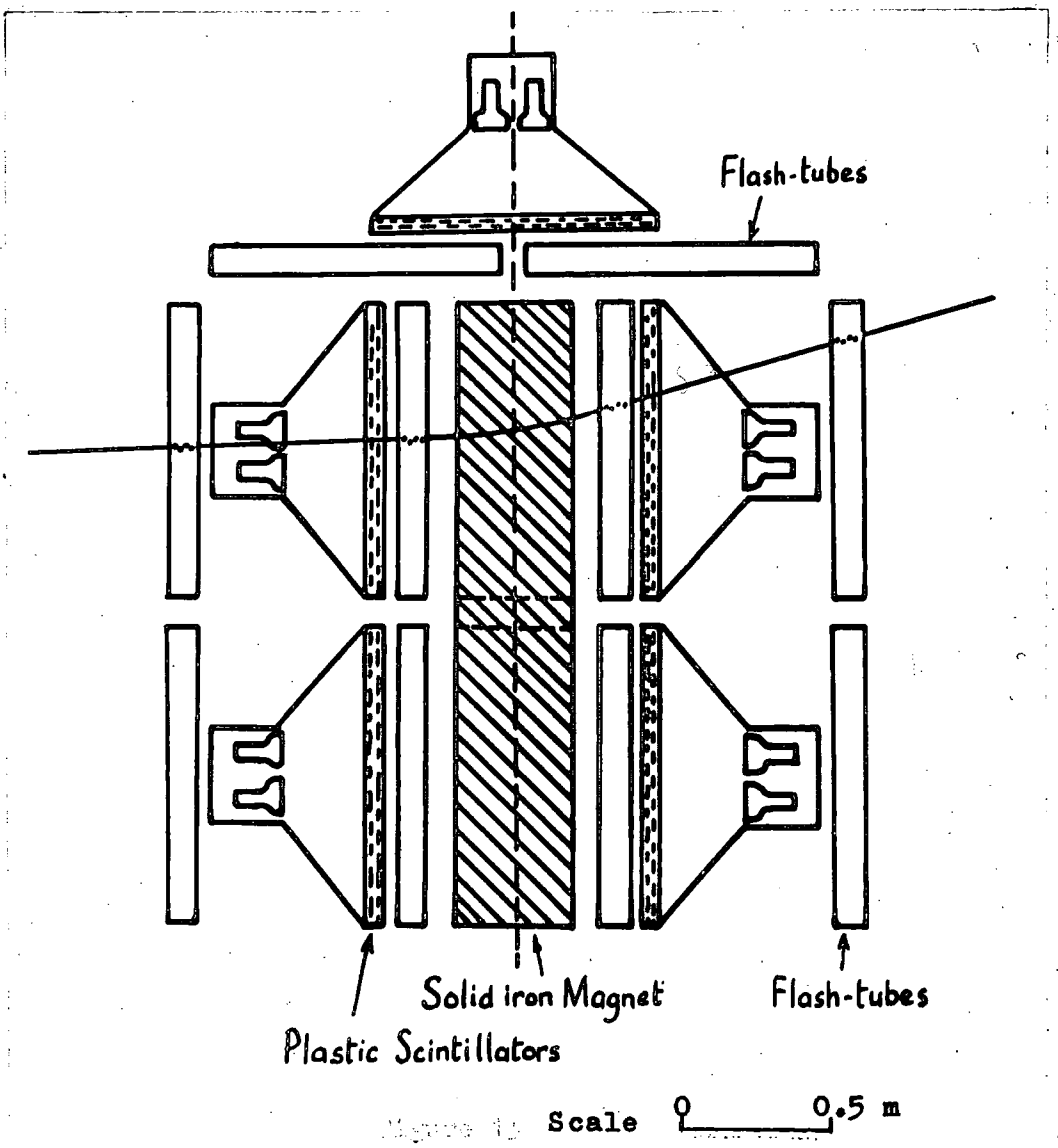

Figure 7.2

Side Elevation of a Spectrograph Solid Iron Magnet

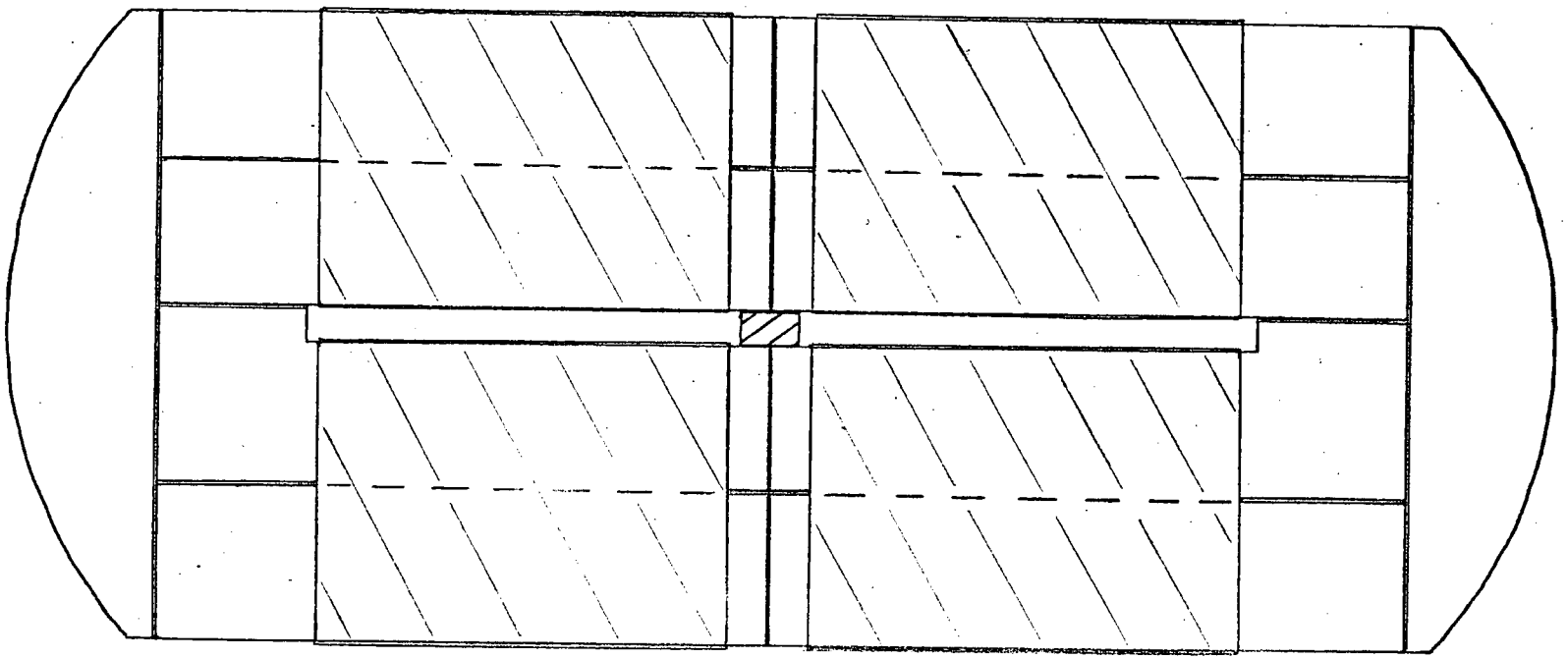

Brass

Aluminium coil

Iron

0 25 50 75 cm

Scale

greater care than had been given to the trays of earlier telescopes, two trays 1 m high by 2 m long placed back to back giving the 4 m long coverage required. Each spectrograph contains 20 flash tube trays arranged as illustrated in figure 7.1. The back-front alignment is estimated to have an average error of $\pm$ 2 mm for any flash tube, giving a maximum detectable momentum of about 40 GeV/c for a particle travelling close to the horizontal, if it is assumed that no scattering takes place.

It can be shown that the Coulomb scattering and magnetic deflection of a muon in the magnet are related by

$$\theta_{mag}/\theta_{scat(r.m.s.)} = 0.38 t_m/\sqrt{t_s}$$

where t_m is the projected path length in the magnet, normal to the flux lines, and t_s is the spatial path length of the muon through the magnet. For a normal incidence $t_m = t_s = 40$ cm and the rms value of Coulomb scattering will be 42% of the magnetic deflection.

The end vertical scintillator elements were masked where the field direction was greater than about 30° to the horizontal so that the spectrograph would not accept particle trajectories that passed through a region of the magnet whose field was greatly different from 14 k.gauss. The differential aperture of one of the spectrographs is drawn out in figure 7.3, the calculation being based on the dimensions given in table 7.2. (Osborne: private communication). It is assumed that the scintillator thickness is negligible, making the differential aperture zero at

Figure 7.3

Differential Aperture of a KGF Magnetic Spectrograph

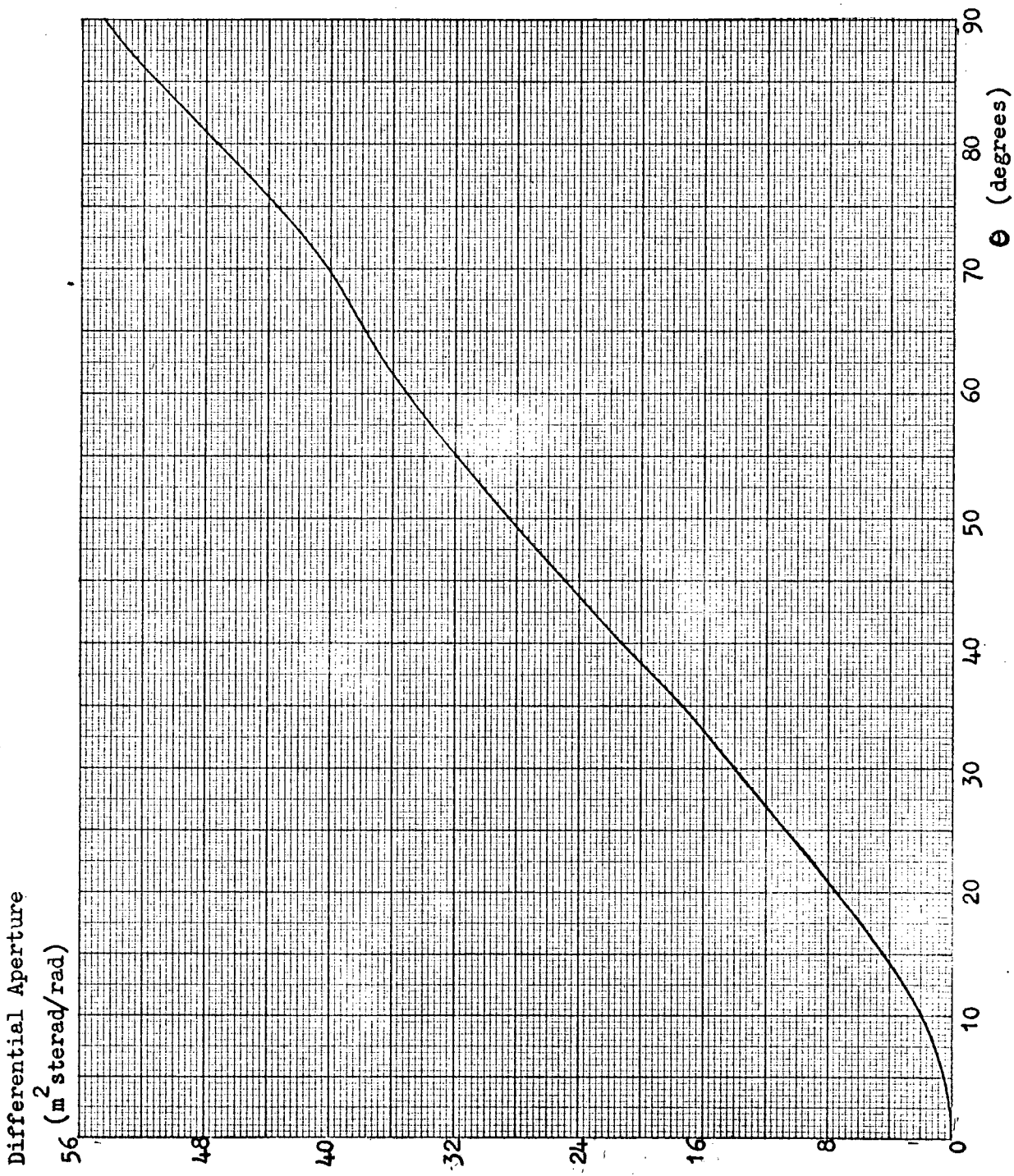

$\theta = 0$. The total aperture for isotropic radiation is 38.8 m^2sterad, a value which should be reduced by about 18% to allow for scintillator gaps and masking.

Table 7.2 Characteristics of the Spectrograph Scintillator Configuration

Scintillator top	Value (cm)
Length	415
Width	100
Separation of horizontal centre plane from top of side scintillator wall	39.0
Scintillator walls	
Length	417
Height	209
Separation (centre to centre)	103.5
Orientation	(^{o}West of North)
Spectrograph 1	15.2
Spectrograph 2	10.5

If an angular distribution of $I_\theta = I_v \cos^{8.25}\theta$ is assumed to hold for atmospheric muons, then the total effective aperture for atmospheric muons is 1.21 m^2sterad. After an allowance for gaps it is estimated that the rate of atmospheric muons through either spectrograph should be approximately 4.10^{-3} hr^{-1}.

Using the rate of neutrino-induced muons observed to traverse telescopes 1 and 2, the expected rate through each spectrograph is in the region of 3.5×10^{-4} hr^{-1}, since the aperture for neutrino-induced muons from both hemispheres is 30.8 m^2sterad after allowing for gaps. Possibly half of these events will pass through the magnet and the outer neon flash tube trays in such a way that the momentum of the muons can be measured to give a useful result.

7.3 Preliminary Results and Further Developments

In the period 12th May to 1st August 1967 a total of 10 events were recorded in the spectrographs in a running time of approximately 2600 spectrograph-hours. These events will not be discussed in detail since their analysis is at a very preliminary stage. All but one of the events is a top-side coincidence, as might be expected, however some of the events fail to show a penetrating particle since there is no absorber between the top and side scintillator elements, other than the magnet.

An event, S6, is illustrated in figure 7.4. This event is a typical downward travelling muon producing secondary particles in the magnet. From the complexity of this and other events it is clear that the interpretation will be difficult unless absorber is placed between the top scintillator elements and the upper horizontal flash tube trays. Initially it is proposed that $1\frac{1}{2}$" of iron will be used (~2.1 radiation lengths) as this is readily

EVENT NO
86

RUN NO
626

DATE
9/7/67

TIME 03.08 IST 21.56 MST

SPECTROGRAPH
1 Back

SCINTILLATORS
S- T4 N3

S CRO T CRO N CRO

TOTAL RUNNING TIME (SPECTROGRAPHS) 1605-00

AZIMUTH ANGULAR RANGE
6°-80° W of spec N

DIRECTION
Downwards

PROJECTED ZENITH ANGLE
11.5°?

SPATIAL ZENITH ANGULAR RANGE
11.5°-49.5°

MAGNET CURRENT
210 A

MAGNETIC DEFLEXION
-

MOMENTUM
-

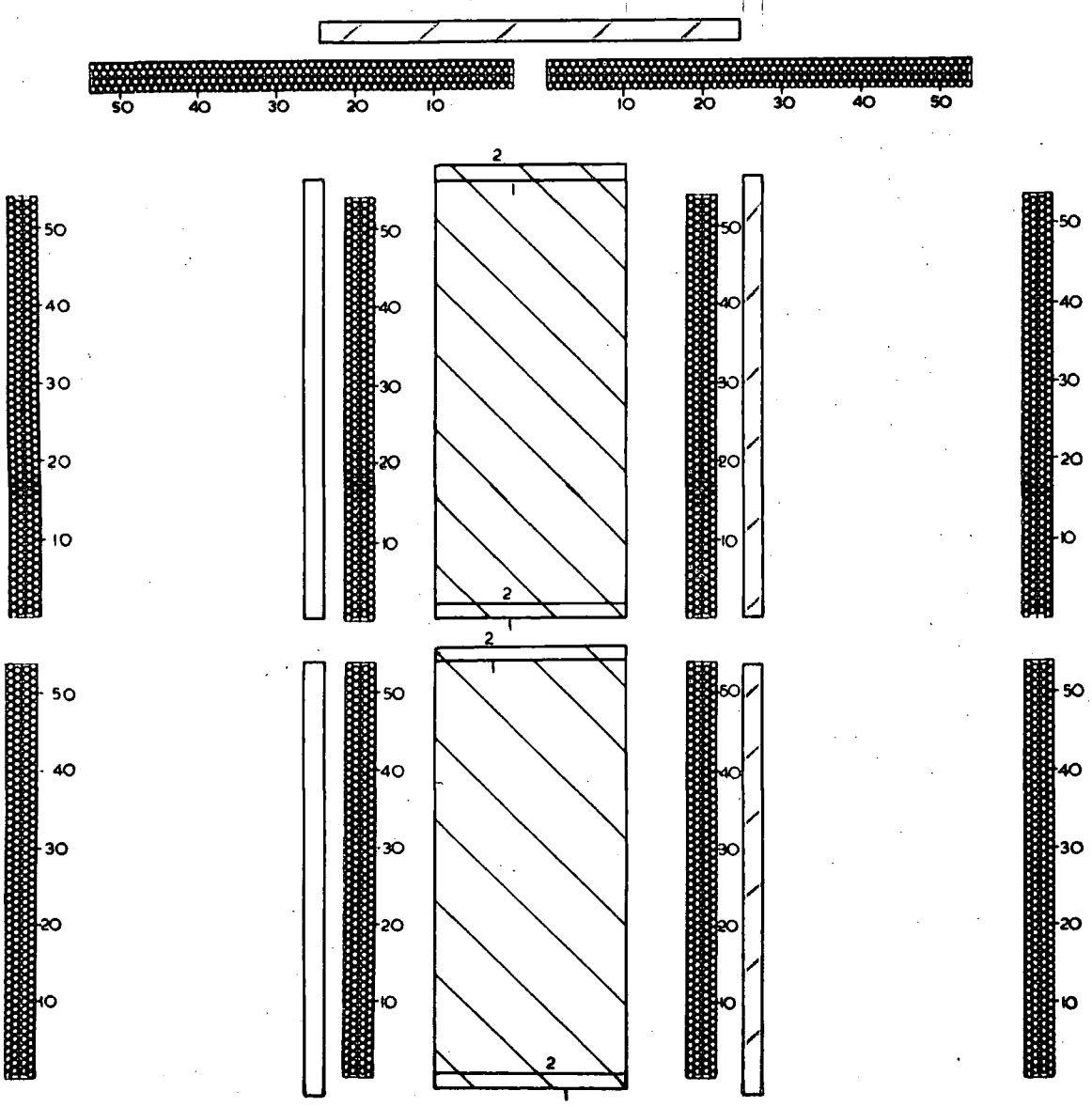

Figure 7.4

available, but ideally 5 radiation lengths of iron would be preferable to eliminate fourfold coincidences triggered by showers from the rock ceiling.

7.4 Conclusion

It is to be hoped that the two spectrographs will provide answers to several of the major problems still outstanding in the KGF experiment.

The top-side scintillator coincidences will give information on the angular distribution and electromagnetic accompaniment of atmospheric muons. The greater accuracy with which the angular distribution can be defined will enable the inference of atmospheric intensities at greater depths and will aid the separation of atmospheric and neutrino-induced components.

More detailed information on the electromagnetic accompaniment will help to confirm the tentative conclusions reached in chapter 3 on the mean energy of atmospheric muons at 7500 m.w.e. and will show up any pairs of muons that arrive from the near vertical direction.

Although the rate of accumulation will be slow, the possibility exists of determining the chief mode of interaction of neutrinos with nuclei from a knowledge of the mean energy, at the detector, of neutrino-induced muons. The increased rate of μ_ν detected by the seven arrays now installed at KGF will enable a more accurate limit to be placed on the μ_ν flux, which coupled with

the momentum data should indicate the form of the inelastic cross-section at energies higher than 10 GeV, as well as allowing a higher upper limit to be placed on the mass of the intermediate boson, or enabling its detection.

Chapter 8

SUMMARY

8.1 Atmospheric Muons

The use of a visual technique in the form of the neon flash tube to detect muons has enabled a wealth of data to be accumulated on the characteristics of muons arriving at a detector at a depth of 7500 m.w.e. The results of the analysis of the experimental information listed in appendix A can be considered under three headings: electromagnetic accompaniment, angular distribution and vertical intensity.

The electromagnetic accompaniment of muons by a soft component was reviewed in chapter 3. The observations of Achar et al. (1965a) at depths less than 5000 m.w.e. were shown to be in accord with an expectation based on the mean muon energy which was derived from the sea level muon energy spectrum and the range-energy relation for Kolar rock. The broad assumption that muons at 7500 m.w.e. with a projected zenith angle of less than 50° were atmospheric in origin lead to the conclusion that their mean energy was in the region of 500 GeV, a value that was higher than that expected from an exponential depth-intensity relation of the type suggested by Menon et al. (1967a). The result could be explained on the assumption that the muon intensity falls as D^{-9}

(where D is the depth below ground level) since this relation predicts a mean energy of 490 GeV for the atmospheric muons observed in the KGF neutrino experiment.

Confirmation of a non-exponential depth-intensity relation was found in an analysis of the angular distribution of the events. When the events expected from an approximately isotropic distribution of neutrino-induced muons are subtracted from the observed distribution, the remaining events have a rather flat distribution. The marked excess of events at about 45° p.z.a. over that expected from an exponential angular distribution can be explained in several ways. Firstly it could represent an upward statistical fluctuation on expectation; this seems unlikely since the excess has a chance occurrence of less than 3.5%.

Secondly it could be caused by neutrino-induced events. An assessment of this possibility has been made by Craig et al. (1967). The only mechanism thought to exist that would give an excess of events specifically at angles in the region 40° - 50° is that of the Glashow resonance since, if it exists, the Earth will no longer be transparent to electron neutrinos of the resonance energy. However to account for the observed excess of events they found that a velocity distribution of the atomic electrons in rock would be needed that was very different from the one believed to exist and that a much higher neutrino intensity at energies of several thousand GeV would be required.

The third, and most likely explanation of the events is that the depth-intensity relation is not exponential and that the

angular distribution follows a $\cos^n\theta$ law even at very great depths, a finding that is in accord with that from an analysis of the electromagnetic accompaniment.

A knowledge of the angular distribution of muons at 7500 m.w.e. enabled an estimate to be made of the depth-intensity relation at greater depths. The single experimental observation of Reines (1966) at 8500 m.w.e. gave a result that was not sufficiently accurate enough to confirm the proposed relation, but the depth-intensity relation obtained from the primary cosmic ray spectrum of Greisen by Craig et al. (1967) was close to that predicted from the observed angular distribution of muons at 7500 m.w.e. Craig et al. used generally accepted models and relationships for the high energy interactions of the primaries, the propagation and multiplicity of the secondaries, and the derivation of the sea level muon spectrum and its translation, via the energy-loss curve and fluctuation correction, to the depth-intensity relation. This therefore tends to indicate that the depth-intensity relation derived from the angular distribution of muons at 7500 m.w.e. is compatible with presently accepted theories.

The continued operation of the seven detectors at KGF should give a total number of events that is large enough to give a relatively unambiguous indication of the angular distribution, and hence the depth-intensity relation at greater depths.

The possible anisotropy observed in the arrival directions of atmospheric muons at 7500 m.w.e. could be explained by a high

magnetic field component normal to the line of sight in the direction of the anisotropy, but until better statics are available such inferences are only speculative.

In response to a paper by Higashi et al. (1965) who claimed that measurements of muon intensities under rock were inaccurate, the results from experiments at depths down to 1500 m.w.e. under sea water and rock were discussed and it was shown that there was no significant difference between sea level muon spectra derived from intensity measurements under the two media. It was further shown that comparable experiments at depths in the region of 4000 m.w.e. in different media could give information on the value of b, the energy loss parameter.

8.2 Neutrino-Induced Muons

It is this aspect of the experiment that has proved to be the most important in terms of new developments in the fields of cosmic ray and high energy physics. The unambiguous registration of a signal from neutrino-induced muons by two experimental teams using different techniques, one in India and the other in South Africa, has opened up the possibility of a new experimental approach to the understanding of weak interactions. The rock walls enclosing an underground detector provide an effective target thickness of many thousands of tons for high energy neutrinos, a condition that cannot be duplicated at present accelerators.

In a paper to be submitted to the Proceedings of the

Physical Society, Craig et al. (1967) have extended the analysis of the expected rates and mean energies of the neutrino-induced muons through the KGF detectors to construct the graph reproduced in figure 8.1. As explained in chapter 5, the instrumental intensity expected at the detectors depends on the energy at which the rising inelastic neutrino-nucleon cross-section saturates and on the mass of the intermediate boson, if it exists. However the mean muon energy $\bar{E}(\mu_\nu)$ is also a function of the type and dominance of each interaction as can be seen from table 7.1, so that in principle it is possible to separate the contribution to the total muon rate of the inelastic mode and the boson mediated mode, if the mean muon energy can be determined. Curves representing different saturation energies for the inelastic cross-section and masses for the intermediate boson, are drawn out and the shaded area represents the region in which most of the detected muons are believed to lie. The only indication of the muon energy to date is that from the electromagnetic interactions of the muons which suggests that $\bar{E}(\mu_\nu)$ lies between threshold and 30 GeV.

The operation of the spectrographs will help the interpretation considerably, and it is possible that the analysis of muon scattering in the lead absorber of the telescopes, which is at present only in the preliminary stages, will enable the upward travelling muons to be distinguished from the downward travelling atmospheric muon background. This analysis assumes that an atmospheric muon can only rarely be expected to show any scattering,

Figure 8.1

The Relation Between the Rate and the Mean Energy of Neutrino-induced Muons

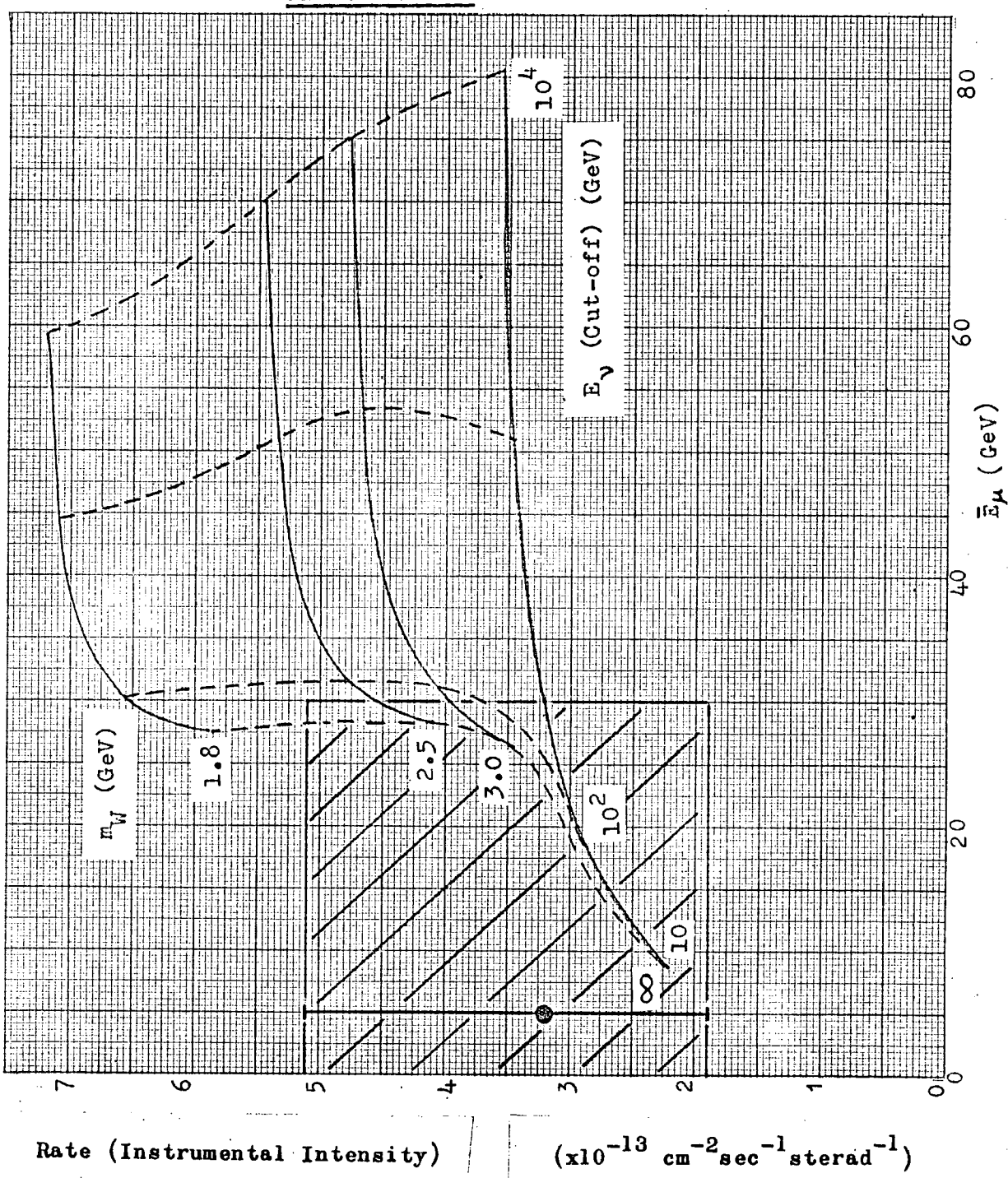

whereas neutrino-induced muons have a high likelihood of being scattered, since their mean energy is thought to be less than about 30 GeV. The difficulties associated with scattering measurements stem from the accuracy of the flash tube alignment. If the tubes are not all exactly parallel, the back-front misalignment of one group of tubes can give rise to an apparent scattering if the particle passed through the backs of the tubes.

Despite the uncertainty in the value of the mean muon energy, some inferences can be drawn from figure 8.1. It is unlikely that the inelastic cross-section saturates at 10 GeV or just above, since the data from accelerators indicates a rising cross-section up to 10 GeV, and, in this case, it is probable that the mass of the intermediate boson is greater than about 2.5 GeV. If there is no boson mediated contribution, the inelastic cross-section appears to saturate at a few hundred GeV, and if the boson contribution is significant this saturation energy is reduced to well below 300 GeV.

The initial results are therefore in accord with expectation: the boson contribution is small if not zero and the inelastic cross-section does not continue to increase indefinitely. However, it has been pointed out by Lee (private communication to A.W. Wolfendale) that the assumption of a constant energy taken by the muon in an inelastic interaction may not be valid, in which case a continuously increasing inelastic cross-section cannot be ruled out.

The possibility of detecting extra-terrestial neutrino sources was discussed in chapter 5. At present the statistics are hardly significant, but if an appreciable number of muons does prove to come from a point source the conclusions reached above will have to be revised.

It is expected that the neutrino experiments in progress will continue for several years since the initial results have proved encouraging. The consquent improvement in statistics coupled with the greater sophistication of the more recent detectors offers hope that the outstanding problems will be solved. Neutrino events in detectors such as telescopes 3 to 5, capable of complete definition of the tracks of several particles, should eventually enable a high minimum limit to be put on the mass of the intermediate boson, although it will not be possible to demonstrate its non-existence. The energy at which the inelastic cross-section saturates should become clear, and the nature of the large electromagnetic showers, as well as the apparent weak photon showers, may be elucidated.

Acknowledgements

The author thanks Professor G.D. Rochester F.R.S. for his interest in this work and for the provision of the facilities made available in Durham.

He is deeply indebted to his supervisor, Professor A.W. Wolfendale, for the encouragement, guidance and help given during the past three years.

This work would not have been possible without the continuous co-operation and good-will of the members of the Kolar Gold Fields team, Messrs. C.V. Achar, M.R. Krishnaswami, V.S. Narasimham, A.M. Vinze and R.M. Wankar of the Tata Institute; Professor K. Hinotani and Dr. N. Ito of Osaka City University and Drs. J.L. Osborne, P.K. MacKeown and J.B.M. Pattison, and Mr. R. Craig of Durham. The author expresses his grateful thanks to the members of the team as well as to his local supervisors in India, Professors M.G.K. Menon and S. Miyake, and Dr. S. Naranan.

The author wishes to thank Dr. E.C.M. Young for many useful discussions on theoretical aspects of the experiment.

The members of the Kolar Gold Mining Undertakings; in particular the Managing Director Mr. M.H. Parthasarathy I.A.S., the Champion Reef Mine Superintendents Messrs. V.V.R. Rao and P.N.V. Raghavan; Mr. B.R. Garudachar, the Chief Electrical Engineer, and the many other officers and men who gave their assistance willingly on so many occasions are thanked for their help and

interest.

Mr. E.W. Lincoln is gratefully thanked for discussions and help in the laboratory and for designing and making much of the electronics sent out to the Durham members in the Kolar Gold Fields.

Finally the Science Research Council are thanked for the provision of a Research Studentship during the past three years.

References.

Achar, C.V., Narasimham, V.S., Ramana Murthy, P.V., Creed, D.R., Pattison, J.B.M. and Wolfendale, A.W., (1965a) Proc. Phys. Soc., 86, 1305. (1965b) Proc. 9th Int. Conf. Cosmic Rays, London, 2, 989.

Achar, C.V., Menon, M.G.K., Narasimham, V.S., Ramana Murthy, P.V., Sreekantan, B.V., Hinotani, K., Miyake, S., Creed, D.R., Osborne, J.L., Pattison, J.B.M. and Wolfendale, A.W., (1965c) Phys. Lett., 18, 196, (1965d) Phys. Lett., 19, 78, (1965e) Proc. 9th Int. Conf. Cosmic Rays, London, 2, 1012, (1965f) Proc. 9th Symp. Cosmic Rays, Elementary Particles and Astrophysics, Bombay, p. 379.

Backenstoss, G, Hyams, B.D., Knop, G., Marin, P.C., and Stierlin, U., (1961) Proc. Int. Conf. Elementary Particles, Aix-en-Provence, 1, 147.

Barnothy, J. and Forro, M., (1948) Phys. Rev. 74, 1300.

Barrett, P.H., Bollinger, L.M., Cocconi, G., Eisenberg, Y. and Greisen, K., (1952) Rev. Mod. Phys., 24, 133.

Bergeson, H.E. and Wolfson, C.J., (1967) Nucl. Instrum. and Methods, 51, 47.

Bergeson, H.E., Hilton, L.K., Keuffel, J.W., Morris, M., Parker, J.L., Stenerson, R.O. and Wolfson, C.J., (1965) Proc. 9th Int. Conf. Cosmic Rays, London, 2, 1048.

Bergeson, H.E., Keuffel, J.W., Martin, E.R. and Stenerson, R.O., (1967) Proc. 10th Int. Conf. Cosmic Rays, Calgary. (to be published)

Bernardini, G. et al. (CERN Spark Chamber and HLBC groups), (1965) Nuovo Cim., 38, 608.

Bethe, H.A., (1932) Z. Phys., 76, 293.

Bethe, H.A. and Heitler, W., (1934) Proc. Roy. Soc., A, 146, 83.

Bhabha, H.J., (1938) Proc. Roy. Soc., 164, 257.

Bollinger, L.M., (1951) Cornell University Ph. D. thesis, (unpublished).

Brooke, G., Hayman, P.J., Kamiya, Y. and Wolfendale, A.W., (1964) Proc. Phys. Soc., 83, 853.

o

Burns, R., Goulianos, K., Hyman, E., Lederman, L., Lee, W., Mistry, N., Rettberg, J., Schwartz, M., Sunderland, J., and Danby, G., (1965) Phys. Rev. Lett., 15, 42.

Carmichael, H. and Stelges, J.F., (1957) Phys. Rev., 105, 1626.

Castagnoli, C., De Marco, A. and Scrimaglio, R., (1964a) Atti. Acc. Lincei, 36, 475, (1964b) Atti. Acc. Lincei, 34, 640, (1965a) Atti. Acc. Lincei, 38, 201, (1964c) Nuovo Cim., 33, 722.

Castagnoli, C., De Marco, A., Longhetto, A. and Penengo, P., (1965b) Nuovo Cim., 35, 969.

Christy, R.F. and Kusaka, S., (1941) Phys. Rev., 59, 414.

Clay, J. and van Gemert, A., (1939) Physica, 6, 497.

Cowsik, R., Pal, Y. and Tandon, S.N., (1966) Proc. Ind. Acad. Sci., 53, 4A, 217.

Craig, R., Osborne, J.L., Wolfendale, A.W. and Young, E.C.M., (1967) Proc. 10th Int. Conf. Cosmic Rays, Calgary, (to be published).

Creed, D.R. and Wolfendale, A.W., (1967) Nuovo Cim., 47, 786.

Creed, D.R., Pattison, J.B.M., Wolfendale, A.W., Achar, C.V., Narasimham, V.S. and Ramana Murthy, P.V., (1965) Proc. 9th Int. Conf. Cosmic Rays, 2, 980.

Crouch, M.F., Gurr, H.S., Jenkins, T.L., Kropp, W.R., Reines, F., Smith, G.R., Meyer, B. and Sellschop, J.P.F., (1966a) Proc. Int. Conf. Weak Interactions, Argonne, ANL-7130.

Crouch, M.F., Kropp, W.R., Gurr, H.S., Sobel, H., Meyer, B., Sellschop, J.P.F. and Reines, F., (1966b) Proc. Rochester Conf. High Energy Physics, Berkeley, (to be published).

Daiyasu, K., Kobayakawa, K., Murota, T. and Nakano, T., (1962) J. Phys. Soc. Japan, Suppl. A III, 17, 344.

Danby, G., Gaillard, J.M., Goulianos, K., Lederman, L.M., Mistry, N., Schwartz, M. and Steinberger, J., (1962) Phys. Rev. Lett., 9, 36.

Davis, R., Jr., (1964) Phys. Rev. Lett., 12, 303.

Ehmert, A., (1937) Z. Phys., 106, 751.

Erlykin, A.D., (1965) Proc. 9th Int. Conf. Cosmic Rays, London, 2, 999.

Fermi, E., (1940) Phys. Rev., 57, 445.

Feynman, R.P. and Gell-Mann, M., (1958) Phys. Rev. 109, 193.

Fowler, G.N. and Wolfendale, A.W., (1958) Prog. Elementary Particle and Cosmic Ray Physics, (Amsterdam: North-Holland), 4, 107.

von Gehlen, G., (1963) Nuovo Cim., 30, 859.

George, E.P. and Evans, J., (1950) Proc. Phys. Soc., A 63, 1248.

Ginzburg, V.L. and Syrovatsky, S.I., (1964) The Origin of Cosmic Rays: Pergamon Press.

Glashow, S.L., (1960) Phys. Rev., 118, 316.

Greisen, K., (1965) Proc.9th Int. Conf. Cosmic Rays, London, 2, 649.

Gupta, M.R., (1958) Nuovo Cim. 7, 39.

Gurr H.S., (1966) Ph.D. thesis, Case Institute of Technology.

Hayman, P.J. and Wolfendale, A.W., (1962) Proc. Phys. Soc., 80, 710.

Hayman, P.J., Palmer, N.S. and Wolfendale, A.W., (1963) Proc. Roy. Soc., A 275, 391.

Higashi, S., Kitamura, T., Miyamoto, S., Mishima, Y., Takahashi, T. and Watase, Y., (1965) Prog. Theor. Phys., 34, 1042, (1966) Nuovo Cim., 43A, 334.

Higashi, S., Kitamura, T., Mishima, Y., Mitani, S., Miyamoto, S., Oshio, T., Shibata, H., Watanabe, K. and Watase, Y., (1962) J. Phys. Soc. Japan, Suppl. A III, 17, 362.

Hilton, L.K., Morris, M.L. and Stenerson, R.O., (1967) Nucl. Instrum. and Methods, 51, 43.

Hiroshige, N. and Matsuda, M., (1965) Prog. Theor. Phys., 33, 764.

Kessler, D. and Kessler, P., (1957) C.R. Acad. Sci., Paris, 244, 1896.

Keuffel, J.W. and Parker, J.L., (1967) Nucl. Instrum. and Methods., 51, 29.

Kobayakawa, K., (1966), preprint of (1967) Nuovo Cim. B47, 156.

Kocharov, G.E., (1965) Proc. 9th Int. Conf. Cosmic Rays, London, 2, 1020.

Lee, T.D. and Yang, C.N., (1960) Phys. Rev., 119, 1410.

Lee, T.D., Markstein, P. and Yang, C.N., (1961) Phys. Rev. Lett., 7, 429.

Lloyd, J.L. and Wolfendale, A.W., (1959) Proc. Phys. Soc., 78, 178.

Mando, M. and Ronchi, L., (1952) Nuovo Cim., 9, 517.

Markov, M.A. and Zheleznykh, I.M., (1961) Nucl. Phys., 27, 385.

Massey, H.S.W. and Corben, H.C., (1939) Camb. Phil. Soc., 35, 463.

Matano, T., Miura, I., Nagano, M., Shibata, S., Suga, K. and Hasegawa, H., (1965) Proc. 9th Int. Conf. Cosmic Rays, London, 2, 637.

Menon, M.G.K. and Ramana Murthy, P.V., (1967) Prog. in Cosmic Ray and Elementary Particle Physics, Vol. 9, (ed. J.G. Wilson and S.A. Wothuysen: North Holland), (to be published).

Menon, M.G.K., Naranan, S., Narasimham, V.S., Hinotani, K., Ito, N., Miyake, S., Craig, R., Creed, D.R., Osborne, J.L. and Wolfendale, A.W., (1966a) Proc. 13th. Rochester Int. Conf. on High Energy Physics, Berkeley, (to be published):,(1966b) Proc. Roy. Soc. Inf. Conf. on Neutrino Physics, London, (to be published); (1967b) Proc. 10th Int.Conf. Cosmic Rays, Calgary, (to be published).

Menon, M.G.K., Naranan, S., Narasimham, V.S., Hinotani, K., Ito, N., Miyake, S., Creed, D.R., Osborne, J.L., Pattison, J.B.M. and Wolfendale, A.W., (1967a) Proc. Phys. Soc., 90, 649.

Miyake, S., Narasimham, V.S. and Ramana Murthy, P.V., (1964a) Nuovo Cim. 32, 1505; (1964b) Nuovo Cim., 32, 1524.

Morris, M.L. and Stenerson, R.O., (1967) to be published in Nuovo Cim.

Murota, T., Ueda, A. and Tanaka, H., (1956) Prog. Theor. Phys., 16, 482.

Narasimham, V.S., (1967) Ph.D. thesis, University of Bombay.

Oda, H. and Murayama, T., (1965) J. Phys. Soc. Japan, 20, 1549.

Osborne, J.L., (1966) Ph.D. thesis, University of Durham.

Osborne, J.L., Wolfendale, A.W. and Palmer, N.S., (1964) Proc. Phys. Soc., 84, 911.

Osborne, J.L., Said, S.S. and Wolfendale, A.W., (1965) Proc. Phys. Soc., 86, 93.

Osborne, J.L., Wolfendale, A.W. and Young, E.C.M., (1967) to be published in Proc. Phys. Soc.

Pattison, J.B.M., (1965) Ph.D. thesis, University of Durham.

Paty, M., (1965) CERN report 65-12.

Randall, C.A. and Hazen, W.E., (1951) Phys. Rev.,81,144.

Regener, V.H., (1951) Phys. Rev., 84, 161.

Reines, F., (1966) Proc. Inf. Conf. on Neutrino Physics, London, (to be published in Proc. Roy. Soc.)

Reines, F. and Cowan, C.L., Jr., (1953) Phys. Rev. 92, 830.

Reines, F., Crouch, M.F., Jenkins, T.L., Kropp, W.R., Gurr, H.S., Smith, G.R., Sellschop, J.P.F. and Meyer, B., (1965a) Phys. Rev. Lett., 15, 429.

Reines, F., Crouch, M.F., Jenkins, T.L., Kropp, W.R., Gurr, H.S., Smith, G.R., Sobel, H.W., Sellschop, J.P.F. and Meyer, B., (1965b) Proc. 9th Int. Conf. on Cosmic Rays, London, 2, 1051.

Reines, F., Kropp, W.R., Gurr, H.S., Lathrop, J., Crouch, M.F., Sobel, H.W., Sellschop, J.P.F. and Meyer, B., (1967) Proc. 10th Int. Conf. on Cosmic Rays, Calgary, (to be published).

Rossi, B., (1952) High Energy Particles, (New York: Prentice-Hall).

Rozental, I.L. and Streltsov, V.N., (1959) Soviet Phys. JEPT 8, 1007.

Said, S.S., (1966) Ph.D. thesis, University of Durham.

Sreekantan, B.V., Naranan, S., and Ramana Murthy, P.V., (1956) Proc. Ind. Acad. Sci., 43, 113.

Sternheimer, R.M., (1952) Phys. Rev., 88, 851; (1956) Phys. Rev., 103, 511; (1959) Phys. Rev., 115, 137.

Ternovski, F.F., (1959) Zh. Eksper. Teor. Fiz., 37, 793.

Uberall, H., (1964) Phys. Rev., 133 B, 444.

Wilson, V.C., (1938) Phys. Rev., 53, 337.

Wu, C.S., Ambler, E., Hayward, R.W., Hoppes, D.D., and Hudson, R.P., (1957) Phys. Rev., 105, 1413.

Young, E.C.M., (1966) Ph.D. Thesis, University of Bristol also (1967) CERN, 67-12.

Zagrebin, V.A. and Zheleznykh, I.M., (1964) Reprint, Lebedev Institute, Moscow.

Zatsepin, G.T. and Mikhalchi, E.D., (1962) J. Phys. Soc. Japan, Suppl. A III, 17, 356.

Zhdanov, G.B., Tret'yakova, M.J., Tsytovich, V.N. and Shcherbakova, M.N., (1963) Soviet Phys. JEPT, 17, 245.

Appendix A

EVENT DATA.

This appendix covers the data on events that occurred in the five KGF neutrino telescopes between 1st April 1965 and 1st June 1967. The basic data for each event is listed in table A.1. In the table the scintillator elements that gave saturated pulses are underlined, where more than one element per wall was triggered. The scintillator nomenclature is illustated in figure 3.10. The following notations are used:

IST = Indian standard time

MST = mean sidereal time

OG = out of geometry, sh = shower event.

The angles quoted are known to approximately $\pm 1^{\circ}$ unless otherwise stated. Features of the events not covered by the table are as follows.

Event 1 The neon flash tube (nft) trays for telescope 2 were still under construction and only scintillator information is available for this event. The event was unambiguously distinguished from a chance four-fold coincidence by the size and position of the oscilloscope display pulses as well as by the statistical unlikelihood of a chance coincidence. The p.z.a. is $> 39^{\circ}$ from the scintillator data.

Event 2 A single track. The centre nft array was not installed

in telescope 1.at this time.

Event 3 A single track. Only the centre nft array was present in telescope 2.

Event 4 This event has been discussed at length by Achar et al. (1965d). (Figure A.1). The two tracks appear to diverge from a point that could be close to the surface of the southern rock wall or up to 1 metre inside it in the projected plane. The tracks diverge at an angle of $3^{\circ} \pm 1^{\circ}$, track 'a' passing through 10 radiation lengths of lead without interaction and track 'b', presumably missing the southern nft array because of its inclination in azimuth angle, passing through 5 radiation lengths. It can be concluded that both tracks are due to either a pion or a muon. It is possible that the point of origin lies in the northern rock wall, either or both of the particles having been scattered by a total of 3°, however the absence of further scattering in the lead reduces this probability. The simplest explanation is that this event is attributable to an inelastic neutrino interaction, the two particles being a muon and a pion, but is is also possible that both are muons observed as a result of the creation of an intermediate boson in the interaction.

Event 5 A single track.

Event 6 A near vertical track that is out of geometry. The S1 scintillator was traversed by a muon and one of the knock-on

Figure A.1

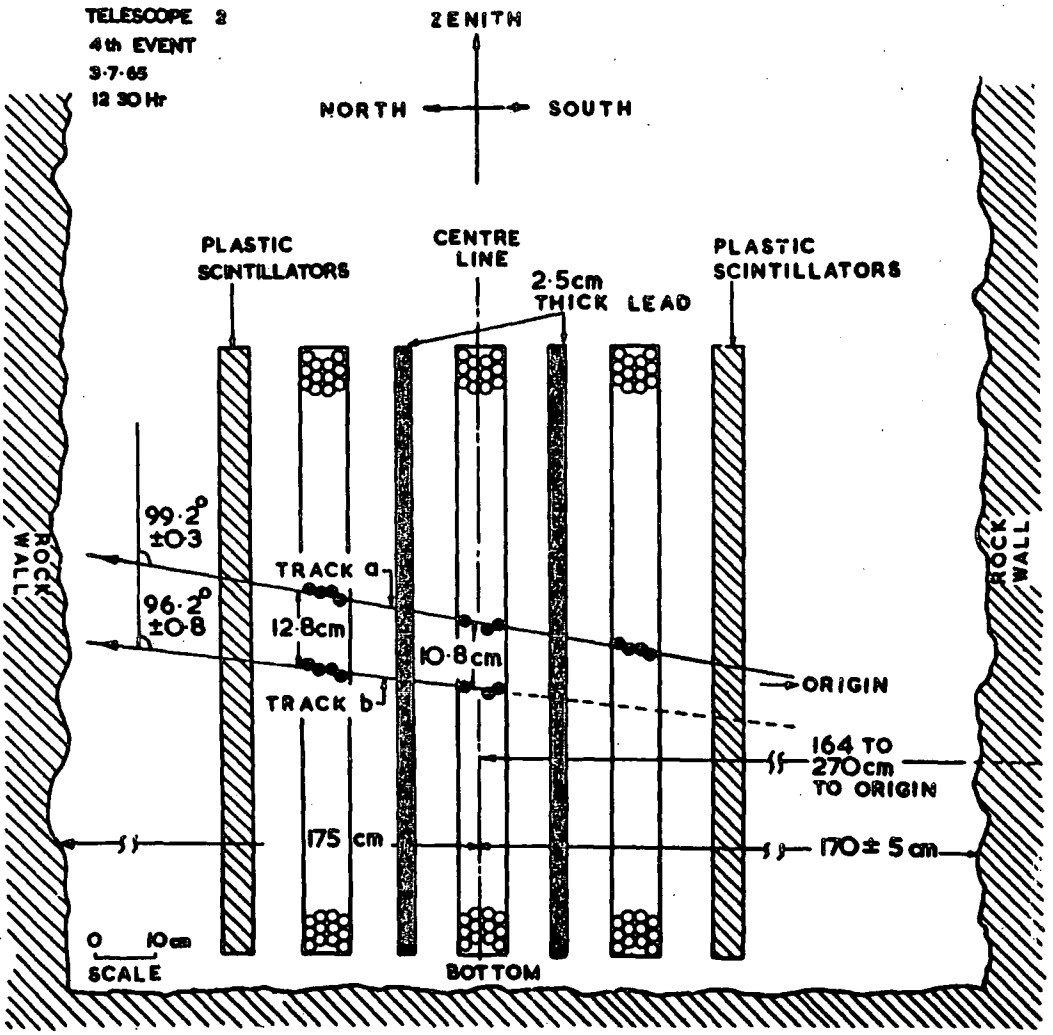

Event no. 4. Only the bottom third of telescope 2 is illustrated. As indicated in the figure, the meeting point is probably just inside the rock wall.

electrons causing the coincidence between S1 and N6 can be seen in the north nft array.

Event 7 A penetrating track with a single knock-on electron from the scintillator visible in the north nft array indicating a downward moving particle.

Event 8 A penetrating track with two knock-on electrons from the lead visible in the centre nft array with a δ-ray produced in the same tray. There is some evidence for a small angle of scatter in the southern lead wall. A downward moving particle.

Event 9 A penetrating track that produced a large electron shower (73 fl.) in the north lead wall. It is possible that this event is out of geometry, the electron shower causing the coincidence in N1. A downward moving particle.

Event 10 An OG event, the single track visible missed the south scintillator wall: presumably a knock-on from the rock caused the coincidence. Probably a downward moving particle that possibly undergoes small angle scattering in the north lead wall. No scintillator data available.

Event 11 A single penetrating track with a single knock-on from the south lead wall. Probably downward moving.

Event 12 A single penetrating track that missed the south scintillator wall, a large electron shower that can be seen coming from the rock causing the coincidence. A low energy

knock-on electron from the south lead wall visible in the centre nft array.

Event 13 A very large electron shower coming from the south rock wall. From the oscilloscope data a large amount of energy was deposited in all six scintillators on the south side of telescope 2, as well as smaller amounts in five of the north wall scintillators. Pulses were also recorded from telescope 1 although few flash tubes fired. Almost all the nfts in telescope 2 south array fired, indicating a shower energy of several hundred GeV. No clear penetrating track that could definately be ascribed to muon could be seen, though it is possible that a particle did traverse the width of the telescope. From the few short tracks in the centre and north arrays the particle initiating the shower was estimated to be travelling in a near horizontal direction at an angle of about 40° to the line of the telescopes.

Event 14 A penetrating track with an electron shower visible in the centre nft array coming from the north lead wall. (27 fl.) A further small shower is visible in the south nft array. (18 fl.) A downward moving particle.

Event 15 A single track.

Event 16 A single track. No flashes are visible in the north nft array. This may be an out of geometry event, but it is difficult to be certain as the photographic technique was poor.

Event 17 There is no nft data for this 'event'. Subsequent analysis of the oscilloscope pulses indicated that this was probably a chance four-fold coincidence, the two-fold rates having been increased considerably since event 1 was recorded.

Event 18 A single track with an additional short track in the south array. This could be a knock-on electron from the south lead wall, the particle moving upwards. There is some slight evidence for small angle scattering in the south lead wall.

Event 19 A penetrating track indicating a downward moving particle that knocked-on two electrons from the north lead wall and possibly one low energy electron from the south lead wall. No oscilloscope data available.

Event 20 A penetrating track with one knock-on electron from the north lead wall visible in the centre nft array indicating a downward moving particle.

Event 21 No clear penetrating track. The coincidence appears to have been caused by a medium sized electron shower generated in the rock ceiling, the direction of propagation of the shower being close to the vertical. There are several widely spaced pairs of flash tubes that fired, possibly caused by electrons generated by photons in the nft arrays.

Event 22 A single penetrating track with a low energy knock-on electron in two of the five nft arrays. A downward moving particle.

Event 23 A single penetrating track. No oscilloscope data available. Some evidence for scattering in the north lead wall.

Event 24 A medium sized electron shower in the south nft array. No evidence of a penetrating track. The direction of the shower is difficult to determine, but it was probably travelling at $>50^{\circ}$ to the zenith.

Event 25 A single penetrating track with a possible low energy knock-on electron in the south nft array from the south lead wall. Probably downward moving.

Event 26 A single penetrating track with a knock-on electron coming from the north lead wall. The unusually large number of single tubes that fired in addition to the main tracks may indicate the presence of a weak photon shower. Probably downward moving.

Event 27 A single penetrating track with, possibly, two δ-rays generated in the south nft array indicating a downward moving particle.

Event 28 An OG event. A near vertical track is visible, with a knock-on electron, in the north horizontal nft array.

Event 29 This event consists of three main tracks. (Figure A.2). The near horizontal track is a penetrating particle assumed to be a muon, although it could be a pion. The two additional shorter tracks appear to converge on the central track at a distance of 60 cm from the south scintillator wall in the projected plane.

EVENT NO.

29

TYPE

I

TELESCOPE

1

SCINTILLATORS

N	S
1, 3, 4	1, 2, 4, 5

TOTAL RUNNING TIME FOR BOTH TELESCOPES

Array Hours

13339-01

RUN NO.

331

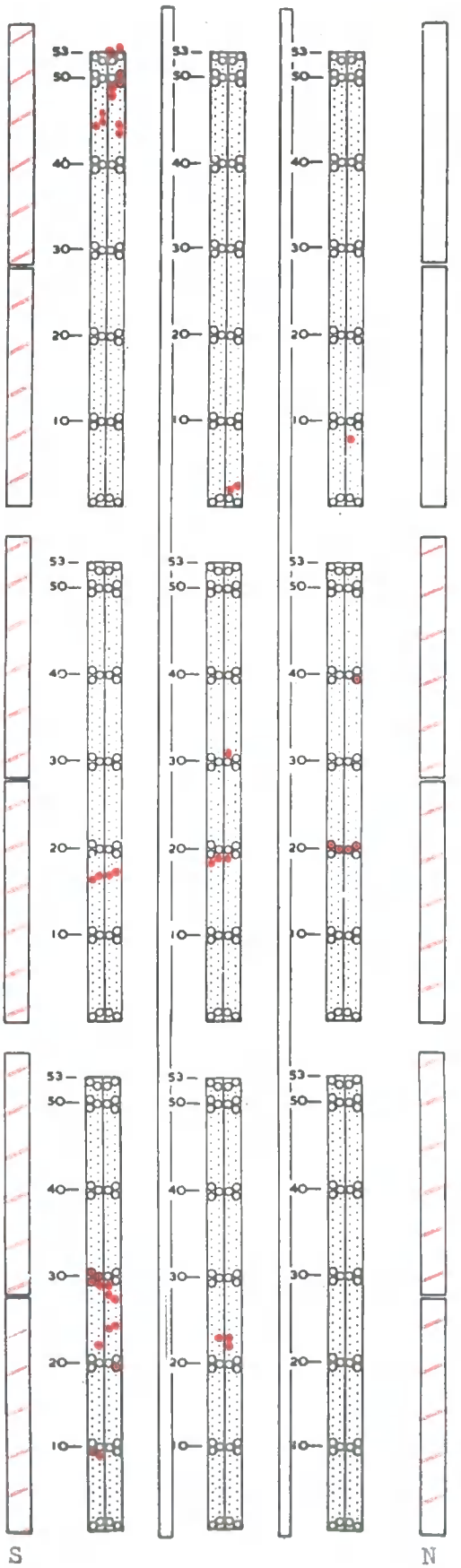

PROJ. Z. A.

$83.5^{\circ} \pm 1^{\circ}$

PROJ. A. A.

64°E of S to 30°W of S

DIRECTION

Upwards

DATE

Day	Month	Year
29	6	66

TIME I.S.T.

22.15

TIME M.S.T.

16.27

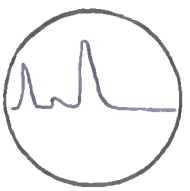

North C.R.O.

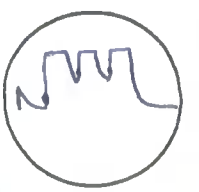

South C.R.O.

Figure A.2

The upper track passes out of the top of the telescope, possibly generating the two low energy knock-on electrons that are visible, the lower track is stopped in the south lead wall with two short tracks nearby, possibly low energy knock-on electrons. The interpretation is the same as that for event 4. An inelastic neutrino interaction, possibly taking place within an iron pillar at 60 cm from the south scintillator wall, gave rise to a muon and a pion and one other particle. This event could also be ascribed to the creation of a W, the upper track being a muon as well as the centre track.

Event 30 A penetrating track that passed through telescopes 4 and 5. No visible accompaniment.

Event 31 A single penetrating track showing evidence of small angle scattering in the north lead wall. This track could be out of geometry because of the scattering of the particle. Presumably the coincidence would then be caused by an unobserved knock-on electron from the rock.

Event 32 This event (figure A.3) shows several tracks. The lower track is most probably a muon which produces a large shower (52 fl.) in the south lead wall, visible in the south nft array. The upper tracks could be caused by a pion, accompanied by an electron from the rock, knocking-on an electron from the north lead wall and stopping in the south lead wall; or by a muon with the same accompaniment which passed out of the telescope missing

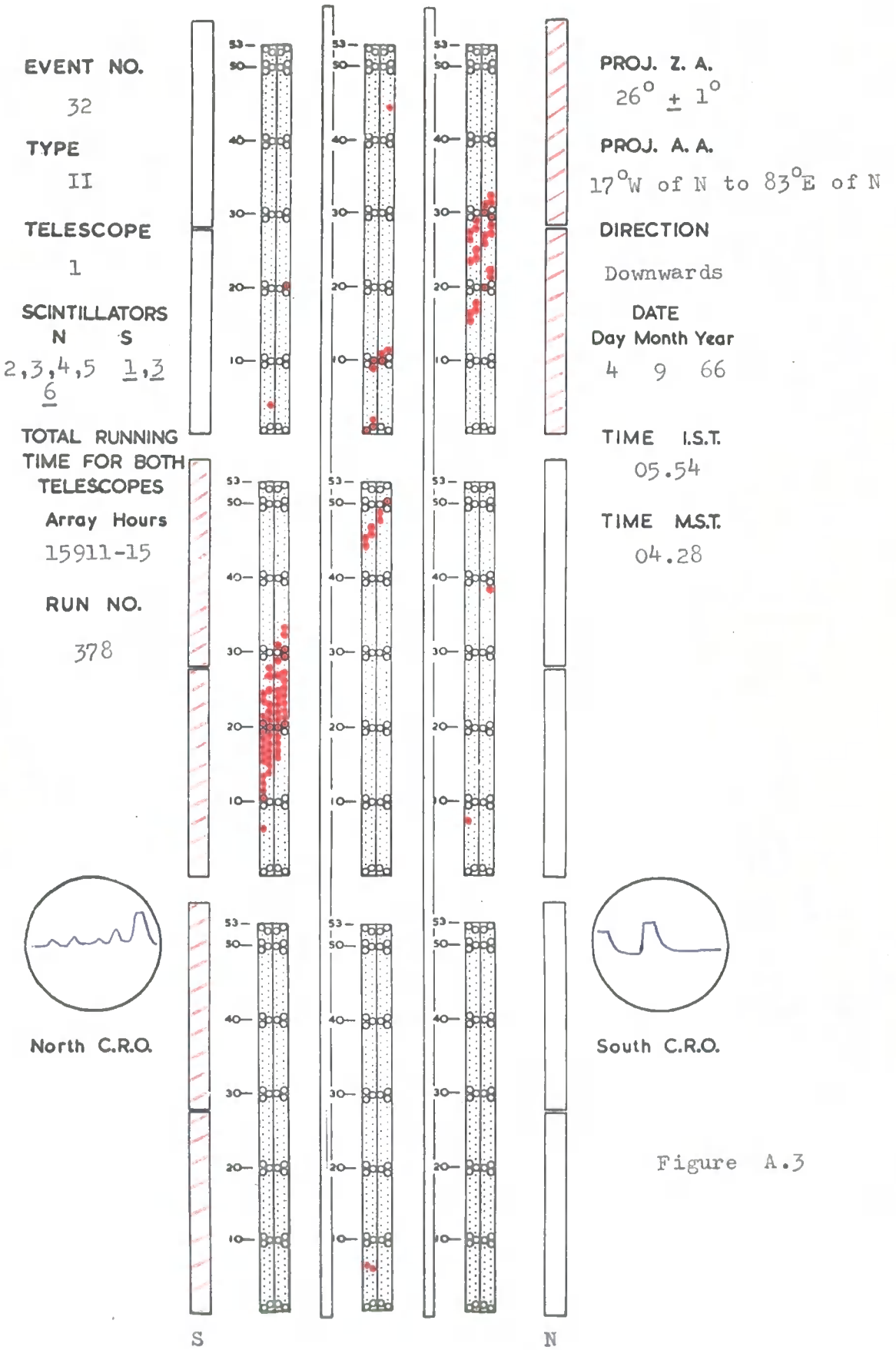
EVENT NO.
32
TYPE
II
TELESCOPE
1
SCINTILLATORS
N S
2,3,4,5 1,3
6
TOTAL RUNNING TIME FOR BOTH TELESCOPES
Array Hours
15911-15
RUN NO.
378
PROJ. Z. A.
26° ± 1°
PROJ. A. A.
17°W of N to 83°E of N
DIRECTION
Downwards
DATE
Day Month Year
4 9 66
TIME I.S.T.
05.54
TIME M.S.T.
04.28
North C.R.O.
South C.R.O.
S
N

Figure A.3

the south nft array. Alternatively, there could be two separate pions, both penetrating the north lead wall, one undergoing scattering. Because of the low p.z.a. and the energetic shower in the south array this is most probably an atmospheric muon event.

Event 33 A single penetrating track accompanied by possibly two electrons from the rock ceiling. A low energy electron is knocked-on from the inner north iron wall, and possibly one is also knocked-on from the south iron wall. A downward moving particle that is out of geometry.

Event 34 A single penetrating track showing some evidence of small angle scattering in one of the lead walls.

Event 35 A single penetrating track showing some evidence of small angle scattering in the south lead wall. A knock-on electron in the north nft array could be from the rock if the particle is downward moving, or from the north lead wall if upward moving, the latter being perhaps the more likely.

Event 36 A single penetrating track that appears to undergo large angle scattering as a result of its traversal of the four iron walls. The particle missed the centre nft array.

Event 37 A single penetrating track.

Event 38 A single penetrating track that undergoes small angle scattering in the south lead wall. A low energy knock-on electron

from the south lead wall is visible. Probably a downward moving particle.

Event 39 A single penetrating downward moving particle producing a small electron shower in the inner south iron wall. (Figure A.4).

Event 40 A single penetrating track.

Event 41 A single penetrating track with a small electron shower (17 fl.) in the centre nft array from the north lead wall, a further development of this shower (43 fl.) being observed in the south nft array. A downward moving particle.

Event 42 A single penetrating track that is out of geometry, the coincidence being caused by considerable energy deposition in the S6 scintillator, the particle passing through the N5 scintillator. Presumably there was considerable accompaniment from the rock.

Event 43 A single, near horizontal track with several other short tracks visible in the lower half of the telescope. (Fig. A.5) The penetrating track did not produce any accompaniment in its passage through the telescope except for one, possible, knock-on electron. The associated tracks could be two pions, each penetrating one lead wall and the high number of random flashes could be due to a photon shower. This event is probably due to an inelastic neutrino interaction.

Event 44 A single penetrating track.

EVENT NO.	TYPE	TELESCOPE
39	II	4
RUN NO.	**SCINTILLATORS**	**DIRECTION**
462	N 1 S 3	Downwards

NORTH C.R.O.

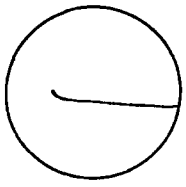

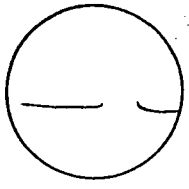

SOUTH C.R.O.

AZIMUTH ANGLE: 23°W of N SPATIAL ZENITH ANGLE: 48°

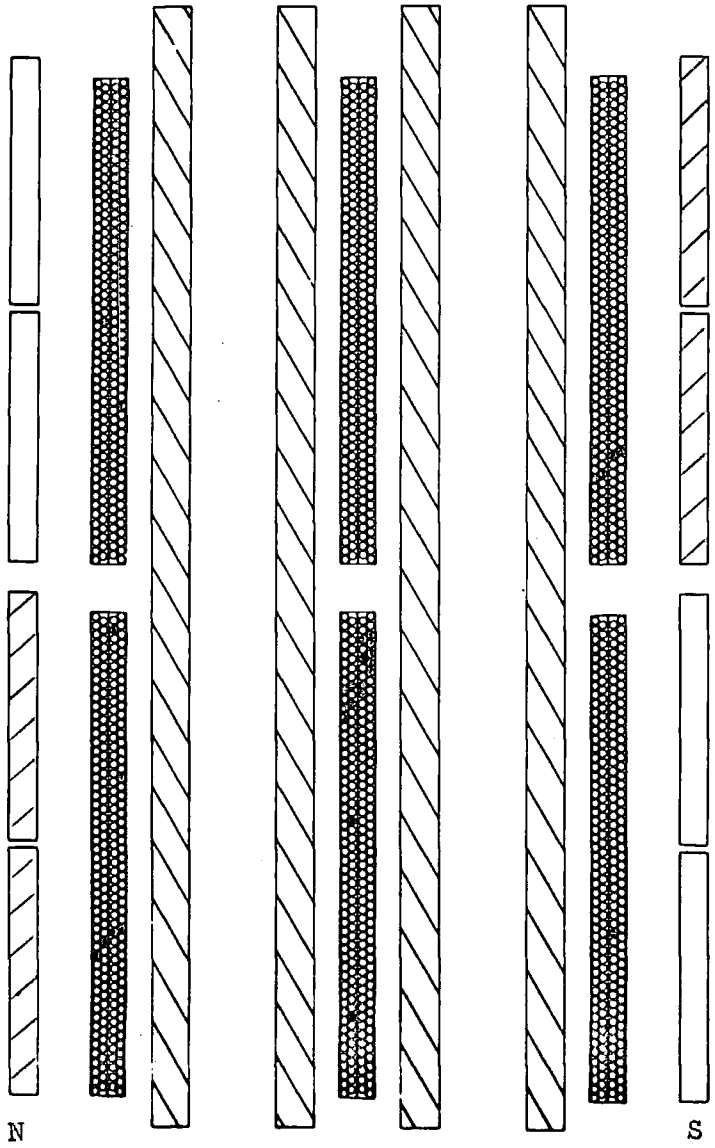

Figure A.4a

DATE			TIME I.S.T.	TIME M.S.T.
day	month	year		
18	12	66	03.50	09.17

TOTAL RUNNING TIME FOR TELESCOPES 3, 4 & 5 – ARRAY HOURS 15,001

PROJECTED ZENITH ANGLE 45°

AZIMUTH ANGLE 23°W of N SPATIAL ZENITH ANGLE 48°

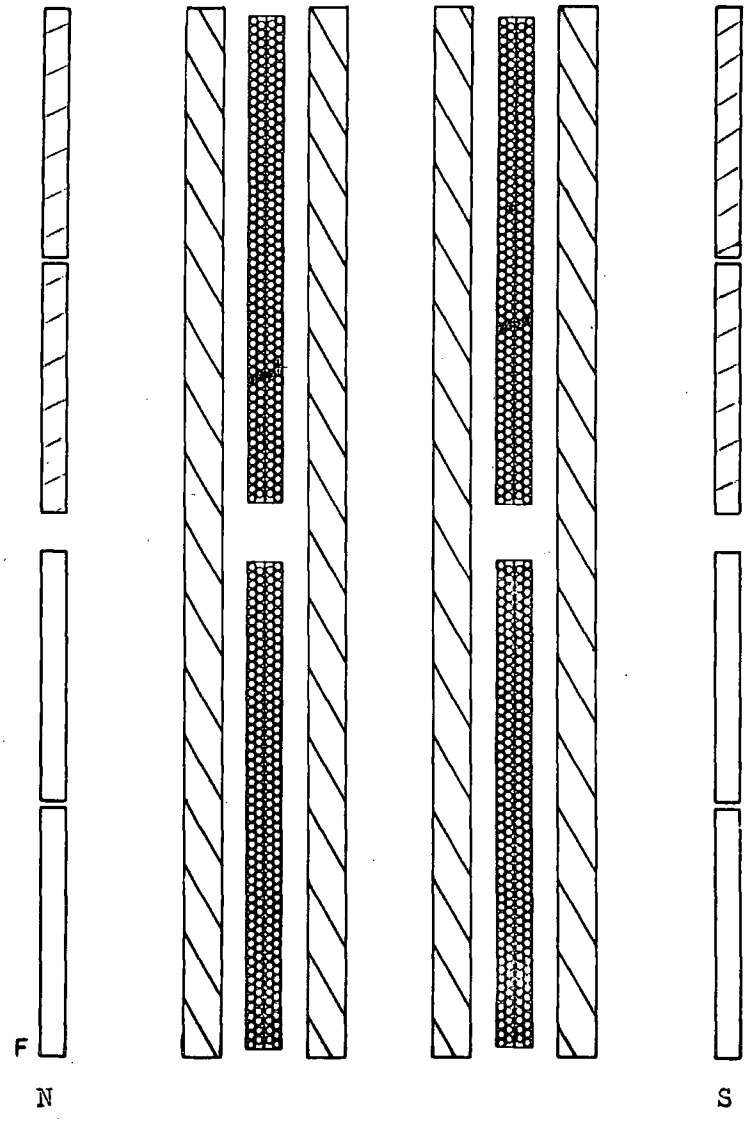

Figure A.4b

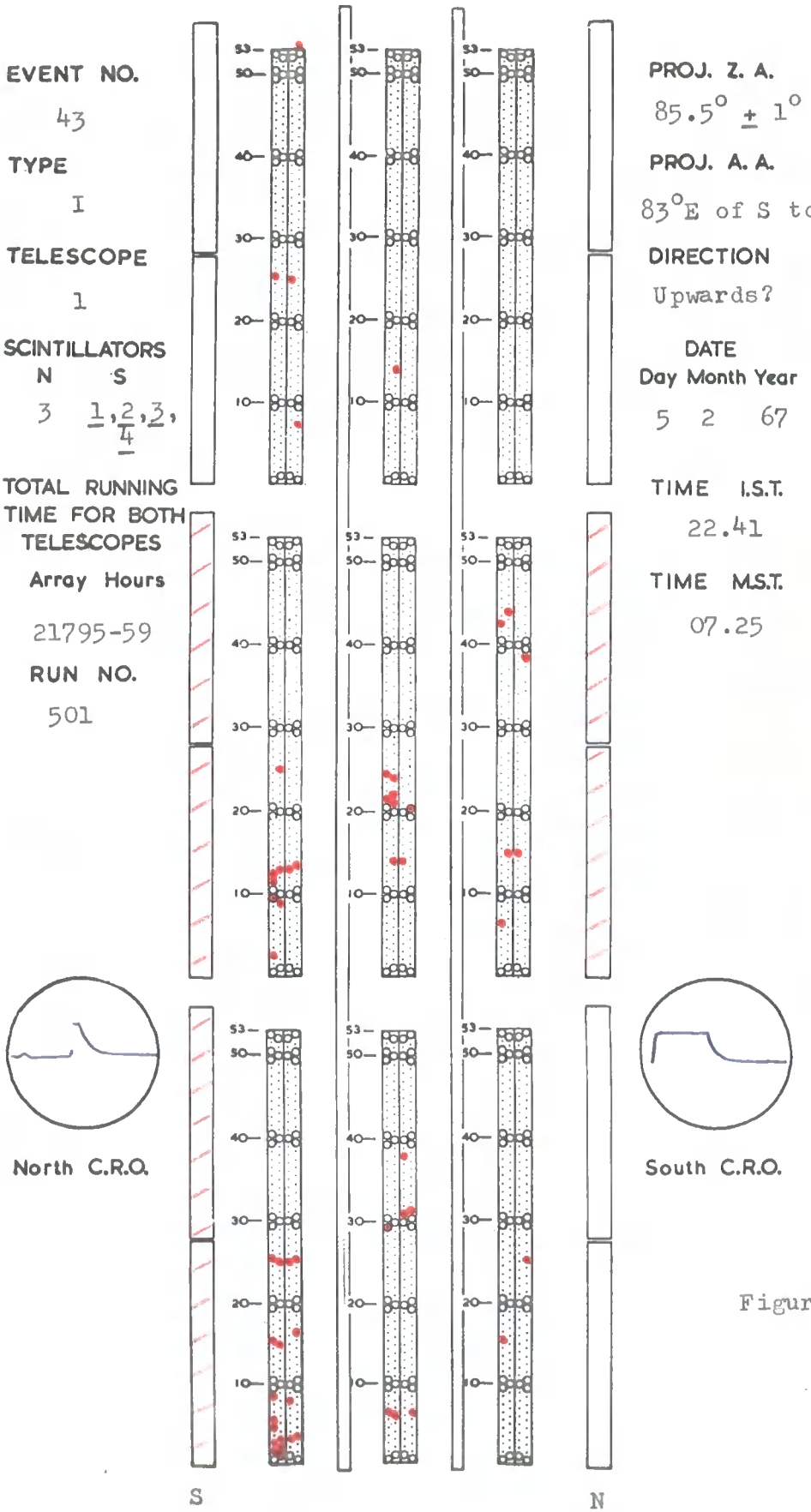
EVENT NO.
43
TYPE
I
TELESCOPE
1
SCINTILLATORS
N S
3 1,2,3,4
TOTAL RUNNING TIME FOR BOTH TELESCOPES
Array Hours
21795-59
RUN NO.
501
PROJ. Z. A.
85.5° ± 1°
PROJ. A. A.
83°E of S to 30°W of S
DIRECTION
Upwards?
DATE
Day Month Year
5 2 67
TIME I.S.T.
22.41
TIME M.S.T.
07.25
North C.R.O.
South C.R.O.
S
N

Figure A.5

Event 45 A single penetrating track. No scintillator information is available.

Event 46 A single penetrating track.

A breakdown of these events is shown in table A.2.

In addition to the events mentioned above, three fourfold coincidences were recorded, 24A, 32A and 45A, that showed evidence of particle tracks or an abnormal number of spurious flashes. In no case was a penetrating particle seen, and the short tracks were tentatively ascribed to electrons. 24A occurred in telescope 5 and shows a track in both the azimuth (vertically orientated) nft arrays, but no tracks in the three zenith (horizontally orientated) arrays. This does not seem to have been due to instrument failure. Event 32A, a coincidence between the N3 (tel. 4) and S2 (tel. 5) scintillators shows only one definite track in one of the nft arrays, but there is an unusually high number of extra single flashes, indicating that the event may be a weak photon shower. A similar explanation is possible for event 45A since, again, there was an abnormally high number of spurious flashes.

In general very few doubtful events were recorded, even though the setting of the amplifier gains and biases was adjusted so that there was a chance fourfold coincidence approximately every 300 telescope-hours.

Table A.1

Events Recorded by the KGF Neutrino Telescopes (1/4/65 to 1/6/67)

Event No.	Date	Time IST	Time MST	Tele-scope	Scintillators	P.z.a. degrees	Comments
1	5/4/65	20.04	08.38	2	N4, S4	>39	no nft
2	27/4/65	18.26	08.30	1	N1, S1	48	
3	25/5/65	20.03	11.58	2	N6, S6	75 ± 15	
4	3/7/65	12.30	06.57	2	N1, S1	96.2 ± 0.8 99.2 ± 0.3	
5	13/7/65	16.13	11.21	2	N4, S356	45	
6	18/7/65	02.52	22.15	1	N36, S12	8.5	OG
7	24/7/65	11.47	07.37	2	N6, S3	37.5	
8	27/7/65	03.24	23.23	1	N6, S3	29.5	
9	29/7/65	19.07	15.18	2	N1, S3	32.5	
10	1/8/65	21.00	17.23	1	-	25	OG
11	2/8/65	03.38	00.02	1	N6, S4	47	
12	11/8/65	17.37	14.38	1	N4, S5	33	OG
13	12/8/65	11.38	08.43	2	N12456, S all	near	
				1	N1246, S1246	horizontal	sh
14	9/9/65	02.22	01.12	2	N5, S13	21	
15	10/9/65	08.20	07.15	1	N6, S3	26.5	
16	13/10/65	12.14	13.23	1	N3, S1	40	
18	26/1/66	03.38	11.40	1	N4, S5	36	
19	27/1/66	02.23	10.29	1	-	33	
20	5/2/66	04.28	13.10	2	N6, S4	51.5	
21	14/3/66	06.02	17.09	1	N246, S5	near vert.	sh,OG
22	9/5/66	13.31	04.21	5	N3, S1	46 (s.z.a.)	
23	9/5/66	17.42	08.33	2	-	44.5	
24	25/5/66	00.01	15.52	1	N4, S135	~50	sh,OG
25	9/6/66	12.47	05.39	2	N3, S1	44	
26	16/6/66	18.32	11.52	2	N2, S45	19.5	
27	27/6/66	16.06	10.09	2	N4, S6	43	
28	29/6/66	21.06	15.18	3	N3, S3	10	OG
29	29/6/66	22.15	16.27	1	N134, S1245	83.5	
30	18/7/66	20.37	16.04	4-5	N1, S1	72 (s.z.a.)	
31	6/8/66	16.33	13.14	2	N6, S13	21 ± 4	
32	4/9/66	05.54	04.28	1	N23456, S13	26	
33	17/10/66	02.17	03.40	5	N4, S2	34 (s.z.a.)	OG
34	31/10/66	19.28	21.49	1	N46, S2	31	
35	1/11/66	08.32	10.55	1	N35, S1	27	
36	13/11/66	22.20	01.32	5	N2, S4	74 (s.z.a.)	
37	20/11/66	20.40	00.20	2	N2, S6	19	
38	15/12/66	09.45	15.02	2	N6, S1	19	
39	18/12/66	03.50	09.17	4	N1, S3	48 (s.z.a.)	
40	29/12/66	01.57	08.08	2	N6, S4	36	

Table A.1 (cont.)

Event No.	Date	Time LST	Time MST	Tele-scope	Scintillators	P.z.a. degrees	Comments
41	8/1/67	23.55	06.49	1	N2, S1$\underline{2}$46	44	
42	16/1/67	22.21	05.46	1	N5, S$\underline{46}$	18	OG
43	5/2/67	22.41	07.25	1	N3, S$\underline{1234}$	85.5 $\pm$ 0.5	
44	10/4/67	20.36	09.32	1	N5, S$\underline{1}$	29	
45	20/4/67	02.41	16.17	1	-	36	
46	4/5/67	01.01	15.28	2	N2, S5	20	

Table A.2

Breakdown of Events.

Type	Telescope		
	1	2	3, 4 and 5
In geometry $\beta < 60^{\circ}$ (incl. event no. 1)	13	15	2
In geometry $\beta > 60^{\circ}$	2	2	2
Out of geometry	4	-	2
Shower events (with no obvious penetrating ptle.)	2	1	-
(Weak photon showers?)	(1)	-	(1)

DURHAM UNIVERSITY 17 JAN 1968 LIBRARY